Drosophila Dunc-115 Mediates Axon Projection Through Actin Binding

by

Christopher Roblodowski

A Dissertation Submitted to the Graduate Faculty in Biology in Partial Fulfillment of the Requirements for the Degree of Doctor of Philosophy The City University of New York

2011

This manuscript has been read and accepted for the Graduate faculty in Biology in satisfaction of the dissertation requirement for the degree of Doctor of Philosophy.

_____
Chair of Examining Committee
Dr. He Qi, Brooklyn College

_____
Executive Officer
Dr. Laurel A. Eckhardt

_____
Dr. Rafael Ovalle, Brooklyn College

_____
Dr. Weigang Qiu, Hunter College

_____
Dr. Chang-Hui Shen, College of Staten Island

_____
Dr. Sujin Bao, Mount Sinai School of Medicine

_____
Supervisory Committee

THE CITY UNIVERSITY OF NEW YORK

Abstract

Drosophila Dunc-115 Mediates Axon Projection Through Actin Binding

by
Christopher Roblodowski

Advisor: Professor Qi He

Axon pathfinding, the process of how neurons reach their correct targets during early neural development, is a critical area in neuroscience research. Though significant progress has been made in identifying the extracellular guidance cues and their membrane receptors, and possible downstream effectors including the Rho GTPases family, little is known regarding how guidance signals are relayed to the actin filaments that are central to the mobility of the growth cone. Our laboratory has identified and characterized *Drosophila* gene *dunc-115* as a possible downstream target in relaying guidance cues further down to the cytoskeleton. Specifically, we have shown that Dunc-115 regulates neural connections in both the eye and the central nervous system in *Drosophila*. In this thesis, I have identified that (1) the surface receptor Roundabout (Robo) is an upstream regulator of guidance signals relayed through Dunc-115, (2) Dunc-115 receives signals from the Rho GTPases, and (3) Dunc-115 binds to actin via its VHD (Villin Head Piece) domain, suggesting a mechanism for Dunc115 to relay guidance signals. Finally, I have analyzed the genomic structure of the *dunc-115* gene in 12 *Drosophila* genomes, which has generated further insights into how this gene has evolved.

To my mother

Acknowledgements

I would like to express my sincere appreciation to my mentor Dr. Qi He for his guidance throughout the doctoral process.

I am grateful for the other members of my committee, Drs. Weigang Qiu, Chang-Hui Shen, Rafael Ovalle, Sujin Bao for being so accommodating and reading this thesis.

I am indebted to Dr. Barbara Studamire for all her help, and thankful for members of the Lipke lab especially Cho Tan and Melissa Garcia for help and advice. My thanks also go to fellow graduate student Katherine Ray for her friendship and support. Many thanks to Takashi Susuki, Greg Bashaw, Julian Ng, Huey Hing and Ruth Fuchs for stocks and reagents.

Finally, I want to thank current and past He lab members for help and time spent especially Sergiy Alyoshkin, Amanda Chicoli, Mame Fall and Daniel Thengone.

On a personal note, I would like to thank my mother whose unrelenting love and support have made everything possible. I would also like to thank the rest of my family, especially Kathleen. Last but certainly not least, my thanks go to Asha Kumar for her emotional support throughout the most pivotal points of my thesis. I will never forget you.

TABLE OF CONTENTS

List of Tables

List of Figures

Chapter 1 Introduction

1.1 Main steps during neural development

The task of connecting neurons to their targets is a huge undertaking. In the adult human brain, for example, each of its almost 10^{12} neurons connects to an average of 1000 target cells, thereby forming a specific circuit whose particular arrangement is critical for the correct function of the system (Barallobre et al., 2005). Such a pattern requires a very precise and reliable process. Such precision is achieved through two overlapping processes: early neural activity-independent mechanisms and late activity dependent refinement mechanisms (Song and Poo, 2001).

These processes are carried out over three main steps of neural development: Neurogenesis and migration, growth of axons, and finally synaptogenesis (Figure 1). The first two steps involve activity-independent pathways. Step one, neurogenesis and migration, involves the formation of neurons and their positioning into distinct regions. Step two involves the communication of these neurons via axon pathways. This step is mediated by a specialized, motile hand-like structure at the tip of growing axons called the growth cone. It detects directional information from guidance molecules and identifies it as attractive or repulsive. The signals provided by the growth cone are then translated via receptors and second messengers into the reorganization of the cytoskeleton, resulting in movement (Song and Poo, 2001; Stoeckli and Zou, 2009; Geraldo and Gordon-Weeks, 2009; O'Donnell et al., 2009).

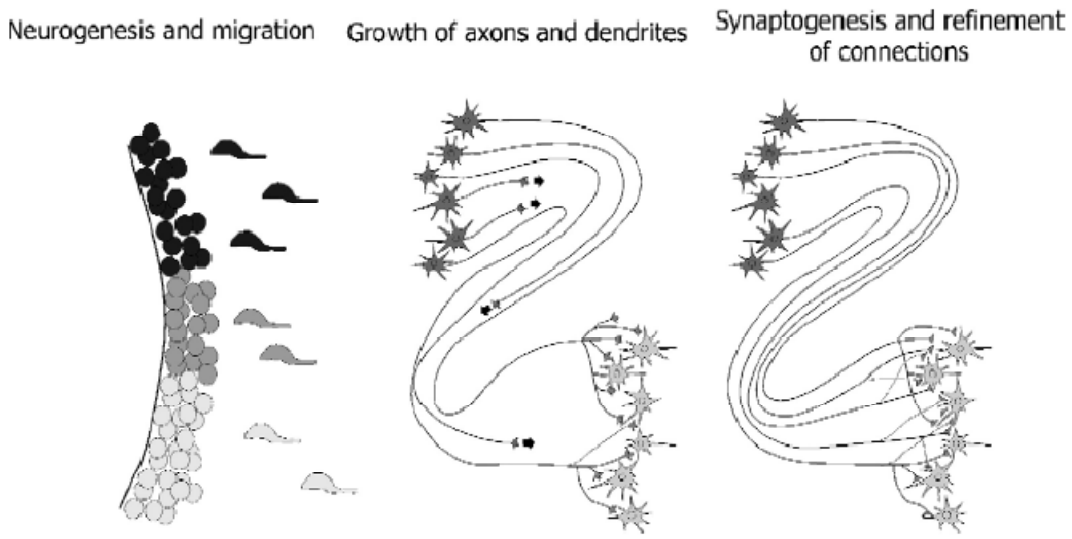

Figure 1. Schematic Representation of the Main Steps in Nervous System Development. The left panel shows a picture illustrating a region with three active neurogenetic areas. Newly generated neuroblasts migrate towards their final destination, directed by their leading process. Next (middle panel), axons grow toward their specific target regions. Finally (right panel), axons reach their target and establish specific synapses, some of which are refined at later stages (Barallobre et al., 2005).

Growth cones are partitioned into subcellular domains P (peripheral), C (central) and T (transition) (Barallobre et al., 2005; Geraldo and Gordon-Weeks, 2009; Lowery and Van Vactor, 2009) (Figure 2). In the P domain, actin filaments, which form filopodia and lamellipodia, predominate. The thin, finger-like filopodia act as sensors, altering the trajectory of the developing axon upon contact with an extracellular target (Chien et al., 1993). They are formed from the bundling together of actin filaments (F-actin). Meanwhile, the large, web-like lamellipodia within filopodia, provide the substrate adhesion and tension necessary for movement and extension. They are composed of a tightly packed branched network of F-actin. When growth cones move along paths established by other axons, they maintain a stable organization. However, when a growing axon reaches a region where a choice must be made about what direction to take, filopodia and lamellipodia expand and retract in order to lead the growth cone to a new

location (Korey and Van Vactor, 2000; Geraldo and Gordon-Weeks,2009; Lowery and Van Vactor, 2009). Such movements occur through interactions between the actin network and receptors that grasp the extracellular environment (Mitchison and Kirschner, 1988). In the C domain, microtubules predominate along with vesicles and membranous organelles like mitochondria and endoplasmic reticulum. The T zone lies at the junction between the C domain and the P domain (Geraldo and Gordon-Weeks, 2009). Here, both cytoskeletal components coexist and membrane rufflings set it apart

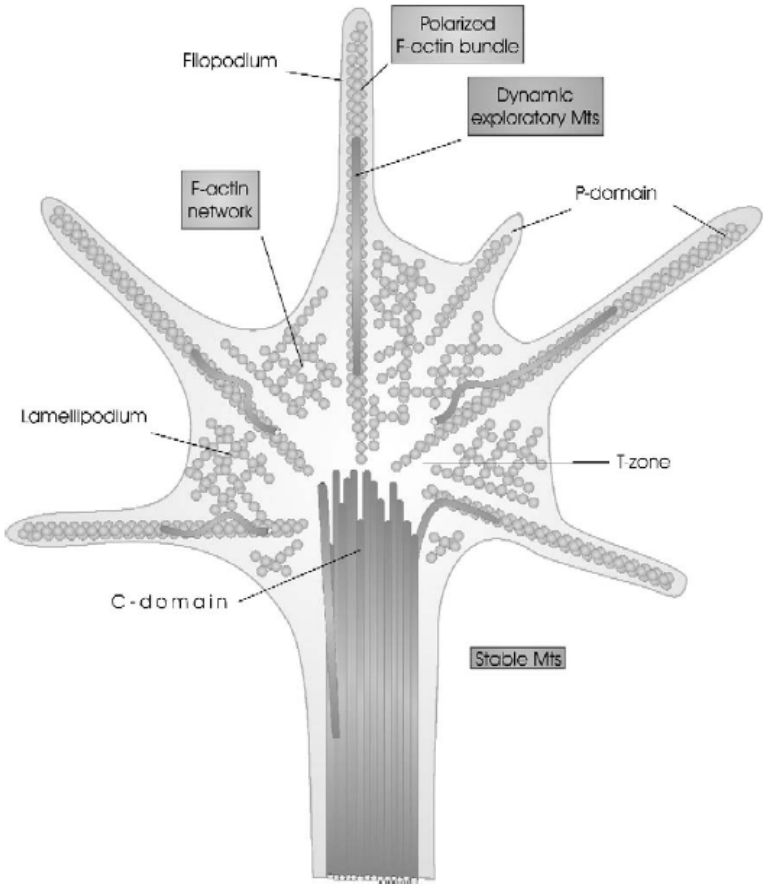

Figure 2. Illustration Summarizing the Organization of the Cytoskeleton at the Growth Cone. Actin filaments are organized into parallel filaments in filopodia and into networks in lamellipodia. Microtubules form stable bundles in the axon shaft. Single dynamic microtubule filaments also emerge into the body and filopodia of the growth cone, extending and retracting in response to several signals at the peripheral region of the growth cone. P-domain, peripheral domain with filopodia and lamellipodia; C-domain, central domain that contains microtubules; and T-zone, transition zone in which distinct components of the cytoskeleton interact (Barallobre et al., 2005).

The final step, synaptogenesis involves activity-dependent pathways. It occurs once the growth cone finds its target. At this point, the terminal region of the axon branches and establishes synapses.

1.2 Guidance Molecules

During axonal pathfinding, the movement of growth cones in a particular direction relies on the presence of specific cues. In addition, the growth cone itself contains specific receptors and transduction mechanisms to respond to these cues. The identity of these cues and the signaling mechanisms that result from the detection of these, have been the subject of much research. These cues can be classified as attractive and repulsive as well as long and short range (Figure 3). Attractive cues are signals that promote axon outgrowth and growth cone expansion whereas negative cues promote retraction and collapse of the growth cone. Diffusible guidance molecules act over long distances whereas non-diffusible (membrane-bound) cues operate over short distances.

1.2aTransmembrane: NCAMS

Neural cell-adhesion molecules (CAMs) are powerful initiators of neurite outgrowth during neural differentiation (Nagaraj and Hortsch, 2006).These proteins are typically transmembrane receptors and are composed of three domains: an intracellular domain that interacts with the cytoskeleton, a transmembrane domain and an extracellular domain. Depending on where this extracellular domain binds, CAMs will mediate either cell-cell or cell-extracellular matrix (ECM) adhesion. CAMs can be subdivided into 4 protein classes: immunoglobulin superfamily (IgSF) CAMs, cadherins, selectins, and

integrins. Cell-cell adhesion involving cadherins and selectins depends on Ca^{2+} ions, whereas interactions involving integrin and Ig-superfamily CAMs do not. Many cells use several different CAMs to mediate cell-cell adhesion. The integrins mediate cell-ECM interactions whereas the other types of CAMs participate in cell-cell adhesion.

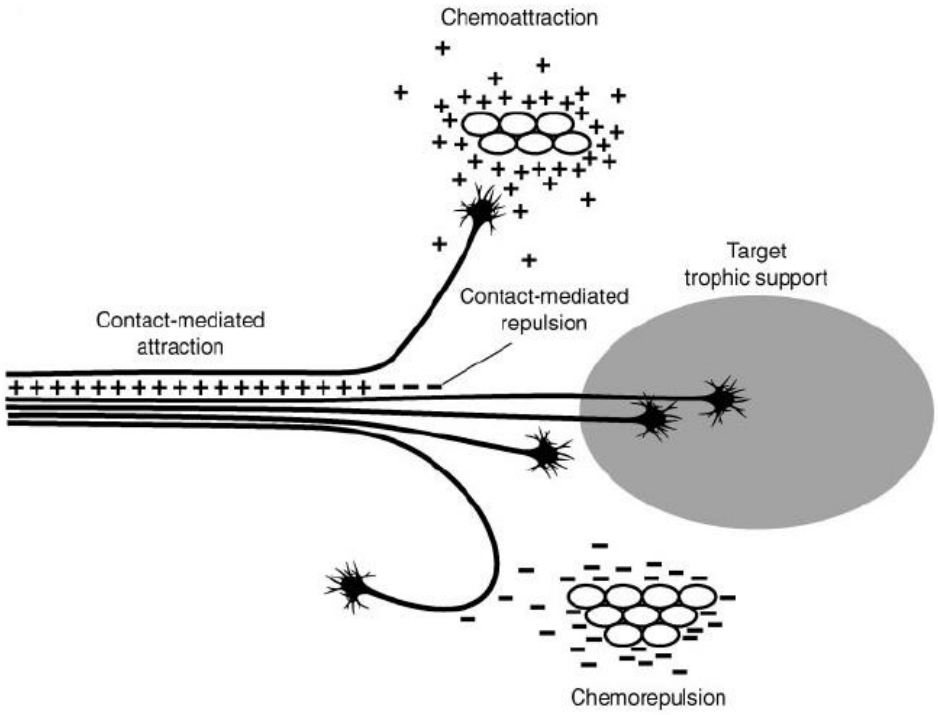

Figure 3. Guidance Cues Can Influence Axons in Different Ways. Guidance cues work on contact or diffuse and function from long distances. Once they interact with the axons, these can either retract or extend depending on whether these molecules are repulsive or attractive, respectively (Barallobre, 2005).

1.2b Diffusible

Another major class of guidance cues consists of those that are secreted by target cells, diffusing from the cells of origin to the growing axons. Early in the past century, Santiago Ramon y Cajal proposed that target-derived signals selectively influenced the movement of axonal growth cones, thereby attracting them to appropriate destinations. Experiments both *in vivo* and *in vitro* have confirmed the existence of these

chemoattractants as well as that of chemorepellents. The problem with finding these molecules had been for a long time, the fact that they are produced in such small amounts in the developing embryo. It took the brain power of Marc Tessier-Levine along with the manual force and patience of his relatives to extract and purify these molecules from extracts of 20, 000 chick embryos over the course of one weekend (Serafini et al., 1994).

Another problem was that of distinguishing tropic molecules—which guide growing axons toward a source—from trophic molecules—which support the survival and growth of neurons and their processes once an appropriate target has been contacted. These problems were solved by intensive biochemical purification and analysis of attractive or repulsive activities from chick embryos, and genetic analysis of axon growth in both *Drosophila* and *C. elegans*. This work eventually led to the cloning of several genes that code for chemotropic factors. Remarkably, the identity and function of chemoattractants and chemorepellents across phyla is highly conserved. There are 4 major families of these chemotrophic molecules and their receptors: Semaphorins, Ephrins, Slits and Netrin (Farrar and Spencer, 2008) (Figure 4).

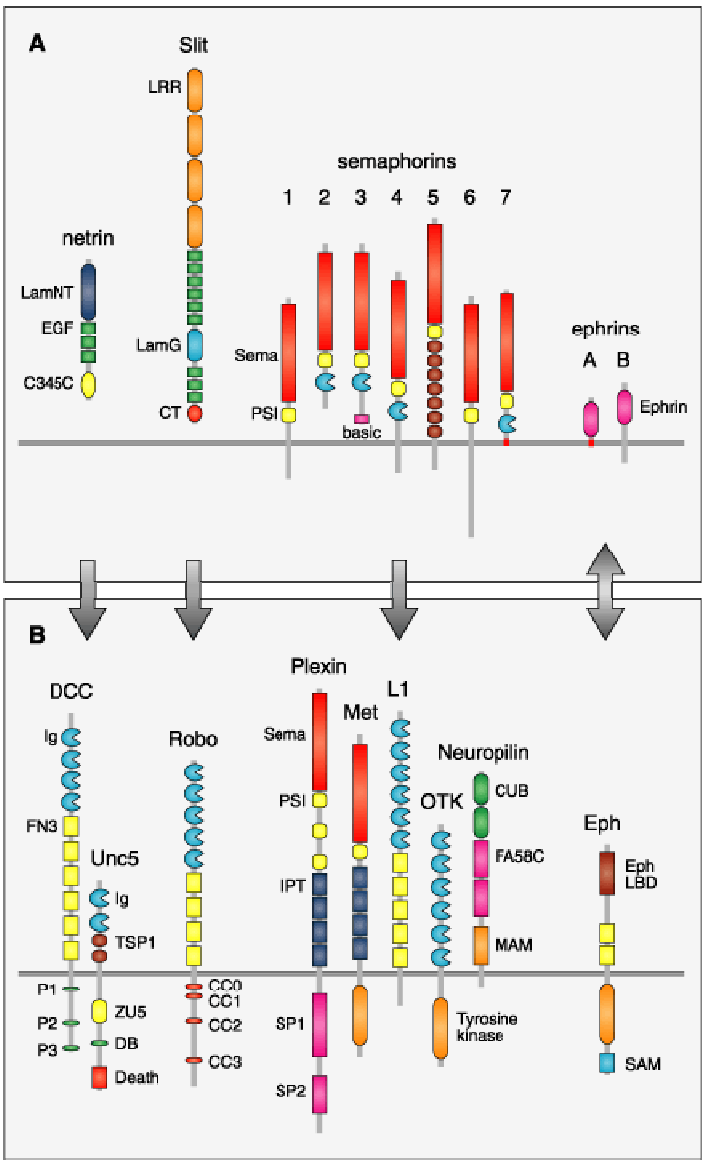

Figure 4. Conserved Families of Four Extracellular Guidance Cues.
A) Structure of ligands B) Structure of receptors. CC0 to CC3, and SP1 and SP2 indicate conserved regions in the cytoplasmic domains of DCC, UNC-5, Robo, and Plexin receptors, respectively (Dickson, 2002).

1.2b.1 Semaphorin pathway

Semaphorins, also known as collapsins, are a family of membrane-associated and secreted proteins that are active during neural development, where they generally act as chemorepellents (Guan and Rao, 2003; Govek et al., 2005; Hall and Lalli,2010). They are defined by the presence of a ~500 amino acid NH2-terminal domain, containing 17

highly conserved cysteines, called the Sema domain (Mueller, 1999; Raper, 2000; Nakamoto et al., 2004). Additionally, they contain a PSI (plexins, semaphorins, and integrins) domain, a C-terminal domain that can either be a C2 type immunoglobulin-like domain in classes 2-4,7 or contain seven thrombospondin repeats in class 5, and a short, unconserved, C-terminal end (Mark et al.,1997; Mueller,1999; Kruger et al., 2005).

There are more than 30 semaphorins, which are divided into 8 classes according to sequence and structural similarity (Figure 5). The first two classes are found in invertebrates while classes 3 to 7 are found in vertebrates. The remaining class (V) is found in viruses (Semaphorin Nomenclature Committee, 1999). The members of classes 1, 4-7 are membrane-associated while those in classes 2, 3, and V are secreted (Kruger et al., 2005).

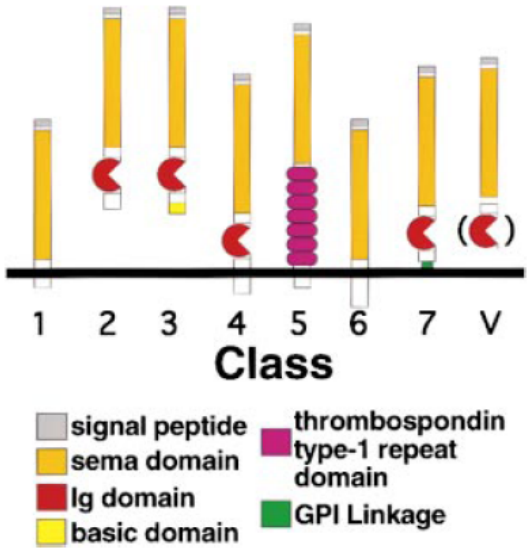

Figure 5. The Semaphorin Family.
Semaphorins exist as secreted, glycosylphosphatidylinositol (GPI)-anchored, or membrane-spanning proteins. Subclasses 1 and 2 represent invertebrate semaphorins, subclasses 3–7 are vertebrate semaphorins, and subclass V compose viral semaphorins (Semaphorin nomenclature committee, 1999)

Semaphorins are known primarily for their repulsive roles in axon guidance of a diverse group of neurons *in vitro*: motor (Shepperd et al., 1996; Valera-Echavarria et al., 1997; Huber et al., 2005), sensory (Luo et al., 1993; Luo et al., 1995; Messersmith et al., 1995; Fan & Raper, 1995), cortical (Bagnard et al., 1998) and hippocampal (Steup et al., 1999; Pascual et al., 2005), to name a few.

Fasciclin IV (Sema I) was the first semaphorin to be identified. It was found to be expressed in distinct bands of epithelial cells in developing grasshopper limb buds (Kolodkin et al., 1992). Here, it inhibits growth cones of tibial pioneer axons from moving forward. To this day, the role of grasshopper Sema I as a repellent or attractant of tibial axons remains unclear. However, grasshopper Sema 2a has been identified as a repellent of tibial pioneer axons (Isbister et al., 1999). It is expressed in a high distal to low promixal gradient in developing limb buds. When Sema 2a is disrupted, tibial axons extend distally in organ culture instead of projecting proximally. When both Sema 2a and Sema I are disrupted, phenotypes show a synergistic effect (Isbister et al., 1999).

Collapsin-1(Sema3A) was the first vertebrate semaphorin to be identified and the first semaphorin to clearly illustrate a role as a repellent of axons. It was isolated from membrane fractions of chick brains and found to induce collapse and paralysis of DRG growth cones, ergo the name collapsin (Luo et al., 1993). Around the same time, semaphorins were also identified in *Drosophila* (D-Sema I&II) and humans (human Sema III) (Kolodkin et al., 1993).

Drosophila Sema 1a, through its receptor Plex A, clearly acts as a repellent of axons (Hung-Hsiang Yu et al., 1998; Winberg et al., 1998). Motor axons avoid muscles expressing Sema 1a ectopically. Moreover, in *sema1a* mutants, motor axons stall at specific choice points, failing to defasciculate and reach their targets. *sema1a* mutants also reveal CNS defects as the lateralmost Fas II- positive longitudinal fascicle appears discontinuous, wavy, and projects abnormally (Hung-Hsiang Yu et al., 1998). Recently, it has been shown that Cyc76C, a receptor guanylyl cyclase, is required for the repulsive effects of Sema 1a on PNS and CNS axons (Ayoob et al., 2004). Therefore, Sema 1a is required for the precise arrangement of neuromuscular connectivity in the PNS as well as longitudinal connective formation in the CNS of the *Drosophila* embryo. Moreover, cGMP production within the growth cone is essential for these effects (Hung-Hsiang Yu et al., 1998; Ayoob et al., 2004).

The first proteins to be identified as receptors for semaphorins were the plexins (Comeau et al., 1998) and neuropilins (Chen et al., 1997; He and Tessier-Lavigne, 1997; Kolodkin et al., 1997).

In contrast to neuropilins, which have only been found in vertebrates, plexins—members of the immunoglobulin superfamily of molecules— are distributed widely in both vertebrates and invertebrates (Fujisawa, 2004). Nine plexins have been identified in vertebrates and these are subdivided into four classes (A to D) based on degree of evolutionary conservation. Like semaphorins, they contain a Sema domain at the NH2

terminal. The Sema domain is believed to interact with the rest of the cytoplasmic domain to silence the receptor when it is unbound to the ligand (Takahashi and Strittmatter, 2001). In addition, plexins have three PSI (plexins, semaphorins, and integrins) domains, three IPT (Ig-like, plexins, and transcription factors) domains, and a large conserved intracellular GTPase-binding domain (Kruger et al., 2005).

In *Drosophila melanogaster*, only two plexins have been identified (PlexA and PlexB). These are able to physically interact *in vivo* and signal through common downstream components such as MICAL (molecule associated with CasL), a multi-domain cytosolic protein essential for semaphorin-mediated repulsion (Terman et al., 2002; Ayoob et al., 2006). PlexA and PlexB serve both unique and common neuronal functions. Both are essential for intersegmental motor axons to defasciculate and find their targets (Ayoob et al., 2006). However, PlexA and PlexB are independently responsible for the formation of two distinct axon bundles within the embryonic CNS: PlexA, for the outermost longitudinal fascicle on either side of the midline, while PlexB is needed for the formation of the medial longitudinal fascicle (Ayoob et al., 2006). The distinct roles for these receptors in the CNS can be linked to their functional associations with different classes of semaphorins: PlexA functionally interacts with Sema-1a and Sema-1b (Winberg et al., 1998; Yu et al., 1998), while Plex B functionally interacts with Sema-2a (Ayoob et al., 2006).

Neuropilins are transmembrane proteins of ~900 amino acids with short cytoplasmic tails that lack intrinsic enzymatic activity. Additionally, they contain three extracellular domains (a1/a2 or CUB, b1/b2 or CF V/VIII, and c, containing the MAM domain) (He &

Tessier-Lavigne, 1997, Kolodkin et al., 1997). The a1/a2 and MAM domains have been implicated in protein-protein interactions (Bork & Beckmann, 1993).

Two neuropilins have been identified so far in vertebrates, Nrp-1 and Nrp-2 (Takagi et al., 1987; Chen et al., 1997). These interact with class 3 semaphorins—Nrp-1 with Sema3a and Nrp-2 with Sema3b, c, and f— to regulate PNS nerve fiber guidance and neural cell migration and accumulation into ganglia (Fujisawa, 2004). *nrp-1* mutant mice have a similar phenotype to *sema3a* mutants. Specifically, they display marked defasciculation of maxillary, mandibular, facial, and vagus nerve bundles, as well as abnormal projections of DRG nerves and specific cranial motor nerves (Kitsukawa et al., 1995; Kitsukawa et al., 1997; Taniguchi et al., 1997). *nrp-2* mutant mice display a similar PNS phenotype to Sema3F mutants but differ in some ways to *nrp-1* mutants. They lack trochlear nerve projections and display excessive defasciculation in the oculomotor, trigeminal and facial nerves, but show normal spinal nerve arborizations (Chen et al., 2000; Giger et al., 2000; Sahay et al., 2003). The difference in PNS phenotype between the neuropilin-1 and neuropilin-2 mutants suggests the cell-type specificity in chemorepulsive functions of neuropilin-mediated class 3 semaphorins (Fujisawa, 2004). Furthermore, it has been demonstrated that the association of neuropilins with semaphorins necessitates the formation of a co-receptor complex with class A plexins (Takahashi et al., 1999; Tamagnone et al., 1999).

Semaphorins and their receptors have also been implicated in the development of various other tissues outside of the NS. They manifest important roles in the immune response,

particularly in lymphocyte activation via CD100/Sema4D (Hall et al., 1996; Comeau et al., 1998; Shi et al., 2000; Billard et al., 2000; Elhabazi et al., 2001;Watanabe et al., 2001; Ishida et al., 2003) as well as in the development of the vascular system via competitive binding on NP/PlexD1 by VEGF and Sema3A,C (Miao et al., 1999;Brambilla et al., 2000; Feiner et al., 2001;Gitler et al., 2004) and having both stimulatory (Sema 3C,F) and inhibitory (Sema A) effects via different class 3 semaphorins in branching morphogenesis during lung development (Ito et al., 2000; Kagoshima and Ito, 2001).

1.2b.2 Slit Pathway

Slit is another important family of chemorepellents (Guan and Rao, 2003; Govek et al., 2007). Slit is a large extracellular matrix protein(~190-kDa) expressed primarily by ventral midline cells, where it promotes crossing of commissural axons and their projection onto the contralateral side of the CNS while preventing crossing of ipsilaterally projecting axons (Dickson, 2002; Huber et al., 2003). Along with its receptor (Roundabout) Robo, it was named for the phenotypes of *Drosophila* mutants in which these genes were first identified (Seeger et al., 1993; Kidd et al., 1999). Slit homologues have since been found in *C. elegans* and many vertebrate species, from amphibians, fishes, birds to mammals. A single Slit has been isolated in *Drosophila*, and *C. elegans*, whereas there are three slit genes (slit1-slit3) and four Robo receptors (Robo1, Robo2, Robo3/Rig-1, and Robo4/magic Roundabout) in mammals (Figure 6B).

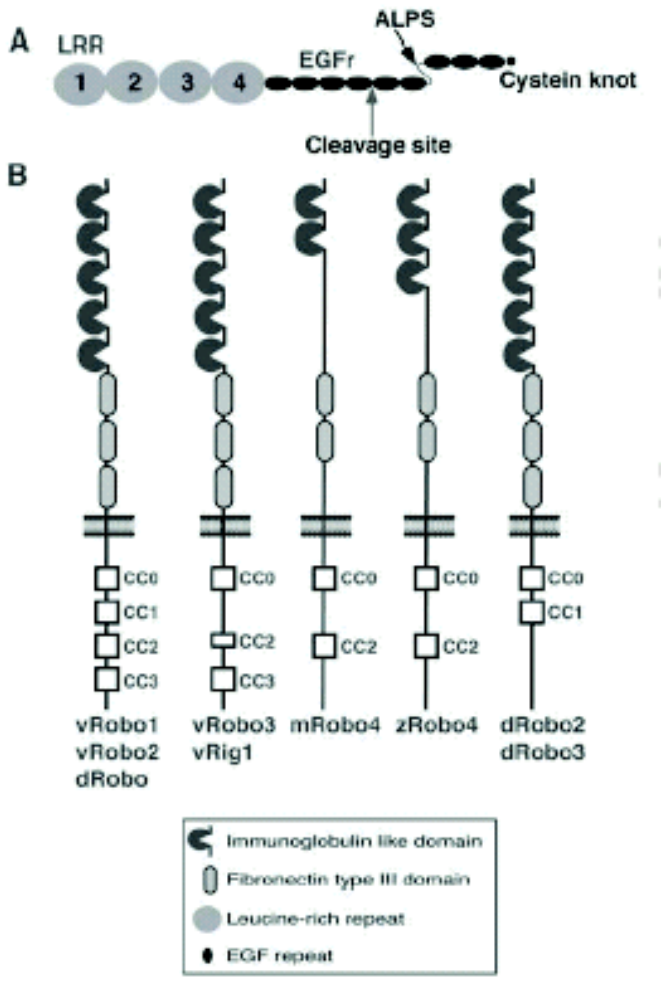

Figure 6. Conserved Slit Family.
A) Structure of the slit proteins. B) Diagrammatic comparison of the structure of Robo receptors in invertebrate and vertebrate species. v: vertebrate; d: Drosophila; z: zebrafish. ALPS: domain found in Agrin, Laminin, Perlecan and Slit.
(Eurekah Bioscience Collection Chapters taken from the Eurekah Bioscience database. Eurekah.com and Landes Bioscience. 2003)

Robo was first identified as part of a screen for mutants affecting midline crossing of commissural axons in the developing *Drosophila* embryo (Seeger et al., 1993). Robo proteins are expressed on the surface of growing axons (Morlot et al., 2007). They have five Ig-like domains followed by three fibronectin type III (FNIII) repeats, a single-pass transmembrane domain and a long intracellular tail containing up to four conserved cytoplasmic motifs, CC0-CC3, with no obvious catalytic domains (Garbe and Bashaw,

2004). The first two Ig domains are the most highly conserved portion and are required for Slit binding. In *robo* mutants, commissures fuse together, become fuzzy, and thicken while the longitudinal fiber tracts are reduced. Additionally, axons that normally do not cross or recross the midline, do so.

Three Robo proteins have been identified in *Drosophila.* Here, Robo1 and Robo2 cooperate during early stages of axon outgrowth to transmit the short-range signal of Slit mediating midline crossing while Robo2 and Robo3 participate during later stages to communicate the long-range signal of Slit specifying the lateral distribution of longitudinal axons with respect to the midline (Rajagopalan et al., 2000b; Simpson et al., 2000a/b). In situ hybridization has provided insight into when Robo receptors are expressed (Simpson et al., 2000): *robo1* begins to be expressed at embryonic stage10. *robo2* first appears at stage 11 and becomes restricted to a smaller subset of neurons by stage 15. *robo3* is first spotted late in stage 13 and is limited to fewer neurons.

Along the midline, Robo1 mediates repulsion of axon crossing. Robo protein levels are low in the growth cones of commissural axons crossing the midline and increase once they have crossed over (Kidd et al., 1998) The specific role of Robo1 in preventing midline crossing can be attributed to two major factors. Firstly, it is attributed to its unique pattern of expression as neither Robo2 nor Robo3 can substitute for Robo1 in the repulsion of axons at the midline. For example, expressing *robo2* or *robo3* at the *robo1* locus via ends-in-homologous recombination results in *robo1* null-type mutant phenotypes: pCC (ipsilateral) axons incorrectly cross the midline (Spitzweck et al., 2010). Secondly, it is attributed to particular structural features of its protein. For

instance, CC1 and CC2 motifs are responsible for the midline repulsive role of Robo1 as a Robo1 construct with a Robo3 CC2 domain was not able to rescue *robo1* excessive crossing mutant phenotype but a Robo3 construct bearing a Robo1 CC2 or CC1 motif did (Spitzweck et al., 2010). In addition, the cleavage of Robo1 ectodomain by transmembrane metalloprotease kuzbananian (Kuz) is also necessary for the repulsive signaling activity of Robo1 at the midline (Coleman et al., 2010). For instance, ectopic expression of an uncleavable form of the Robo1 receptor(Robo1-U) does not effectively rescue *robo1* mutants as medial-most fascicles still cross the midline in many segments (Coleman et al., 2010).

Most recently, evidence points to an attractive role for the Robo2 receptor at the midline. Moderate levels of Robo2 overexpression lead to thickened commissures and ectopic midline crossing (Evans and Bashaw, 2010). Moreover, Robo2 proteins that promote midline crossing are expressed strongly on crossing axons (Evans and Bashaw, 2010). Furthermore, in *NetAB, robo2* double mutants, there is a significant increase in commissural disruption versus *NetAB* single mutants (Spitzweck et al., 2010). This ability of Robo2 is dependent on its ectodomain (Spitzweck et al., 2010; Evans and Bashaw, 2010). It can be pinpointed to its Ig2 domain, as a Robo2 construct that has had its Ig2 domain swapped for that of Robo1 is unable to promote midline crossing. Conversely, a Robo1 construct that has its Ig2 domain replaced with that of Robo2 inherits its midline crossing activity. (Evans and Bashaw, 2010)

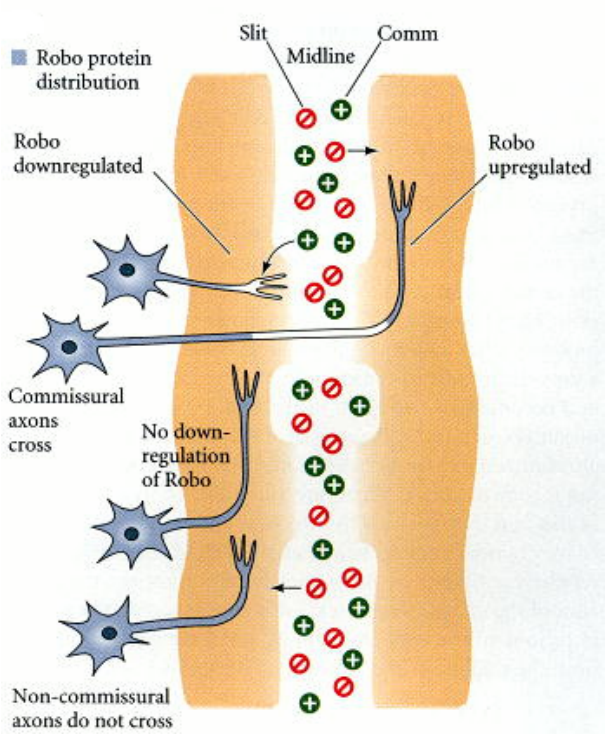

Figure 7. Robo and Slit Production at the Midline. Robo proteins are expressed at the axonal surface. For commissural axons, Robo protein expression is downregulated upon crossing the midline and upregulated once crossing has occurred to prevent recrossing. For ipsilateral axons, Robo protein expression is not downregulated. Slit is produced at the midline and is activated upon Robo binding (Thomas, 1998).

But how is Robo downregulated in commissural axons once they cross the midline? *Comm* was discovered during the same large-scale screen for mutations that influence CNS development in Drosophila (Seeger et al., 1993) and it encodes a 370 amino acid long transmembrane protein (Tear et al., 1996). Fluorescent in situ hybridization has shown that *comm* is spatially confined to commissural axons and temporally correlated with midline crossing as *comm* expression is turned off once axons cross the midline (Keleman et al., 2002). In mutations of *comm,* growth cones that normally extend across the midline fail to do so (Seeger et al., 1993). In *comm robo* double mutants, the phenotype is robo mutant-like as ipsilateral axons cross and commissural axons recross. Thus, *comm* serves to suppress Robo-mediated repulsion (Seeger et al., 1993).

Furthermore, in *comm* gain-of-function mutants, Robo protein expression drops to low or undetectable levels (Kidd et al., 1998b).

Then how does Comm downregulate Robo? It has been shown that Comm colocalizes with Robo and recruits it to late endosomes and lysosomes by sorting it directly from the trans-Golgi network (Keleman et al., 2002). In fact, direct visualization of Robo-GFP trafficking *in vivo* shows that Comm blocks Robo from traveling down the axon and reaching the growth cone (Keleman et al., 2005).

Once Comm was established as the switch that controls midline crossing (Keleman et al., 2002), it remained to be seen how *comm* expression is turned off and on during midline axon crossing. Most recently, it has been shown that *comm* is transcriptionally activated by *frazzled in* neurons as they cross the midline (Yang et al., 2009).Firstly, removing one copy of *comm* in hypomorphic *fra* mutants (fra^4/fra^6; $comm^{e39}/+$) exacerbates the commissural defects as shown by thin or missing commissures in many segments as well as increased instances of failure to cross in eagle commissural neurons (Yang et al., 2009). Secondly, *comm* mRNA expression, measured in individual eagle neurons as relative fluorescent intensity of *in situ* probes, is reduced between 1.7-2.4X in *frazzled* mutants. Thirdly, overexpressing *frazzled* via UASFra-myc in a subset of apterous (ipsilateral) neurons, which normally do not express *comm*, induced ectopic *comm* mRNA expression. What's more, it caused these ipsilateral neurons to cross the midline often. Lastly, expressing UASComm in eagle neurons of *frazzled* mutants partially rescues guidance defects. In summary, *frazzled* is both necessary and sufficient for

comm mRNA expression in commissural neurons and elucidates how crossing is ensured and premature repulsive responses are prevented at the midline (Yang et al., 2009).

Along longitudinal tracks, it has been the belief for over a decade that Robo receptors form a combinatorial code: Robo 1 is distributed across the entire width, Robo 3 is expressed in the lateral 2/3's, and Robo2 is expressed in the outermost 1/3 (Rajagopalan et al., 2000b) (Figure 8). In *robo 2* and *3* loss-of-function mutants, there is a shift of axons closer to the midline: In *robo 2* null mutants, the outermost fascicle merges with the middle one while in *robo3* nulls, the middle fascicle merges with the innermost fascicle with thinning of the outermost fascicle. The converse also holds as either *robo2* or *robo3* gain-of-function mutant axons follow a more lateral path. Moreover, in double gain-of-function mutants, axons shift even further laterally. So in the Robo Code, the differential distribution of Robo receptors determines how axons will be patterned longitudinally.

Most recently, new findings have raised some doubt into the combinatorial Robo code that controls longitudinal pathways. For instance, when *robo2 and robo3* are separately misexpressed in apterous neurons, these follow a more lateral pathway further from the midline. Ectopically expressing *robo2* in *robo1*, *robo3*, and *robo3/robo1* double mutant backgrounds or *robo3* in *robo1* and *robo2* mutant backgrounds, still results in the lateral redirection (Evans and Bashaw, 2010). Similarly, targeting the coding region of *robo2* and *robo1* into the *robo3* locus by ends-in-homologous recombination, resulted in normal formation of longitudinal fascicles (Spitzweck et al.,2010) These results show that it is

the individual expression of each protein rather than the combinatorial expression that determines longitudinal positioning of axons at the midline (Evans and Bashaw,2010).

If this is the case, then what determines the roles the different receptors play in positioning axons along longitudinal pathways? Recent evidence points to the Robo family immunoglobulin domains as being the essential factors. In apterous neurons ectopically expressing a Robo 2 construct, whose Ig1-3 domains were swapped with those of Robo1, disrupts its lateral positioning activity. Conversely, a Robo1 construct whose Ig1 or Ig3 domains were replaced by those of Robo2, shows similar lateral positioning activity to that of full-length Robo2 (Evans and Bashaw, 2010).

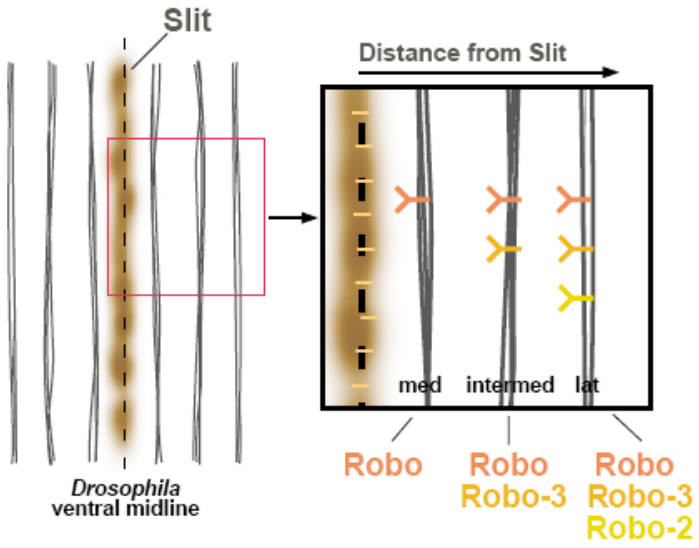

Figure 8. The Robo Code at the Drosophila Ventral Midline. Robo1 alone guides axons along longitudinal axons in the medial fascicle. Robo1 and Robo3 control the intermediate fascicle. Finally, all three Robos help guide axons along the lateral-most fascicle (Yu and Bargman, 2001)

In *C.elegans,* Robo function depends largely on its regulation of transport to the plasma membrane. A case for its positive regulation by a downstream component has been shown. VAB-8L, a kinesin-related Rac GTPase, is responsible for promoting the

posterior migration of growth cones during CNS development (Wolf et al., 1998). During this process, it is able to enhance the Robo response to Slit (Watari-Goshima et al., 2007). This finding is surprising as RacGTPases are normally associated with downstream signaling of guidance receptors. VAB-8L most likely increases the activity of SAX-3 by positively regulating its concentration at the cell surface. This may be achieved directly, by promoting its transport to the cell surface or indirectly, by inhibiting its endocytosis. Additionally, this increase in SAX3 levels necessitates direct protein interactions between the cytoplasmic domains of VAB-8L and SAX-3 and spectrin repeats in the N-terminal domain RhoGEF-1 of UNC73/Trio (Watari-Goshima et al., 2007).

In contrast to VAB-8L's ability to positively regulate its orientation, RPM-1 negatively regulates SAX-3-mediated axon outgrowth in *C. elegans* (Li et al., 2008). For instance, when *rpm-1* is ectopically expressed in PLM axons, their extension is significantly shorter—a phenotype which is also observed in *sax-3* loss-of-function mutants. Conversely, *rpm-1* loss-of-function mutants display a PLM overextension phenotype. Notably, this phenotype is reduced in *rpm-1; sax-3* double mutants. RPM-1 likely regulates axon guidance and termination by controlling the trafficking of SAX-3 receptors to cell membranes. For example, in *rpm-1* loss of function mutants, the expression of a SAX-3::GFP fusion protein becomes restricted to the plasma membrane as opposed to being concentrated in the cytoplasm of the wild type (Li et al., 2008). Furthermore, it has been shown that when regulating axon guidance of PLM axons, RPM-1 functions through the GLO-4 pathway. In *glo-4* mutants, the Sax-3::GFP signal is more widely detected, just like in *rpm-1* mutants. This is important as it has been shown

that through the GLO-4 pathway, RPM-1 promotes vesicular trafficking (Grill et al., 2007). So in summary, RPM-1 likely regulates axon outgrowth that affects axon guidance and termination by controlling the trafficking of SAX-3 receptors to cell membranes (Li et al., 2008).

Subsequent experiments in *Drosophila* proved that Slit was the midline ligand for the Robo receptor (Kidd et al., 1999). It is a large extracellular protein containing four N-terminal leucine rich repeats (LRRs)— which are flanked by conserved amino and carboxy-terminal sequences— a stretch of seven to nine EGF repeats, an Agrin-Laminin-Perlecan-Slit (ALPS) conserved spacer motif, and a C- terminal cysteine knot (Brose et al., 1999;Dickson and Gilestro, 2006) (figure 6A). In *Drosophila*, a single Slit protein (Slit1), which is secreted by neuronal cells in the midline, has been identified. In *slit* loss-of-function mutant embryos, pCC (ipsilateral) and SP1 (commissural) axons freely enter the midline like in *robo* loss-of-function mutants. However, they never leave it, instead choosing to fasciculate into a single tract (Kidd et al., 1999). Moreover, *slit* and *robo1* transheterozygotes display a dosage-dependent genetic interaction, establishing that they are in a common molecular pathway (Kidd et al., 1999). Lastly, cell overlay binding assays show that Slit binds Robo directly with a high degree of specificity (Brose et al., 1999). These interactions are evolutionarily conserved— further cementing Slit as the Robo ligand.

The Slit-Robo interaction is mediated by the second LRR domain of Slit and the first two Ig domains of Robo. Although *in vitro* pull down assays have shown that Slit-Robo

binding requires both domains (Liu et al., 2004), it has recently been demonstrated that the Ig1 domain is responsible for the primary interaction with Slit (Morlot et al., 2007). Firstly, *in vitro* surface plasmon resonance spectroscopy (SPR) has shown that when compared to the binding ability of both domains together, Ig1 has a relative binding ability that is 10 times that of Ig2. The crystal structure of Ig1 shows that this binding involves electrostatic and hydrophobic regions within Ig1 and the concave surface of Slit. Secondly, sequence alignment of metazoan homologues reveals that Slit-binding residues in Ig1 are highly conserved in other family members while those in Ig2 show high divergence.

Three Slits have been identified in mammals (Slit1, -2, -3) which share a common domain structure as well a high sequence similarity with *Drosophila* Slit (Brose et al., 1999). Like in *Drosophila*, mammalian Slit isoforms selectively bind to Robo receptors (Brose et al., 1999; Long et al., 2004), which is necessary for its repulsive axon guidance effects at the floor plate. They differ from *Drosophila* by an additional LRR in the LRR-3 and two additional EGF repeats. Like *Drosophila* Slit, they are all expressed by cells at the ventral midline. Slit1 is expressed broadly throughout the floor plate while Slit 2 is restricted to the medial and basal-most region of the floor plate. Slit3 is expressed at levels significantly lower than both Slit1 and Slit2 (Brose et al., 1999). The importance of having all three isoforms present at the floor plate is evidenced by the highly penetrant phenotypes of *slit* triple mutants: Commissural axons stall at the floor plate or recross it (Long et al., 2004). On the other hand, *slit* double mutants (i.e. Slit1; Slit2) display no obvious commissural axon guidance defects (Plump et al., 2002). Most recently, it has

been shown that deubiquinating enzyme USP33 is required for Slit responsiveness of commissural axons at the floor plate as siUSP33 knockdown abolishes Slit-induced growth cone collapse *in vitro* (Yuasa-Kawada et al., 2009). Moreover, siUSP33 - electroporated spinal cords show commissural axons stalling at the midline— a phenotype similar to *slit* triple mutants (Yuasa-Kawada et al., 2009).

An additional receptor has been identified for Slit (Fujisawa et al., 2007). Enhancer of ventral-axon guidance defects of unc40 mutants (Eva-1) is a transmembrane protein 461 amino acids long, that most likely acts as a co-receptor with SAX-3/Robo for SLT-1/Slit to repel AVM and PVM pioneer axons toward the ventral nerve cord. In *eva-1* mutants, AVM (anterior ventral microtubule) axons—which normally extend to the VNC (ventral nerve cord) before following a path toward the head—travel from the cell body toward the head without the turn toward the VNC (Fujisawa et al., 2007).

The debate over whether Slit/Robo signaling inhibits axon guidance directly or indirectly has been mired in controversy. In the case of direct repulsion, its primary role would be to repel axons at the midline. It would suggest that guidance decisions are determined by a balance of attractive versus repulsive signals at the growth cone. In the case of indirect repulsion, the major role of Slit/Robo signaling is to inhibit Netrin- mediated attraction (Bhat 2005; Hiramoto 2006). It would suggest that the activation of one receptor inhibits another. The initial study by the Bhat laboratory supported the indirect approach: It was shown that Slit-Robo signaling specifies lateral positioning of longitudinal axons by inhibiting Netrin-frazzled mediated attraction (Bhat, 2005). *slit/robo; fra* double mutants

had a *fra*-like appearance and *robo; net* double mutants looked *net*-like. A Robo/Fra chimeric protein caused midline crossing of longitudinal tracts and recrossing of commissural tracts. When this chimeric protein was expressed in a *net* mutant background (UAS-$Robo_e$-Fra_i/elav-GAL4; UAS-$Robo_eFra_i$/+; net/Y), the embryos had a *netrin* mutant phenotype. This led to the conclusion that the inhibition of Netrin attraction is epistatic to Robo repulsion (Bhat, 2005).

However, the work of the Bashaw laboratory contradicted the findings of the Bhat laboratory and supported the direct approach (Garbe and Bashaw, 2007). Using Bhat's stocks, Bashaw and coworkers repeated Bhat's experiment with the Robo/Frazzled chimera ($Robo_e$-Fra_i-Myc). In embryos carrying this protein, many Fas II axons ectopically attracted across the midline in response to Slit. Netrin mutants overexpressing $Robo_e$-Fra_i-Myc still displayed inappropriate crossing. Additionally, expressing Robo in *fra, robo* double mutants not only repelled axons at the midline in absence of Frazzled, but further intensified the loss of attraction associated with *fra* mutants (Grabe and Bashaw, 2007). Furthermore in apterous (ipsilateral) and eagle pioneering neurons, axons of *fra,robo* double mutants still crossed and recrossed—indicating that Robo-mediated midline repulsion is independent of whether Frazzled is there or not. Thus, Robo plays a direct role in axonal repulsion. Even if Robo silencing of Frazzled occurs at the *Drosophila* midline, these results indicate that Robo repulsion on its own is sufficient to prevent recrossing. Nevertheless, one cannot discount the possibility that the silencing of other attractive guidance cue pathways may be essential (Grabe and Bashaw, 2007).

Upon a repeat of their original experiments, the Bhat laboratory later rescinded their initial claims. They indicated they had incorrectly recorded a gene that was called "*fra-like*" as *frazzled* and that their use of balancers may have caused a variety in penetrance (Bhat, 2007). When redoing the experiments, the *robo; fra* double mutants were predominantly *robo*-like but results were mixed in other cases, leading them to proclaim that the picture in Slit-Robo signaling is so complicated that one can't decisively say one way or another whether the repulsive nature of Robo signaling is direct or indirect. Taking these studies together, one can conclude that the Robo-Slit signaling pathway does repel axons independent of silencing of Frazzled.

1.2b.3 Ephrin Pathway

Ephrins and Eph receptors comprise a family of guidance molecules most known for their axon-repulsive role in establishing topographic maps in the visual system (Cutforth and Harrison, 2002; Guan and Rao, 2003). Eph receptors and Ephrins are able to initiate bidirectional signaling, meaning that the signal is initiated from the ligand or receptor-expressing cell (Holland et al., 1996; Kullander and Klein 2002; Davy and Soriano, 2005).The Ephrins are distributed in a graded fashion in the optic tectum (or superior colliculus) and the lateral geniculate nucleus, while the Eph receptors are found in a complementary gradient in the retina.

Eph receptors belong to the single transmembrane domain tyrosine receptor kinase family which is comprised of 16 identified members in mammals (ten EphA and six EphB), and directly transduces a signal from Ephrins. The Ephrins, of which 9 have been identified in

mammals, are cell adhesion-like molecules that can be either transmembrane or GPI-anchored proteins. In *Drosophila melanogaster,* only one Eph receptor and one Ephrin have been identified while one Eph receptor and 4 Ephrins have been discovered in *C. elegans* (Davy and Soriano, 2005). Ephrins can be further subdivided into Ephrin A (GPI-anchored) or Ephrin B (transmembrane) and Eph receptors can be further subdivided into Eph-A or Eph-B (Huber et al., 2003; Nakamoto et al., 2004; Pasquale, 2005; Chilton, 2006). Disruption of the genes for the Ephrins or their receptors results in subtle disruptions in the topographic organization of the retino-collicular or retino-thalamic projection.

The optic chiasm is the choice point where retinal ganglion cell (RGC) axons cross from the eye to the ventral midline of the brain (Mann et al., 2004). Studies in *Xenopus* and mice have shown that Ephrin-B is localized at the optic chiasm, where it repels Eph B-expressing optical nerves to route ipsilateraly (Nakagawa et al., 2000; Mann et al., 2002; Williams et al, 2003). This mechanism seems to also be applicable to vertebrates as Ephrin B cannot be detected at the ventral midline of the diencephalon of chick embryos, which lack permanent ipsilateral connections (Nakawaga et al., 2000). Gain and loss-of-function experiments in mice have indicated that zinc-finger transcription factor Zic 2, is expressed exclusively in RGCs and is required for axons to be repelled at the chiasm and to project ipsilaterally (Herrera et al., 2003).

In the optic tectum, retinal ganglion cell (RGC) axon terminals are arrayed in a topographic order. The nasal-temporal axis of the retina maps along the anterior-posterior

axis of the optic tectum, where it is mediated through EphrinA/EphA in a repulsive manner (Mann et al., 2004; Chilton, 2006) (Figure 9A). Both Ephrin-A2 and Ephrin-A5 are maximally expressed in the posterior tectum while Eph A3 is maximally expressed in the temporal retina (Nakamura, 2001). Therefore, RGC temporal axons with a high level of Eph-A3 receptors are repelled by Ephrin-A2 and Ephrin-A5, whereas RGC nasal axons with low Eph-A3 receptor levels are permitted to cross and innervate the posterior tectum. Temporal axons terminate normally in *ephrin-A2* or *ephrin-A5* single mutant mice and in half of the mice, an additional more posterior arborization can be seen (Frisen et al., 1998; Feldheim et al., 2000). In one study (Frisen et al., 1998), *ephrin A5* single mutants actually overshoot the tectum into the inferior colliculus. Nasal axons terminate normally in *ephrinA2* single mutants while presenting an additional anterior arborization in most *ephrin A5* single mutant mice (Feldheim et al., 2000). *Ephrin A2/A5* double mutant mice show a synergistic phenotype with A-P organization being almost but not completely lost (Feldheim et al., 2000). The phenotype of *ephrin A2/A3/A5* triply mutant mice is even more severe than that of *ephrin A2/A5* double mutants (Pfeiffenberger et al., 2006), showing that all three ligands are critical for the proper organization of the target region.

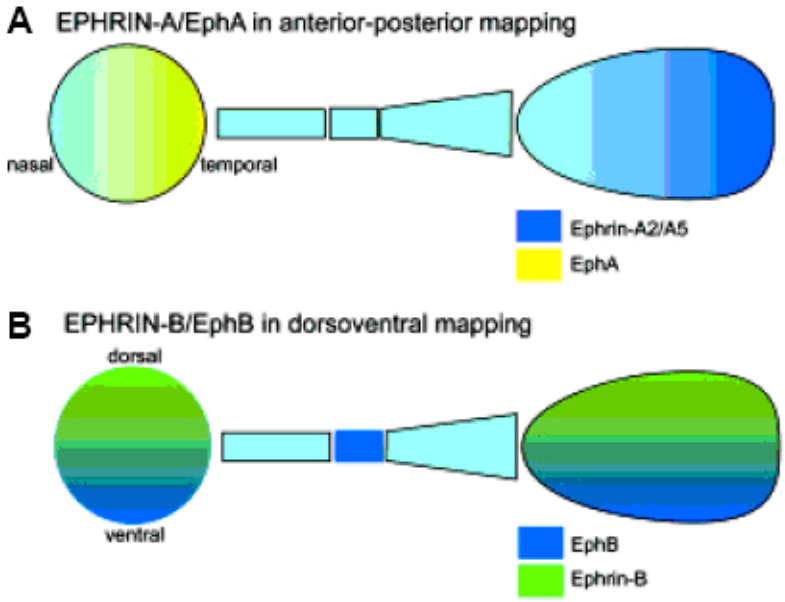

Figure 9. Summary of Distribution and Role of A- and B-Type Ephrins and Receptors in the Developing Visual Pathway.
Eye: dorsoventral axis is top to bottom, nasotemporal axis left to right. Tectum: mediolateral (mammals) and dorsoventral (frogs) is top to bottom, anterior-posterior axis is left to right (Mann et al., 2004).

Some recent experiments point to a possible attractive role for Ephrin A ligands. *In vitro* studies have shown that Ephrin-A2 can actually promote retinal axon outgrowth at low concentrations (Hansen et al., 2004) while Ephrin- A5 induces an axon turning response that is substratum-dependent: repulsive on a fibronectin substrate while attractive on laminin (Weinl et al., 2003). So Ephrin-A ligands might not regulate topographic mapping in the visual system exclusively via repulsive mechanisms (Pasquale, 2005).

The dorsal-ventral retinal axis maps along the ventral-dorsal tectal axis where it is mediated by Ephrin B/ EphB receptors in an attractive manner (Mann et al., 2004) (Figure 9B). The EphB receptor is expressed in a high-ventral to low-dorsal gradient in

the retina while Ephrin-B is expressed in a high-dorsal to low-ventral gradient in the tectum. Ephrin-B is not expressed at the chiasm until metamorphosis which coincides with the initiation of the ipsilateral projection (Mann et al., 2004). The cytoplasmic tail of Ephrin-B is necessary for this regulation (Mann et al., 2002). Additionally, *in situ* hybridization studies of *Xenopus* embryos have indicated that translational regulation might control the levels of EphB and Ephrin-B protein expression at the growth cone (Brittis et al., 2002).

Eph receptors and Ephrins have been found to regulate integrin functions (Nakamoto et al., 2004). For example, the binding of Ephrin B1 to Eph B1 and expression of EphA8 activates integrins while the activation of EphB2 by Ephrin B1 has an inhibitory effect on integrins (Kullander and Klein, 2002). Some differing reports have suggested that Eph-Ephrin signaling can depend on the expression level of a protein. One report indicates that activation of EphA2 by Ephrin A1 suppresses integrin signaling and subsequently promotes dephosphorylation of FAK (Kullander and Klein, 2002) while another shows it stimulates integrin signaling and promotes FAK phosphorylation (Carter et al., 2002).

1.2b.4 Netrin Pathway

The word Netrin comes from the Sanskrit language, where it means “to guide”. In actuality, Netrins are bifunctional: chemoattractive for some neurons and chemorepellent for others, as well as being able act at long or short range. Netrins act during development and control a wide range of outgrowing axons and migrating neurons.

The secondary structure of the family is highly conserved in all species. All Netrins are structurally related to the short arms of the ECM protein Laminin and contain the Laminin VI and V domains (Barallobre et al., 2005) (Figure 10). They also contain positively charged C-terminal domains, termed NTR modules. These domains show the greatest variation between species and serve as binding sites for components of the ECM or cell surface. In vertebrates, four secreted Netrins have been identified: Netrin-1 in chickens, mice, zebrafish and humans; Netrin-2 in chickens; Netrin-3 in mice and humans; and Netrin-4 in mice and humans. In invertebrates, three secreted netrins have been identified: UNC-6 in *C. elegans* and Netrin-A and B in *Drosophila*.

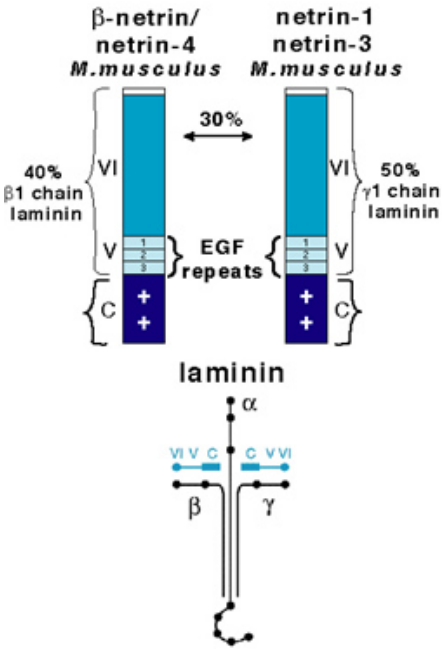

Figure 10. Scheme Illustrating the Structure of Laminin and Netrins and the Homology Between Them. Classic Netrins (Netrin-1, -2 and -3) and Netrins-G present regions with high similarity with the V and VI domains of the Laminin gamma chain. In contrast, Netrin-4/h is closely related to domains V and VI of the Laminin Beta Chain. (http://bio.research.ucsc.edu/people/hinck/netrinoverview.html)

Netrins act at a variety of sites in the developing vertebrate nervous system where axons must choose whether to cross the midline or remain ipsilateral. The first evidence of

Netrin's chemotropic ability came from cell culture experiments in the developing spinal cord (Serafini et al., 1994). When dorsal spinal cord explants from chick embryos are plated onto collagen gels, the presence of floor plate cells near them promotes the outgrowth of commissural axons. Serafini and his co-workers took fractions of embryonic chick brain homogenate and tested them to see if any of the proteins therein mimicked this activity. This process resulted in the identification of Netrins.

Subsequent experiments confirmed the role of Netrins in directing the growth of commissural axons crossing the floor plate at the midline. When Netrin genes are inactivated in mice by homologous recombination, the midline crossing of commissural axons is disrupted. Netrins and their receptors have also been implicated in midline crossing at a variety of other sites in the central nervous system, including the optic chiasm, the corpus callosum, and the decussation of the trochlear nerve. Thus, these and other chemoattractant signals help organize the major crossed pathways in the brain.

The attraction and repulsion responses produced by Netrin-1 are a result of its interaction with two receptor families: Deleted in Colorectal Cancer (DCC) and UNC-5. Both families belong to the immunoglobulin (Ig) superfamily of receptors and cross the membrane only once.

In vertebrates, the DCC family has two members, DCC and neogenin, that consist of four Ig domains, six extracellular fibronectin type III repeats, and three cytoplasmic domains (P1, P2 and P3) that mediate interactions with other receptors. The UNC5H family has

four members, UNC5H1-H4, that contain two Ig and two thrombospondin type I (TSP) domains extracellularly and ZU-5, DCC binding and C-terminal death domains (DD) intracellularly (Barallobre et al., 2005). When DCC homodimerizes, Netrin transmits an attractive signal (Stein et al., 2001; Keleman and Dickson, 2001; Huber et al., 2003; Govek et al., 2005; Hall and Lalli, 2010). With UNC5H alone or bound to a yet identified receptor X, Netrin transmits short range repulsive signals (Keleman and Dickson, 2001; Round and Stein, 2007). When DCC and UNC5H form a heterodimer, Netrin transmits a long range repulsive signal (Hong et al., 1999; Keleman and Dickson, 2001; Guan and Rao, 2003; Govek et al., 2007; Hall and Lalli, 2010). So it is believed that DCC strengthens the UNC5 response (Figure 11).

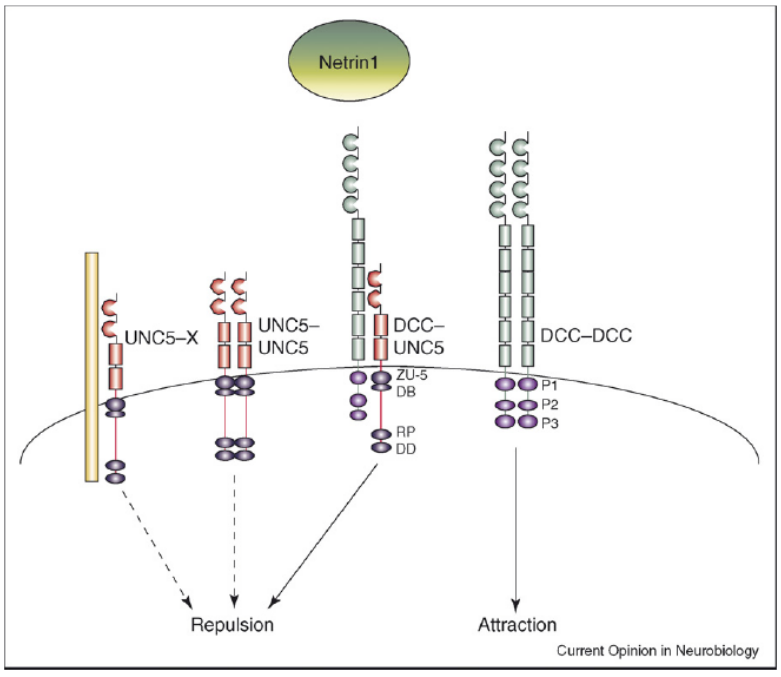

Figure 11. Netrin and its Receptors.
Netrin transmits an attractive signal through DCC homodimers and short range repulsive signals through UNC5 homodimers or an interaction between UNC5 and a yet to be determined receptor. When the two receptors form a complex, Netrin transmits a long range repulsive signal (Round and Stein, 2007).

In *Drosophila,* Netrin-A and Netrin-B are expressed by midline cells of the CNS and by specific muscles in the periphery. The DCC family receptor that interacts with Netrin is Frazzled (Kolodziej et al. 1996). Netrins attract commissural and motor axons expressing *frazzled.* *Frazzled* is expressed on axons in the embryonic CNS, on motor axons in the periphery, and on the epidermis and gut epithelium. The phenotypes of *frazzled* null mutants strongly resemble those of a deletion in *Drosophila* Netrin-A and Netrin-B, with defects in CNS and motor axon guidance (Kolodziej et al. 1996). In photoreceptor axons, *frazzled* is not required in photoreceptor neurons but in their targets (lamina) (Gong et al., 1999). However, it has been shown that *frazzled* can be expressed in dMP2 neurons, where it captures Netrin and presents it for recognition by other receptors (Hiramoto et al., 2000). Its cytoplasmic domain is both necessary and sufficient for proper localization. The UNC5 receptor is a repulsive Netrin receptor that contributes to motor axon guidance. Analogous to the situation in vertebrates, ectopic expression of UNC5 on CNS axons can elicit short-range repulsion from the midline. Meanwhile, long-range repulsion requires Frazzled (Keleman and Dickson, 2001).

In *C. elegans*, the DCC family receptor that interacts with Netrin is UNC-40. It is required primarily for ventral migrations directed toward UNC-6 (Netrin homolog), but also participates in many dorsal migrations away from UNC-6. UNC-5, in contrast, is required only for dorsal migrations away from UNC-6 (Hamelin et al., 1993).

1.3 Signal Transduction by Rho GTPases

1.3a small GTPases

Small GTPases are small (20-25 kD) proteins that relay extracellular cues to cytoplasmic signaling cascades by cycling between inactive GDP-bound and active GTP-bound forms. They regulate a wide range of processes in the cell, including growth, morphogenesis, membrane transport, cell motility and organization of the cytoskeleton, and cell polarity (Jaffe and Hall 2002).

1.3b Rho subfamily GTPases

Rho(Ras- homologous) GTPases form a subfamily of the Ras superfamily of small GTPases (Negishi and Katoh, 2002; O'Donnell et al., 2009; Hall and Lalli, 2010). This subfamily consists of some 21 genes in humans, encoding at least 23 signaling proteins. They were originally found during a search for proteins homologous to Ras proto-oncoprotein (Satoh et al. 1992). Of these, only Rho (isoforms A, B, and C), Rac (isoforms 1, 2, 3) and Cdc42 have been studied in detail.

Rho GTPase function is conserved in evolution, with members identified in mammals, yeast, plants, slime mold, worms, and flies. *C. elegans* and *Drosophila* have homologues of all three small GTPases, and downstream effector proteins are also conserved. Rac is absent from yeast, but both the Cdc42 and RhoA (Rho1) homologues are present.

In neurons, Rho GTPases coordinate the spatial and temporal changes in the actin cytoskeleton that lead to cellular movement (Nobes and Hall, 1995). Early work helped

shape a model for the mode of action of Rho GTPases—that the activation of Cdc42 and Rac1 stimulates axonal growth while the activation of RhoA inhibits growth or induces growth cone retraction and collapse (Negishi and Katoh, 2002; Govek et al., 2007;O'Donnell et al., 2009) (Figure 12). In this model, each is thought to control the formation of a distinct cytoskeletal element. For example, Rho stimulates the bundling of actin and myosin filaments into stress fibers and focal adhesions (Ridley and Hall, 1992; Hall 1998). Rac reorganizes actin at the leading edge of the growth cone to form lamellipodia (Ridley et al., 1992). Finally, Cdc42 is associated with the formation of another group of actin-rich structures, filopodia (Nobes and Hall, 1995; Kozma et al., 1995).

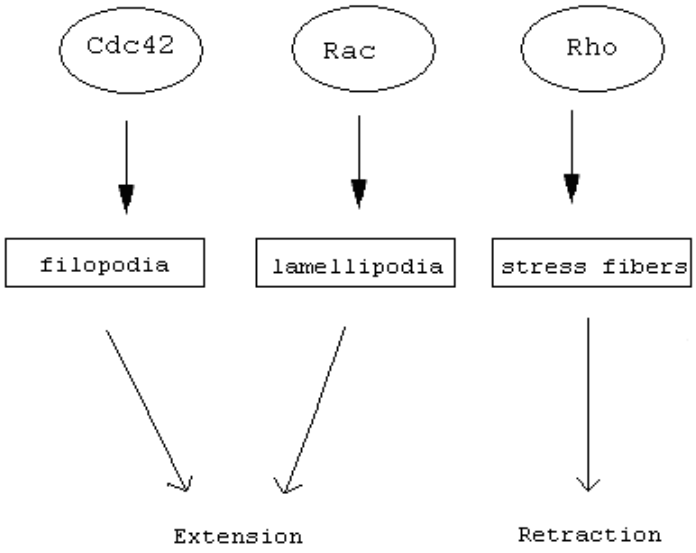

Figure 12. Extracellular Signals Cause Membrane Extension or Retraction by Regulating the Activity of the Rho GTPases.
Rac and Cdc42 activity typically leads to filopodia/ lamellipodia formation and membrane extension while Rho activity leads to stress fiber formation and membrane retraction.

1.3b.1. Rac

Rac small GTPases of the Rho subfamily control the structure and dynamics of the actin cytoskeleton (Hall, 1998). For example, microinjection of Rac1 recombinant proteins into fibroblast cells promotes increased actin polymerization, which is needed for the formation of lamellipodia and membrane ruffles (Ridley et al., 1992). This increase is inhibited in Rac1 mutants.

There are three Rac genes in the C. elegans genome: *ced-10, mig-2 and rac-2.* It has been shown that these serve redundant, non-cell autonomous functions in axon guidance, outgrowth, fasciculation in CAN and PED neurons with *ced-10* and *mig-2* having greater roles than *rac-2* (Lundquist et al., 2001). Increasing severity of defects in double and triple mutants suggests that complete removal of Rac activity results in complete failure of axon outgrowth and cell migration. It has also been demonstrated that the Nck-interacting kinase (NIK kinase) MIG-15 acts in pathways defined by these three Rac GTPases to control axon pathfinding (Shakir et al., 2006).

In both *C. elegans* and *Drosophila*, the different *Rac* mutant defects appear independently of one another (Lundquist, 2003). For example, in *C. elegans,* defects in axon guidance and outgrowth can occur with or without branch formation defects while in *Drosophila*, branch formation defects occur without defects in axon guidance or outgrowth (Lundquist, 2003). In *Drosophila*, there are three Rac genes as well: *rac1, rac2 and mtl* (Mig2-like). In the CNS, visual system, and in mushroom bodies, these have overlapping functions in axon guidance and outgrowth (Hakeda-Suzuki et al., 2002; Ng et al., 2002). Unlike in *C. elegans,* Rac activity in *Drosophila* is dose-sensitive: different levels of Rac proteins are needed to regulate distinct processes at the growth cone (Luo, 2002;

Lundquist, 2003). For instance, removing Racs in the sequence Rac1, Mtl, and Rac2, leads to progressive defects in axon branching, guidance, and outgrowth (Ng et al., 2002). Moreover, axon branching and guidance require high levels of RacGTPase activity while axon outgrowth demands only modest amounts (Ng et al., 2002). This is why only in Rac GTPase triple mutants does one observe severe axon stalling by dorsal cluster sensory neurons on their way to the CNS (Hakeda-Suzuki et al., 2002). This is attributed to the latter's lack of reliance on CRIB-domain effector proteins for Rac function (Ng et al., 2002).

Recently, a link between Racs and repulsive axon guidance at the *Drosophila* CNS midline has been revealed (Fan et al., 2003). Slit mediates the recruitment of SH3-SH2 adaptor protein Dock to the Robo receptor cytoplasmic domain and leads to Rac1-mediated changes at the cytoskeleton. To start with, pan-neural expression of a dominant negative form of Rac1 in a *slit-robo* transheterozygous mutant background enhances the defects induced by *slit and robo* mutants. Additionally, loss-of-function *rac1* mutants show a partial disruption of Slit-mediated axon repulsion. Finally, GST pull-down experiments show that Rac1 activity is increased upon Slit stimulation. Although there is an increase in Rac2 and Mtl activity upon Slit stimulation, the increase of these Rho GTPases is not as significant. Thus, although Rac has been established as a positive regulator of axonal outgrowth (Luo, 2000), it is necessary for Slit-mediated axonal repulsion at the CNS midline.

1.3b.2. Cdc42

Cdc42 induces formation of filopodia in growth cones and significantly increases neurite outgrowth rates (Brown et al., 2000). Time lapse analysis shows that microinjection of Cdc42 recombinant proteins into fibroblast cells promotes increased actin polymerization which leads to the formation of filopodia within minutes (Nobes and Hall, 1995; Kozma et al., 1995). Furthermore, staining with fluorescently labeled phallotoxins reveals that Cdc42 expression also redistributes actin into the growth cone's peripheral domain and depletes it from the central domain (Brown et al., 2002). In addition, when microinjected with a dominant negative form of Cdc42, fibroblast cells with existing filopodia show a rapid loss of filopodia (Kozma et al., 1995). This result shows that Cdc42 is not only necessary for the formation, but also the maintenance of filopodia. Lastly, live filopodial studies in *Drosophila* have shown that Cdc42 controls filopodial formation/ maintenance and growth cone pathfinding via separate downstream events (Kim et al., 2002). For instance, expression of constitutively active Cdc42 causes a significant increase in filopodial formation without causing defects in axonal pathfinding. Meanwhile, mutations that affect interactions with CRIB-domain containing proteins suppress defects associated with constitutively active Cdc42 without affecting filopodial activity.

1.3b.3. Rho

Rho is responsible for the induction of stress fiber and focal adhesion formation associated with microtubule depolymerization (Liu et al., 1998). Microinjection of Rho recombinant proteins into fibroblast cells promotes increased bundling of actin and myosin which leads to the formation of stress fibers associated with focal adhesion

complexes (Ridley and Hall, 1992). Additionally, inhibition of Rho protein function via ADP-ribosylation prevents the increase in stress fiber formation and simultaneously, the assembly of proteins into focal adhesions (Ridley and Hall, 1992; Enomoto, 1996). Furthermore, the application of agents that disrupt actin-myosin interactions to cells microinjected with Rho also disrupts the formation of these structures (Chrzanowska-Wodnicka and Burridge, 1996). However, actin staining reveals that actin polymerization is not inhibited in these cells. Thus, actin-myosin bundling and not actin polymerization is necessary for stress fiber and focal adhesion assembly.

1.3b.4. Complexity of Rho GTPase signaling

Although painting a pathway in which the Rho GTPases act independently of each other with Rac1 and Cdc42 exclusively regulating axon extension while RhoA always regulates axon retraction is convenient, in reality, the picture is much more complicated.

To begin with, Rho GTPases can participate in both axon attraction and retraction. It all depends on the partners they are signaling with. For instance, in addition to its widely reported role in axon extension, Rac1 has been shown to participate in growth cone retraction induced by two repulsive guidance cues: ephrin and semaphorin. Firstly, Rac-1 is required for ephrin-A2- induced growth cone collapse. For instance, using an antisense oligonucleotide, applying a Rac1 inhibitory peptide, or creating a dominant negative form of Rac1 blocks ephrin-A2-induced retinal growth cone collapse as growth cones become immotile (Jurney et al., 2002). Additionally, reducing Rac1 protein levels inhibits the ephrin-A2 induced endocytosis to the plasma membrane of retinal and DRG growth

cones (Jurney et al., 2002). Secondly, expressing a dominant negative from of Rac1 nearly abolishes Semaphorin3A-induced DRG and spinal cord motor growth cone collapse (Jin and Strittmatter, 1997; Kuhn et al., 1999). Similarly, application of a Rac1 inhibitory peptide also negates semaphorin 3A-induced DRG and retinal growth cone collapse and additionally, inhibits its endocytosis (Vastrik et al., 1999, Jurney et al., 2002).

Another detail that complicates our GTPase cascade picture is the fact that there is considerable crosstalk between these pathways (O'Donnell et al., 2009). For example, in *Xenopus*, BDNF- induced growth cone repulsion requires basal levels of Cdc42 working along with RhoA as dominant negative versions of either Cdc42 or RhoA convert the spinal growth cone repulsion to attraction (Yuan et al., 2003). This relationship is dependent on the regulation of myosin: higher levels of RhoA stimulate myosin activity which leads to growth cone collapse while increased Cdc42 inhibits myosin function which leads to growth cone extension.

1.3c GEFs and GAPs

Signals originating from cell surface receptors control the activity of Rho family GTPases by acting on two classes of regulatory molecules: Guanine nucleotide exchange factors (GEFs) activate Rho family GTPases by enhancing the exchange of GDP for GTP while GTPase-activating proteins (GAPs) inhibit Rho family GTPases by stimulating their hydrolysis of GTP to GDP (Luo 2002; Guan and Rao 2003; Govek et al., 2007; Lowery and Van Vactor;2009; Hall and Lalli, 2010) (Figure 13). Such upstream regulation

allows these factors to direct Rho family GTPase signaling in a manner that is both tissue-specific and temporal during axon guidance (O' Donnell et al., 2009).

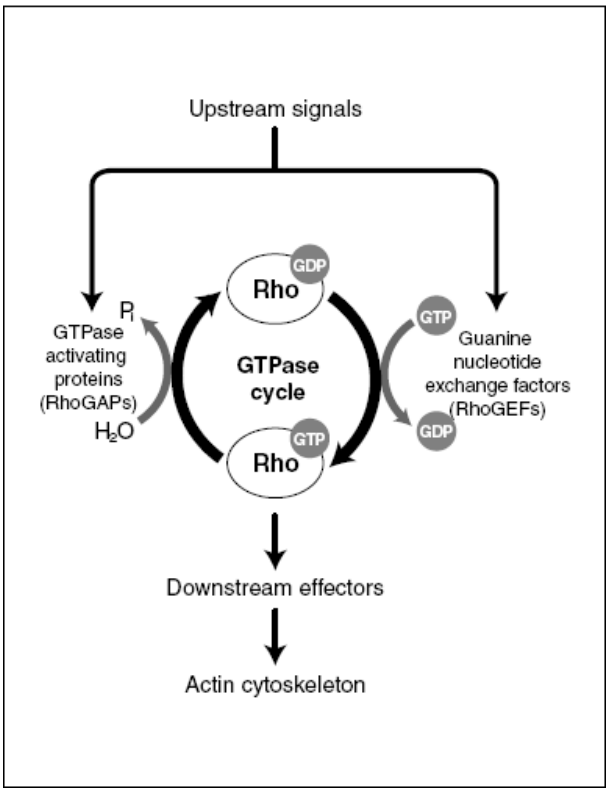

Figure 13. The Rho GTPase Cycle.
Guanine exchange factors (RhoGEFs) facilitate the conversion from the GDP-bound to the GTP-bound form and thus are activators. GTPase activating proteins (RhoGAPS) enhance GTP hydrolysis and are thus negative regulators. When bound to GTP, Rho GTPases bind to downstream effectors that transduce signals to regulate the actin cytoskeleton (Luo, 2002).

In *Drosophila melanogaster,* there are 22 Rho-family GEFs and 20 GAPs (Hu et al., 2005). Of these, eight GEFs (rtGEF, SOS, Sif, RhoGEF2, Pebble, Vav, Trio, and GEF64C) and nine GAPs (Rotund, Rlip, P50GAP, CrGAP, CdGAPr, RhoGAP100F, RhoGAPp190, RhoGAP19D, and Tumbleweed) show high embryonic CNS expression (Hu et al., 2005).

1.3c.1 GEFs

Trio is a GEF that has been shown to be the primary activator of Rac proteins during axon outgrowth (Hakeda-Suzuki et al., 2002). For example, *C. elegans* UNC-73/Drosophila Trio is a GEF that activates Rac activity (Lundquist, 2003). In both *C. elegans* (UNC-73) and *Drosophila* (Trio), mutants have strong axon outgrowth and guidance defects (Steven et al., 1998; Hakeda-Suzuki et al., 2002). For example, in *C.elegans*, *unc-73* mutants show similar defects on axon outgrowth and guidance as *Rac* double mutants, indicating that UNC-73 regulates multiple Rac proteins for axon guidance *in vivo* (Lundquist et al., 2001). In *Drosophila*, *rac1* and *rac2* loss-of-function mutations are able to suppress *trio* gain-of-function visual system axon projection and morphological defects (Hakeda-Suzuki et al., 2002). Thus, Trio does indeed signal through Rac proteins.

First identified in *Drosophila*, SOS (son-of-sevenless) is mainly known for its role as a GEF for Ras proteins during eye development. Here, it functions downstream of Sevenless and EGF receptor tyrosine kinases to activate the Ras signaling cascade that leads to the specification of R7 cells as photoreceptors (Rogge et al., 1991). However, SOS has also been shown to function as a Rac-specific GEF during Slit-mediated midline axon repulsion (Yang and Bashaw, 2006). Firstly, removing one copy of *slit* in an *sos* mutant background enhances the ectopic midline crossing phenotypes of *sos* single mutants. These defects are rescued upon *sos* wild type overexpression. At the same time, removing just one copy of *rac1* promotes a 5-fold increase in the *sos* single mutant phenotype. Additionally, this function of SOS is mediated by its Rac-binding domain as

overexpression of an *sos* missing this domain does not rescue axon guidance defects caused by removal of one copy of *slit* in an *sos* mutant background. Furthermore, GST pull-down and coimmunoprecipitation assays reveal that SOS, Robo, and adaptor protein Dock form a triple complex, with Dock acting as the linker for Robo-SOS signaling. This recruitment of SOS to Robo via Dock is triggered by Slit as SOS, Robo, and actin can be seen colocalizing in membrane ruffings upon Slit stimulation. In addition, Adam family metalloprotease Kuzbanian(Kuz), which cleaves the Robo1 ectodomain, is required for this recruitment as expressing a dominant-negative form of Kuz blocks the Slit-induced localization of SOS to the plasma membrane in HEK293T cells (Coleman et al., 2010). This presents a signaling cascade which begins when Kuz cleaves Robo1's ectodomain upon slit activation, and leads to the strengthening of Robo1's interaction with Dock, recruitment of SOS to the plasma membrane, activation of Rac1, and subsequent actin cytoskeleton changes that lead to axonal repulsion and retraction (Coleman et al., 2010).

1.3c.2 GAPs

CrGAP (Cross GAP) is a GAP involved in downregulating Rac during Robo-mediated axon repulsion (Hu et al., 2005). Firstly, disrupting *CrGAP* function via RNAi in a *slit-robo* transheterozyous mutant background enhances the *slit-robo* mutant phenotype (Hu et al., 2005). Moreover, *CrGAP* overexpression results in both ectopic midline crossing and axonal outgrowth defects, opposing Robo-mediated midline repulsion. Furthermore, GST pull-down and coimmunoprecipitation assays prove that CrGAP and Robo interact directly. Likewise, *CrGAP* overexpression in a Rac dominant negative mutant background causes increased ectopic midline crossing. Finally, expressing a homozygous

mutant of *sos*—a positive regulator of Robo-mediated repulsion—in a *CrGAP* heterozygous mutant background, enhances midline defects (Yang and Bashaw, 2006). These results validate the role of CrGAP as a downregulator of Rac activity, indicative of the highly sophisticated regulation in place during Robo-mediated midline repulsion.

1.4 Binding Proteins Involved in Remodeling the Actin Cytoskeleton

The final target of all the signaling cascades in the growth cone is the actin filament network (Dent and Gertler, 2003). It is the constant remodeling of this network that drives directional movement of the growth cone. Actin filaments have a distinct polarity due to the fact that all subunits are oriented in the same direction. The end that undergoes faster (five to ten times) subunit addition is labeled the positive end while the slower growing end is labeled negative (Geraldo and Gordon-Weeks, 2009). These ends have been designated barbed and pointed, respectively, because of the arrowhead appearance of myosin heads when bound to the actin filament.

A wide variety of proteins can bind to actin. The ABPs, actin-binding proteins, facilitate the association and dissociation of actin monomers that lead to growth cone movement. ABPs can be generally distinguished by their ability to either promote actin filament polymerization or depolymerization.

1.4a. Actin filament polymerization

Actin filament polymerization at the barbed end is initiated with the formation of a small aggregate consisting of three actin monomers, a process known as nucleation. Upon filament assembly, actin subunits undergo ATP hydrolysis and gamma-phosphate dissociation. ADP-bound monomers are less likely to undergo repolymerization. Nucleation is triggered upon the activation of the Arp2/3 complex (Pollard and Borisy, 2003), a stable assembly of two actin related proteins (Arp2 and Arp3) along with five smaller proteins (ArpC1-ArpC5).

1.4.b. Actin Binding proteins involved in each step

1.4b.1.Arp2/3: nucleation

Real time microscopy has been helpful in showing the primary role of the Arp2/3 complex: It accelerates polymerization by increasing the rate of nucleation (Mullins et al., 1998). As a result, a new filament is generated as a branch joined by its pointed side to the side of a pre-existing filament (Amann and Pollard, 2001). In this way, filaments are produced that elongate from their barbed ends (Kelleher et al., 1995). Additionally, biochemical and microscopic analysis has determined that the Arp2/3 complex caps pointed ends with high affinity, inhibiting the rate of elongation of these ends (Mullins et al., 1998). Thus, based on the above data, the Arp 2/3 complex promotes formation of actin filaments that elongate only at their barbed ends.

Since nucleation is the rate-limiting step of actin filament polymerization, signaling proteins that induce actin filament polymerization function primarily by activating

Apr2/3. For example, Rho-family GTPase Cdc42, can bind and turn on Neuronal homolog of Wiskott-Aldrich syndrome protein (N-WASP). It does so by inducing a conformational change that relieves the intramolecular binding that causes N-WASP to be inactive (Kim et al., 2000). Other SH3 domain proteins such as phosphatidylinositol 4, 5 bisphosphate (PIP2), NICK, and WISH also help to activate N-WASP (Miki and Takenawa, 2003). Subsequently, N-WASP functionally and physically interacts with Arp2/3 via its WA domain to induce nucleation of actin filaments.

1.4b.2 Villin: barbed end capping/actin bundling

As new branches grow, filament length is regulated by proteins that cap barbed ends. The importance of barbed-end capping is two-fold (Pollard and Borisy, 2003). Firstly, it ensures that the filaments are stiff enough to push on the membrane (Pollard and Borisy, 2003). Secondly, it limits the number of free barbed ends in contact with the cell surface, avoiding the unnecessary utilization of actin subunits elsewhere in cell (Pollard and Borisy, 2003). An example of a protein involved in barbed-end capping is Villin, a Gelsolin family protein. It serves this function via its Gelsolin-like domain.

Additionally, Villin is also involved in actin bundling via its headpiece domain. Actin bundling is the process of assembling actin filaments into larger structures by cross-linking actin into bundles. The actin bundling activity of Villin promotes the formation of special protrusions of the cell surface known as microvilli. When ectopically expressing Villin, fibroblast cells become covered with microvilli containing bundled actin (Friederich et al., 1999). In cells transfected with a form of villin lacking the headpiece

domain, villin is unable to bind to actin and therefore does not form actin bundles (Friederich et al., 1999).

1.4b.3. Treadmilling: cofilin

As the growth cone moves forward, turnover of actin filaments is a necessary occurrence. This process of continually balancing polymerization at the barbed end with depolymerization of the pointed end is referred to as treadmilling (Figure 14). The rate at which actin filaments depolymerize is the rate-dependent step in this process (Maciver and Hussey, 2002). First isolated from chick brains (Bamburg et al., 1980), Cofilin is a ~160aa long actin filament side-binding protein which is largely responsible for increasing actin-filament turnover. It has been shown to promote depolymerizization of actin in two ways. The first involves the severing of actin filaments into short segments (Maciver et al., 1991), which generates more ends. Alternatively, it accelerates the rate of actin monomer release (22-fold) from the pointed ends without affecting the rate of assembly at the barbed ends (Carlier et al., 1997).

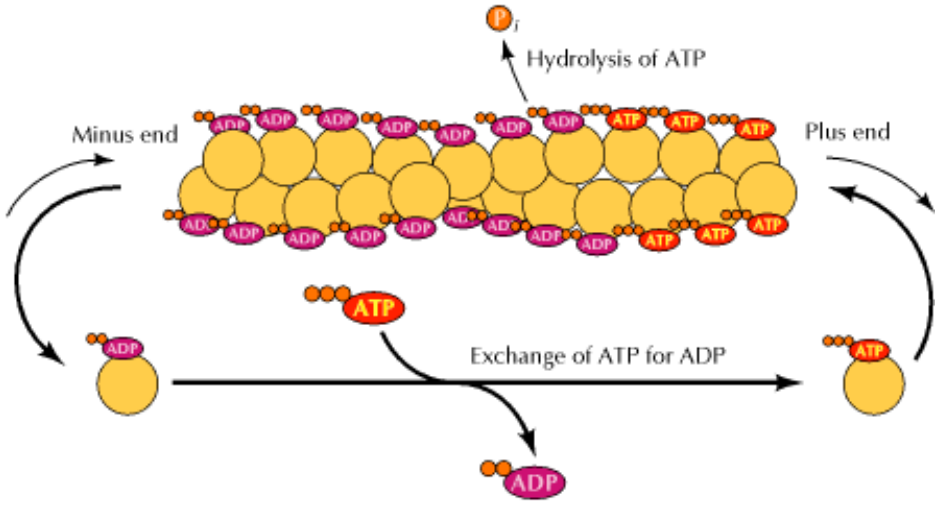

Figure 14. Treadmilling.
The minus ends grow less rapidly than the plus ends of actin filaments. There is a net dissociation of monomers (bound to ADP) from the minus end, balanced by the addition of monomers (bound to ATP) to the plus end (Cooper, 2000).

The presence of Cofilin has been shown to be essential for the preservation of cell motility. For example, mutations in *twinstar*, the gene that encodes *Drosophila* Cofilin, induce an especially high accumulation of actin filaments in developing ovaries (Chen et al., 2001). This change in actin cytoskeleton composition leads to the disruption of cell movements during ovary development and oogenesis. Additionally, in *Dictyostelium discoideum*, cells overexpressing Cofilin move significantly faster than control cells (Aizawa et al., 1996).

A question that remains is how are actin filaments marked for recognition by Cofilin? As actin subunits undergo ATP hydrolysis, Cofilin will preferentially bind to actin filaments with a higher concentration of ADP-bound monomers (Carlier et al., 1997). Moreover, binding of Cofilin to these actin filaments, increases their twist—a quality that makes it

unique among the ABPs (McGough et al., 1997). As a result, Cofilin alters the binding site of competing proteins such as Profilin. Profilin is the nucleotide exchange factor for actin, catalyzing exchange of ADP for ATP and returning subunits to the pool of ATP-actin bound to Profilin for assembly into filaments (Pollard and Borisy, 2003).

1.5 AbLIM Family

The abLIM family of actin-binding proteins represents a distinct cytoskeletal signaling mechanism downstream of Rac (Yang and Lundquist, 2005). Since the discovery of abLIM in humans (Roof et al., 1997), orthologs *C.elegans* UNC-115(Lundquist et al., 1998) and *Drosophila* Dunc-115 (Garcia et al., 2007) have been identified. They all share N-terminal LIM domains, a UAD domain (Unc-115, AbLIM, Dematin) and a C-terminal villin headpiece domain (VHD). Additionally, both abLIM (Roof et al., 1997) and UNC-115 (Struckoff and Lundquist, 2003) have been shown to bind to actin *in vitro* via its VHD domain while the actin-binding ability of Dunc-115L has been indicated from *in silico* studies (Garcia et al., 2007).

1.5a. Mammalian abLIMs

AbLIM1 was isolated from a screen for dermatin-like proteins in the vertebrate retina (Roof et al., 1997). It is composed of N-terminal LIM domains, a UAD domain, and a C-terminal villin headpiece. Three isoforms have been isolated in abLIM1: abLIM-S (small), abLIM-M, (medium), and abLIM-L (long) (Lu et al., 2003) (Figure 15). abLIM-L and abLIM-M each have four while abLIM-S lacks LIM domains. They all have a C-terminal VHD domain. AbLIM-M and abLIM-S are widespread and are relatively constant through development. At the same time, abLIM-L is primarily expressed in

retinal ganglion cells. It is upregulated postnatally and temporally correlates with the period of retinal ganglion cell (RGC) axon remodeling (Lu et al., 2003).

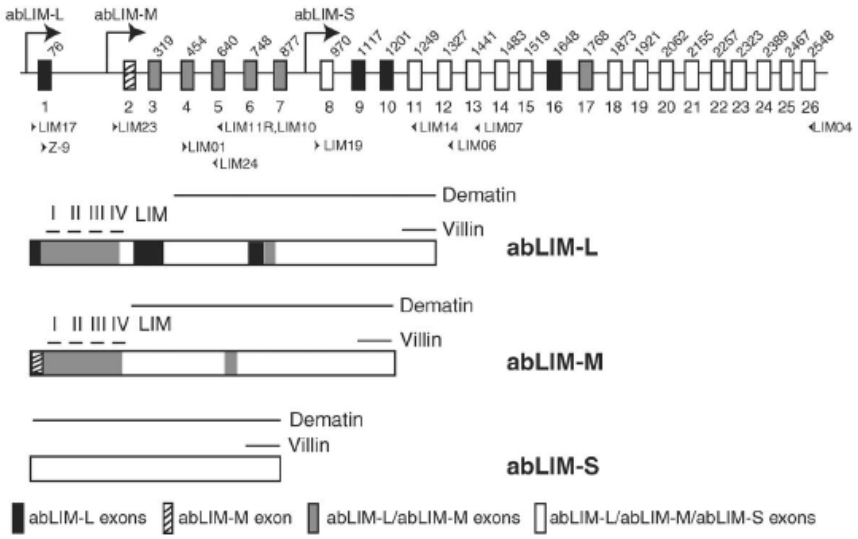

Figure15. Characterization of Three Major Variants Transcribed from the Murine abLIM Gene.
Gene structure of murine abLIM gene. There are 26 exons. The number below each exon indicates exon number and the number above indicates the starting nucleotide number of that exon (numbering begins with the transcription start site of abLIM-L as 1). Transcription start sites are marked by arrows. Small arrowheads show oligonucleotide primers used in PCR analyses. Below the gene structure are schematic diagrams of the abLIM proteins. GenBank accession numbers for these variants are: abLIM-L, AF404774; abLIM-M, AF404775; abLIM-S, AF404776 (Lu et al., 2003).

In vitro and *in vivo* analyses have shown that abLIM1 binds actin via its VHD domain (Roof et al., 1997). Additionally, expression of an abLIM construct that is missing its VHD domain, results in pathfinding defects in chick retinal ganglion cells. Unlike wild type , these RGC axons turn away from the optic disc, follow a wave-like trajectory, and undergo abnormally high levels of fasciculation (Erkman et al., 2000). However, disruption of abLIM-L in mice results in normally projecting RGCs (Lu et al., 2003).

Most recently, a yeast two-hybrid screen for proteins that interact with STARS(Striated Muscle Activator of Rho Signaling)—a muscle-specific actin-binding protein—in striated muscle tissue, has led to the isolation of two additional abLIM proteins (Barrientos et al., 2007). Human abLIM-2 expression is relatively constant throughout development and is strongest in skeletal muscle while expressed more modest in the brain. On the other hand, human and mouse abLIM-3 expression is downregulated in adulthood while being strongest in the heart and somewhat in brain tissue. The expression of these two isoforms in the brain is largely distinct. *In vitro* and *in vivo* assays have shown that like abLIM-1, both abLIM-2 and abLIM-3 bind to actin. The discovery of two additional abLIM proteins may explain why phenotypic studies with abLIM1-L (Lu et al., 2003) resulted in no obvious pathfinding defects.

1.5b. C. elegans UNC-115

UNC-115 was first reported as part a screen of *C. elegans* behavioral mutants for genes involved in guiding axons along the ventral nerve cord (Wightman et al., 1997). It has been found to be involved in the pathfinding of later-extending as opposed to early pioneering neurons (Wightman et al., 1997; Lundquist et al., 1998). Mutations in UNC-115 lead to uncoordinated locomotion and the fasciculation of axons at the VNC (Wightman et al., 1997; Lundquist et al., 1998). For example, in adults, mutations in *unc-115* cause HSNL axons, hermaphrodite-specific motor axons that normally travel in the left fascicle of the VNC, to travel in the right side (Wightman et al., 1997). Additionally, axon guidance and locomotion defects have been proven rescuable upon transgenic

expression of *unc-115* full length cDNA (Lundquist et al., 1998; Yang and Lundquist, 2005).

UNC-115 has been shown to act as a cytoskeletal adaptor protein. For instance, molecular modeling and actin co-sedimentation assays have shown that like abLIM, UNC-115 indeed does bind with actin via its VHD domain (Struckhoff and Lundquist, 2003). Additionally, UNC-115 has been shown to act as a downstream cytoskeletal effector of Rho-family GTPase Rac-2 in axon pathfinding of both postderid sensillum (PDE) and excretory canal (CAN) axons (Struckhoff and Lundquist, 2003) (Figure 16). Furthermore, loss of *unc- 115* function suppresses the increase in lamellipodia and filopodia-like structures caused by constitutively activating *Rac-2* (Struckhoff and Lundquist, 2003).

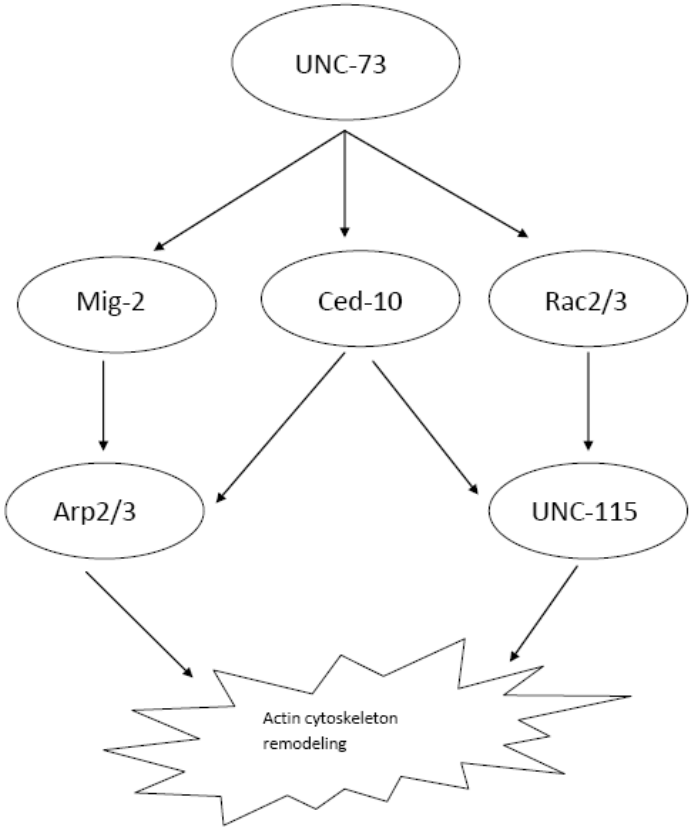

Figure 16. UNC-115 Acts Downstream of Rac Signaling in CAN and PDE Axon Pathfinding.
The genetic relationships between the three *racs*, *unc-73* and *unc-115* are shown. Arrows indicate that the genes act in the same pathway. Three *rac* genes *ced-10, mig-2* and *rac-2/3*, define three parallel pathways with overlapping function. *unc-73* acts in all three pathways, and *unc-115* acts downstream of *rac-2* and *ced-10*. *Arp2/3 acts downstream of Mig-2.*

A functional link between UNC-115 and external guidance cue Netrin has been reached in axon pathfinding and neuronal morphogenesis (Gitai et al., 2003). The generation of a gain-of-function UNC-40 mutant (MYR::UNC-40), causes axon guidance defects, accompanied by excessive axon and cell body outgrowth. Furthermore, these defects are suppressed by expressing UNC-115 loss-of-function mutations in this background—proving that it acts downstream of UNC-40. Additionally, double mutants of Rac protein CED-10 and UNC-115 result in no added suppression of MYR::UNC-40, indicating that they are all part of the same pathway. Lastly, guanine exchange factor UNC-73 has been

shown to bind to the cytoplasmic domain of UNC-40 (Watari-Goshima et al., 2007). In summary, UNC 40 recruits CED-10 via UNC-73, which signals to UNC-115 to promote actin cytoskeleton rearrangements (Figure 17).

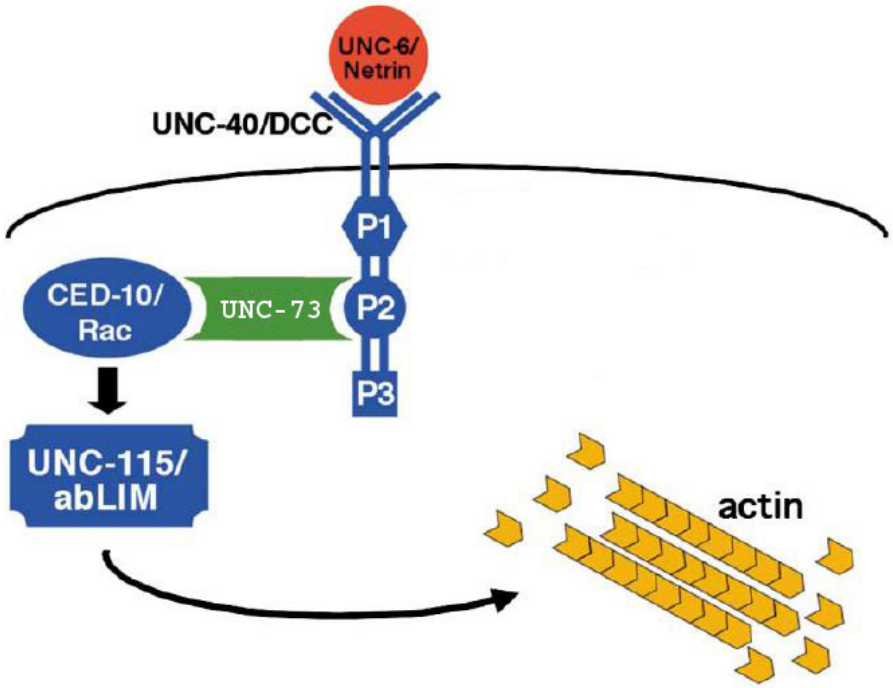

Figure 17. Model for UNC-115 Mediated Actin Rearrangements via UNC-40 Signaling. Shown here is a model for UNC-40 signaling in which UNC-6 induces UNC-40 receptor dimerization. The P2 domain of UNC-40 recruits CED-10 and UNC-115 to promote actin rearrangements via UNC-73. UNC-115 acts downstream of CED- 10 due to its ability to directly bind actin (Modified from Gitai et al., 2003).

Most recently, UNC-115 has also been shown to be crucial to growth cone morphology and dynamics during outgrowth (Norris et al., 2009). In both *C. elegans* neurons and mouse fibroblast cells, UNC-115 overexpression has been shown to induce filopodial and lamellipodial formation (Yang and Lundquist, 2005). Moreover, UNC-115 regulates the filopodia initiation rate *in vivo*: In *unc-115* loss-of-function mutants, filopodia are generated 1 every 5.9 minutes per neurite in comparison to the wild type where they are

generated 1 every 4 minutes (Norris et al., 2009). This control of growth cone dynamics most likely depends on the distinct guidance cue environment witnessed by different neurons (Norris et al., 2009). In PQR neurons, for example, UNC-115 redundantly controls the number of filopodia that are formed per neurite along with seven protein member complex, Arp2/3. Conversely in VD neurons, *unc-115* mutants do have significant drops in filopodia formed when compared to wild type.

Investigations from both invertebrates and vertebrates have brought us closer to understanding how axons are directed to their targets in early development. They have brought to light the existence of secretable proteins that provide directional information to the cell by binding to receptors at the cell membrane. They have also brought to light the existence of signaling proteins like Rho GTPases that relay this information to the cytoplasm. Although we are learning more about actin-binding proteins that mediate interactions between the actin cytoskeleton and cytoplasmic targets, further inquiries are needed to complete this picture. For example, studies of mammalian abLIM and *C.elegans* UNC-115 have shown that these proteins are necessary for proper pathfinding decisions at the embryonic midline and elsewhere. By studying the fly ortholog, Dunc-115, we hope to fill in the gaps that still remain in our understanding of how cytoskeletal changes lead to directional movement of the growth cone during axon pathfinding.

1.5c. *Drosophila* Dunc-115

1.5c.1 Identification of *Drosophila* Dunc-115

The *dunc-115* gene (85E6) spans some 10.7 Kb and contains eleven exons that are alternatively spliced to generate three isoforms *dunc-115l*, *m*, and *s* (Garcia et al., 2007) (Figure 18). Both *dunc-115m* and *dunc-115s* contain the stop codon TAA, while *dunc-115l* has TAG. All cDNAs contain a polyadenylation signal and a poly A tail (Garcia et al., 2007).

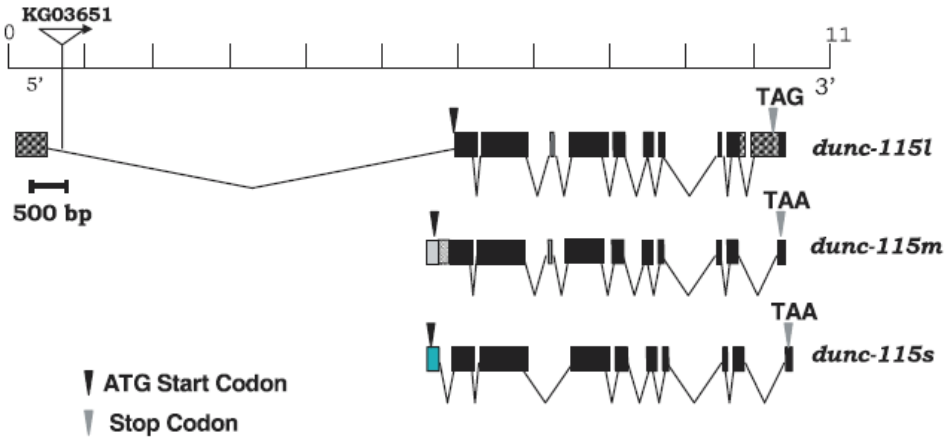

Figure 18. Genomic Structure of Dunc-115 Isoforms. A total of eleven exons have been identified. Black boxes are the sharesd exons while different fillings represent isoform-specific ones. The location of the P-element in mutant strain *dunc-115*^{KG03651} is indicated (Garcia et al., 2007).

There are three protein isoforms of Dunc-115 as a result of alternative splicing: Dunc-115L (806 aa), Dunc-115M (769 aa), and Dunc-115S (766 aa) (Garcia et al., 2007) (Figure 19). All three proteins have four N–terminal LIM domains as well as a UAD domain with Dunc-115L being the only one having a VHD domain. Moreover, molecular modeling shows that the VHD domain of Dunc-115L is likely to bind to actin (Garcia et al., 2007) (Figure 20).

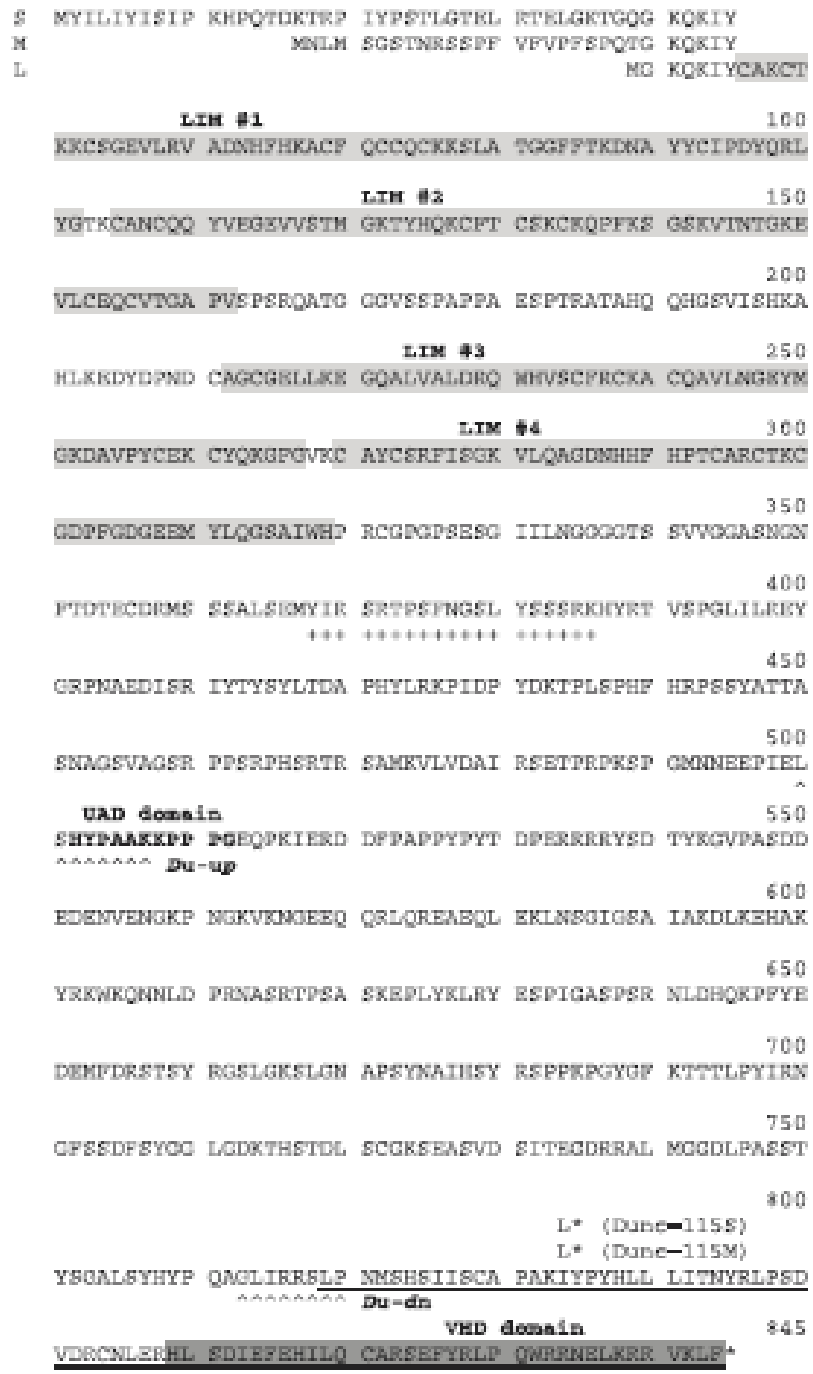

Figure 19. Protein Sequence Comparison of Dunc-115 Isoforms. All four isoforms share 4 LIM domains and a UAD domain. Dunc-115L is the only isoform to contain a VHD domain. Note that Dunc-115S and M have different N-terminal sequences and terminate before the VHD domain as separately marked. Shaded areas are LIM domains and the VHD
domain and the UAD domain is in boldface. The stretch marked by (+) following the LIM domains is deleted in Dunc-115S (Garcia et al., 2007).

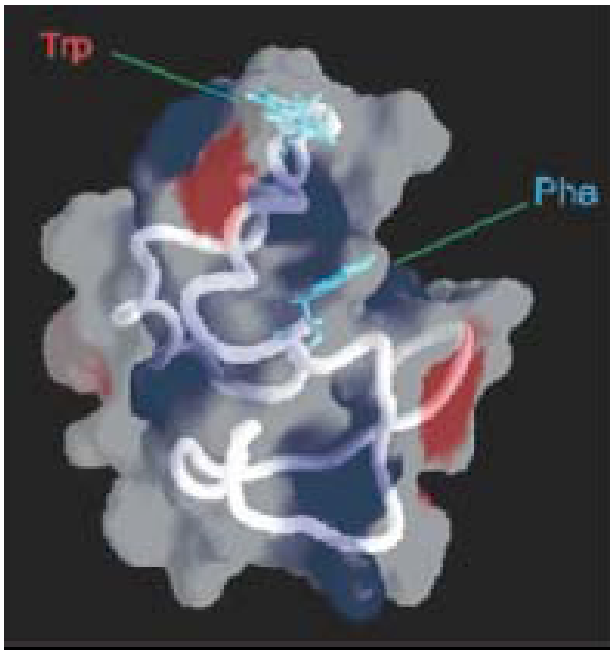

Figure 20. Model of Dunc-115L VHD Domain. There are four conserved residues in the human villin headpiece domain involved in binding to actin and the corresponding four residues in Dunc-115 VHD have been found. Two of the four residues are Trp and Phe shown here and the other two are Arginines. Blue, red and white colors represent positive, negative and neutral charges, respectively (Garcia et al., 2007).

1.5c.2 Phenotypic Analysis

Drosophila visual system is a well-studied model for retinal axon pathfinding where axons from photoreceptor neurons project from the eye disc through the optic stalk to their brain targets in a retinotopic fashion. Disruption of genes required for axon projection results in defects ranging from stalled axons to the formation of gaps and crossovers. To determine the functions of Dunc-115, axon projections in the visual system have been examined. Using the antibody 24B10 for the photoreceptor neuron specific marker chaoptin, retinal axon projection in *dunc-115* mutants has been analyzed where abnormal gaps and crossovers are apparent (Figure 21) (Garcia et al., 2007), suggesting that Dunc-115 is involved in retinal axon navigation to the target.

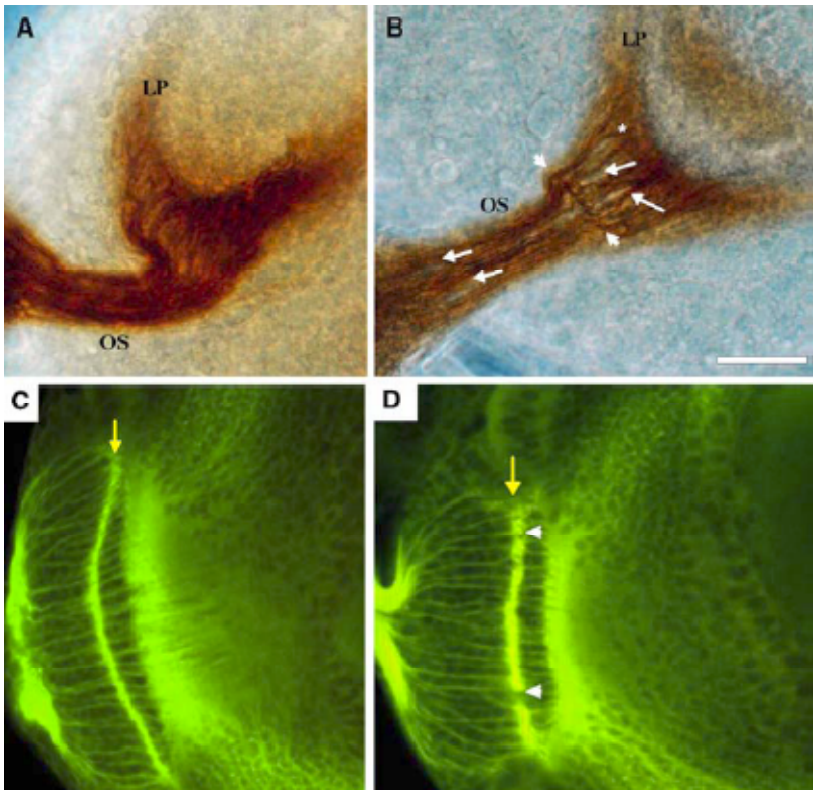

Figure 21. Dunc-115L Mediates Retinal Axon Projection. Dunc-115 mediates retinal axon projection.
(A), (C) wild-type and (B), (D) *dunc-115*^{KG03651}. (A), (B) were stained with the 24B10 antibody. Long arrows in B indicate some of the gaps formed by adjacent axon bundles and the star points to one crossover event, while the two short arrows indicate abnormal folding of the axons.
(C), (D) were stained with a panneural FITC-conjugated anti-HRP antibody and viewed from the lamina plexus perspective where the targets of R1-6 cells formed a continuous crescent shape (arrow in (C)) in the wildtype. In *dunc-115*^{KG03651} D, the lamina plexus was disrupted by frequent gaps (arrowheads).
OS optic stalk; LP lamina plexus. Scale bars: 50 lm in (A) and (B), 30 lm in c and 38 lm in (D). (Garcia et al., 2007).

The embryonic CNS is another intensively investigated target for axon navigation. Our lab has also examined the involvement of Dunc-115 in this process. As one of the markers for the CNS, fasciclin is an immunoglobulin superfamily cell adhesion molecule that delineates the three longitudinal pathways on each side of the midline: medial, intermediate, and lateral. CNS staining with the antibody for Fasciclin II 1D4 shows that

in *dunc-115* mutants, the outermost fascicle experiences frequent breaks while the middle and intermediate fascicles fuse together (Garcia et al., 2007) (Figure 22C). Additionally, axon bundle thickening occurs at each neuromere (Figure 22D, E). Together, these data indicate that Dunc-115 is necessary for proper axonal projection of longitudinal axons at the midline.

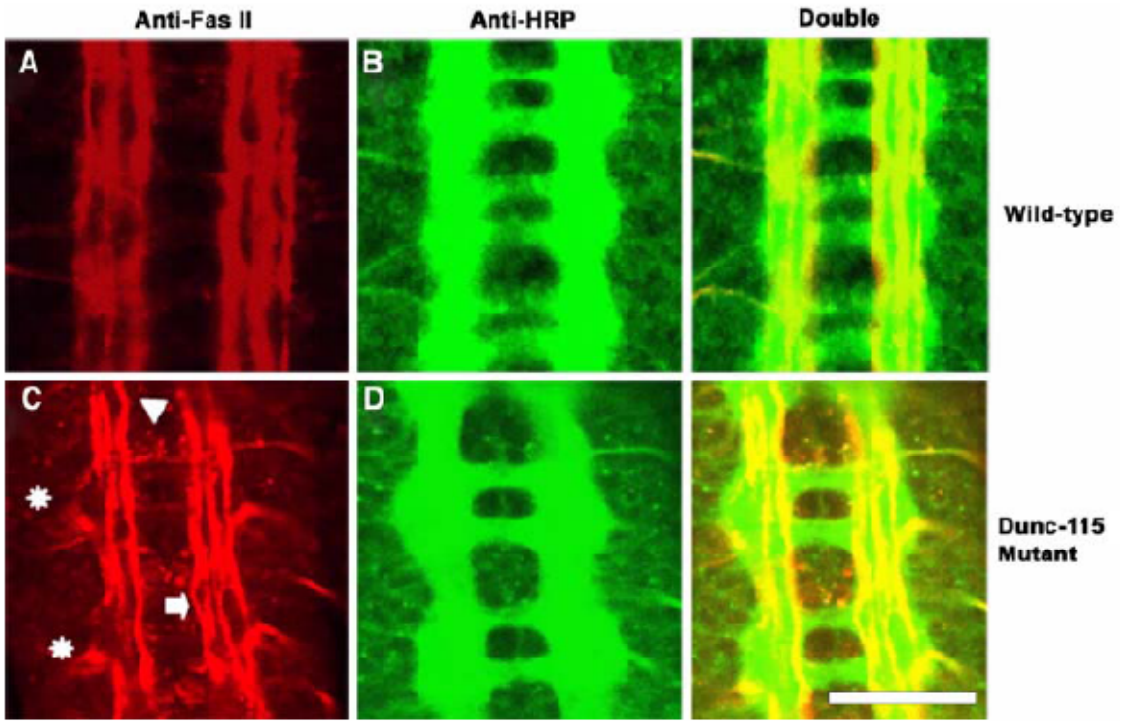

Figure 22. Dunc-115 is Involved in Longitudinal Axon Fasciculation. (A) Fas II staining in the wild type reveals three continuous longitudinal bundles running in parallel in each of the two longitudinal tracks. (B) Wild-type CNS is seen with the anti-HRP staining. (C) Anti-Fas II staining of the *dunc-115*^{KG03651} CNS shows large breaks along the longitudinal bundles (stars) and fasciculation defects of abnormal gaps (arrow). Arrowhead marks the center of the CNS. (D) The large longitudinal breaks coincide with axon bundle thickening at each neuromere when the *dunc-115*^{KG03651} CNS is seen with double labeling of anti-HRP and anti-Fas II. Scale bar: 25 lm for all panels. (Garcia et al., 2007)

Given all of the above data, Dunc-115 functions in choice point decisions and influences defasciculation at the midline.

1.6 *Drosophila melanogaster* as model for studying axon pathfinding.

Drosophila melanogaster is a well-established genetic model for studying *in vivo* functions of genes. Moreover, the wide range of molecular, cellular and genetic techniques in fruit flies provides a unique system to investigate the axon guidance pathways. It is very easy to manipulate genetically since it has very large chromosomes, its entire genome has been mapped, and it has a life cycle that takes 9 days to reach adulthood. Furthermore, the high level of conservation across species has extended the understanding obtained from *Drosophila* to other systems including humans.

1.6a *Drosophila* motoneurons

In the embryos and larvae of *Drosophila,* the muscular system is organized into a segmentally repeating pattern of 31 or fewer distinct muscle fibers per hemisegment (Figure 23A)—each of which is innervated by motoneurons (Johansen et al., 1989). Just as is the case with vertebrates, Drosophila motor neurons leave the CNS in two major axon bundles termed fascicles. These are the intersegmental (ISN) nerve roots and segmental nerve (SN) roots. These bundles separate into five branches as they enter the periphery to reach their muscle targets, a process called defasciculation. These five pathways are the SNa, SNc, ISN, ISNb, and ISNd. (Figure 23B) The ISN innervates the dorsal muscle fibers while SN innervates the ventral muscle fibers (Johansen et al., 1989).

The SNa and SNc pathways derive from the segmental nerve cord while the ISN, ISNb and ISNd separate from the intersegmental nerve cord. The SNa branch is the main

branch and the first to appear of the SN (Johansen et al., 1989). It extends past the ventral muscle domain to the lateral muscle region. It then divides into a lateral and a dorsal branch, innervating muscle fibers 5 and 8 and then bifurcates again to innervate muscle fibers 21-24 (Johansen et al., 1989; Kauffmann et al., 1998; Winberg et al., 1998) (Figure 23C) These set of six fibers are the most distant targets of the SN (Johansen et al., 1989) The SNc, ISNb, and ISNd branches emerge simultaneously—innervating more proximal targets. Of these, the ISNb branch has been most extensively investigated (Kauffmann et al., 1998). It separates from the ISN after exiting the CNS and proceeds into the ventral domain forming three major branches, one between muscle fibers 6 and 7, and one each at the ventral edges of muscle 13 and 12 (Winberg et al., 1998)(Figure 23C).

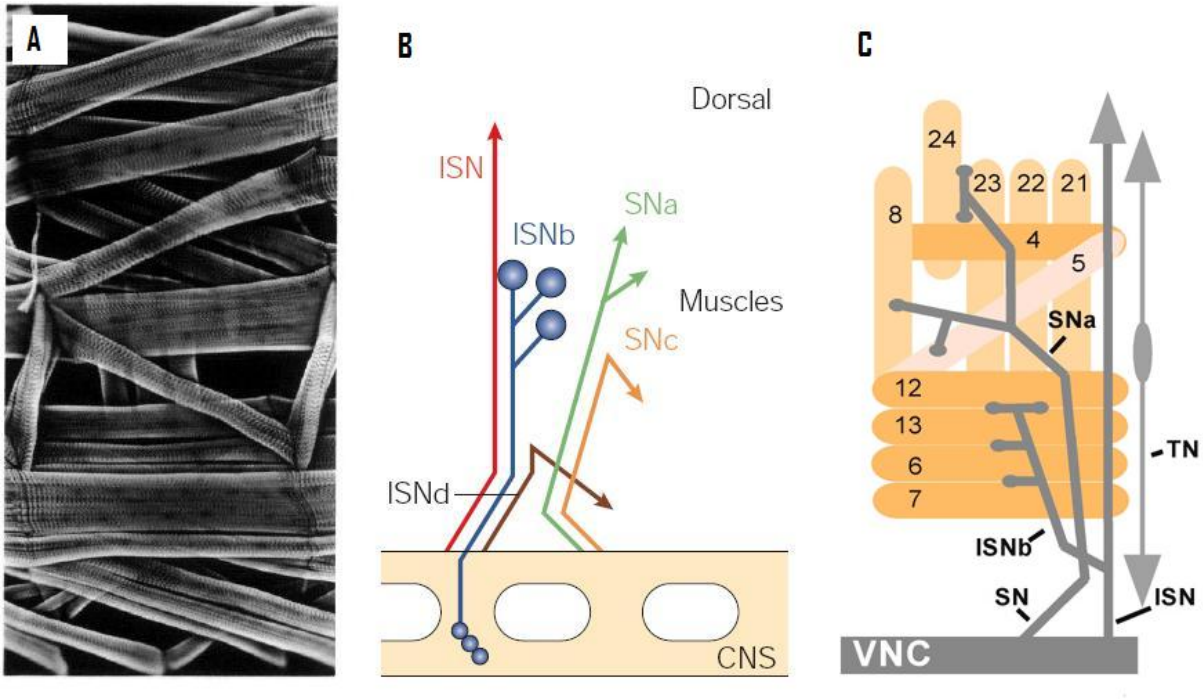

Figure 23.Connections of Motor Axons to Muscles (A) Muscle fibers of an abdominal hemisegment labeled by rhodamine-conjugated phalloidin (Johansen et al., 1989). (B) The ISN and SN exit the CNS in ISN, ISNb, INSd, SNa, and SNc branches (Araujo and Tear, 2003).(C) Schematic of a hemisegment in the wild-type stage 17 embryo illustrating the innervations of individual muscle fibers by motoneuron axons. ISN, intersegmental nerve; ISNb, the b branch of ISN; SN, segmental nerve; SNa, the a branch of SN; TN, transverse nerve; VNC, ventral nerve cord. Anterior is to the right and dorsal up in all panels. Schematics were based on and inspired by Ayoob et al. (2006).

1.6b Drosophila Ventral Nerve Cord

In both vertebrates and invertebrates, the midline of the developing CNS is an important choice point for pathfinding axons. These project toward and across the midline, forming axon commissures (Tessier-Lavigne&Goodman, 1996).These commissural axons must extend significant distances toward the midline and then must decide whether or not to cross over to the opposite side of the CNS (Garbe and Bashaw, 2004). After reaching the midline, axons execute right angle turns on the ipsilateral (same) and contralateral (opposite) side of the midline, respectively. Subsequently, these axons must further decide whether to extend in the rostral or caudal direction parallel to the midline.

Both classes of axons are barred from the midline once they begin to extend in the longitudinal direction. Specialized midline cells function as intermediate targets that provide growth cones with long- and short-range guidance cues which positively or negatively influence axonal extension. Thus, proper axon guidance in this region relies upon the growth cone's ability to correctly integrate a variety of extracellular guidance signals (Kaprielian et al., 2001).

The *Drosophila melanogaster* ventral nerve cord (VNC) has been studied extensively and provided significant findings in the field of neuroscience. It possesses a relatively simple nervous system which makes it optimal for scientific research. The VNC develops from a sheet of neuroectodermal cells within a 24 hour period (Skeath and Thor, 2003). The VNC has the appearance of a railroad track with two longitudinal connectives running along the A-P axis and two commissures extending from one side of the midline to the other, forming the 'rungs' of the track. A hemisegment is a bilateral half of a segment and is the unit of the VNC (Skeath and Thor, 2003).The VNC is subdivided into 14 hemisegments with 300 neurons per hemisegment of ventral nerve cord (VNC) (Skeath and Thor, 2003; Araujo and Tear, 2003).

One difference between *Drosophila* and vertebrates is that the axons crossing the midline are subdivided into anterior and posterior commissures (Hummel et al., 1999; Kaprielian et al., 2001) The formation of these commissures takes place during Stage 12 (8.5-10hours) of embryonic development (Klambt and Goodman.1991; Kaprielian et al., 2001). They are formed in several steps: The pioneering of the posterior and anterior

commissures, the migration of posterior glia, and the resulting separation of anterior and commissures (Klambt and Goodman, 1991). Three pairs of glia are present at the midline and these are connected to the longitudinal and commissural bundles (Klambt et al., 1991).

Several proteins are involved in making sure all axons reach their desired destinations in the Drosophila midline. Netrins A and B are attractive cues that are initially secreted by midline glial cells during stage 12 of Drosophila development (Harris et al., 1996). Removing both *Netrin-A* and *Netrin-B* results in missing or thinning commissures and frequent disruptions of the longitudinal connectives (Harris et al., 1996). The presence of one of the two is sufficient for the correct crossing of commissural axons across the midline. Reintroducing either Netrin-A or Netrin-B rescues the Netrin-A and B double mutant non-crossing phenotype to a similar extent (Harris et al., 1996). Moreover, commissural axons in single mutants of Netrin-A and B project normally (Brankatschk and Dickson, 2006). Netrins and B interact with *frazzled* receptors, which are expressed in the surface of extending axons (Kolodziej et al., 1996). *Frazzled* null mutants strongly resemble the phenotype of *netrin-A* and *netrin-B* mutants (Kolodziej et al., 1996). Also controlling midline crossing are repulsive cue Slit and its receptor Robo-1. Robo-1 is expressed on the surface of the developing embryo while Slit is secreted by neuronal cells at the midline. Robo-1 is upregulated at the surface of ipsilateral axons to prevent them from crossing the midline, downregulated to allow commissural axons to respond to Netrin and cross the midline, and then upregulated again once they have crossed correctly to prevent recrossing (Kidd et al., 1998).

1.6c *Drosophila* visual system development

The *Drosophila* compound eye is a stereotyped structure consisting of 750 repeating eye units called ommatidia, each consisting of 20 cells: Eight photoreceptors(R1-R8),six glial-like support cells, four cone cells, and two primary pigment cells (Bao et al., 2010) (Figure 24). Of the 8 photoreceptors, R1-R6 respond to green light while R7 and R8 react to blue and UV light (Harris et al., 1976). In early embryogenesis, 20-40 cells set up imaginal discs. Imaginal discs are groups of larval cells from which adult structures form. The eye develops in the flat epithelial layer of the eye imaginal disc of the larva. There are no cells directly above or below this layer, so the interactions are confined to neighboring cells in the same plane.

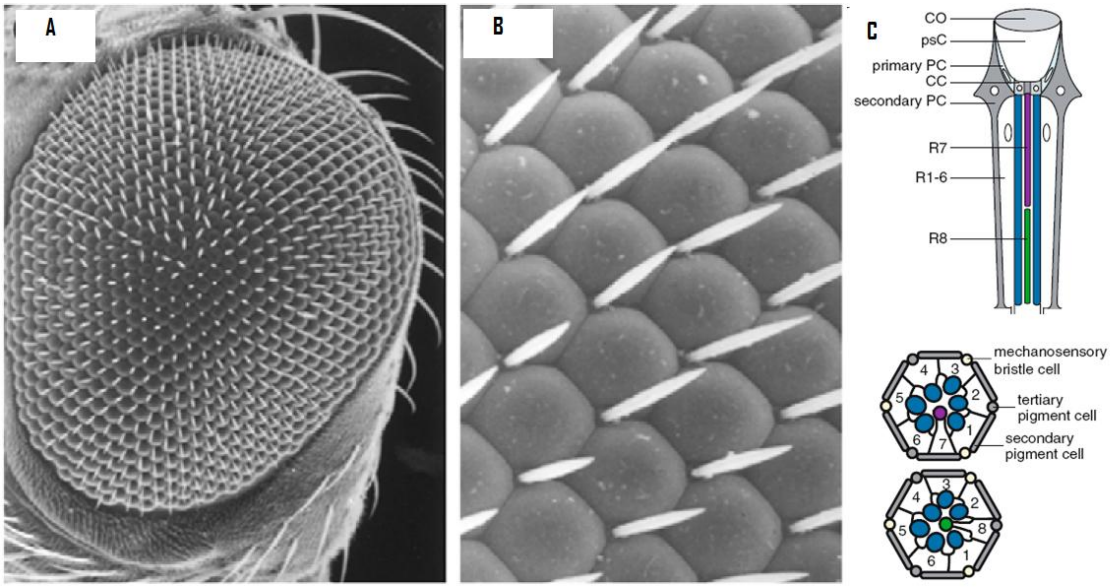

Figure 24. The Drosophila Eye (A) Scanning electronmicrograph of the eye of an adult fly showing its repeating eye unit organization. (B) higher magnification image showing the hexagonal shape of each ommatidia, which are outlined by a bristle growing every other vertex. (C) Cellular organization of single ommatidia. co, cornea; primary PC, primary pigment cell; psC, pseudocone; secondary PC, secondary pigment cell; R1–6, photoreceptor cells 1–6; R7, photoreceptor cell 7; R8, photoreceptor cell 8. A+B (Knust, 2007) C (Wang and Montel 2007)

1.6c.1. R cell fate specification

The differentiation of these randomly arranged epithelial cells into the retinal photoreceptors and their surrounding lens tissue occurs during the third larval instar stage. An indentation forms at the posterior margin of the imaginal disc, and this morphogenetic furrow sweeps across it over a 2 day period in a wave of development from posterior to the anterior of the epithelium (Ready et al., 1976; Roignant and Treisman, 2009). This progression of the furrow is mediated by segment polarity protein Hedgehog (HH) and TGFB superfamily member Decapentaplegic (DPP) (Heberlein et al., 1993). HH is expressed in differentiating cells posterior to the morphogenetic furrow and diffuses anteriorly to mediate the expression of DPP in the furrow. In *hh* mosaic mutants, a portion of the eye is missing and morphogenetic furrow progression is arrested early. Also, in both *hh* single mutants and in mutations that stop the progression of the morphogenetic furrow, *dpp* expression is abolished. Moreover, *dpp* expression is restored before morphogenetic furrow progression resumes. Thus HH and DPP are critical to the ability of the furrow to traverse the eye disc.

As the morphogenetic furrow passes through a region of cells, those cells behind it begin to differentiate in a defined order. The first cell to differentiate is the central (R8) photoreceptor. R8 cell is thought begin a cascade of induction that starts with the differentiation of the R2 and R5 photoreceptors. R3 and R4 follow, then R1 and R6 and finally R7 is differentiated (Roignant and Teisman, 2009). The other cells around these photoreceptors become the lens cells.

Several proteins are involved in controlling the steps of this induction cascade. Firstly, transcription factor Atonal (Ato) is responsible for triggering the onset of R cell differentiation by specifying the R8 cell (Jarman et al., 1994). Ato is initially expressed anteriorly to the morphogenetic furrow as a stripe spanning the optical disc and is refined to R8 cells as the furrow moves. In *ato* mutants, the eye is devoid of any photoreceptors and thereby reduced to a mass of pigment cells. As a consequence of Atonal activity, the R8 cell begins to express serine proteases Rhomboid (Rho) 1-3 which cleave and subsequently activate EGFR ligand Spitz (Wasserman et al., 2000; Yogev et al., 2008). The secretion of Spitz from the R8 cell sets off a cascade of differentiation of R1-R7 cells (Freeman et al., 1996; Roignant and Treisman, 2009). In the presence of seven-up (Svp) and high activity of the Ras pathway, R precursor cells become R1/R6 cells. In the absence of Svp, they become R7 cells at high levels of Ras signaling and cone cells at low levels of Ras signaling (Begeman et al., 1995; Kramer et al., 1995; Shi and Noll, 2009).

Receptor tyrosine kinase Sevenless, transmembrane proteins Boss and Delta and transmembrane receptor Notch work together to regulate R7 cell fate. Sev is expressed in all presumptive R cells as well as cone cells (Banerjee et al., 1987).Meanwhile, Boss is first expressed in cells posterior to the morphogenetic furrow and then later expressed in R8 photoreceptors (Kramer et al., 1991). The ligand Boss binds to receptor tyrosine kinase Sev, which internalizes Boss to the R7 cell (Kramer et al., 1991). In sev and boss single mosaic mutants, R7 precursor cells are converted to cone cells (Tomlinson and Ready, 1986; Kramer and Van Vactor, 1990). Additionally, Delta and Notch specify the

R7 cell by providing a signal from the R1/R6 photoreceptor pair (Kramer et al., 1991). In mosaic mutants in which at least one member of the R1/R6 pair lacks Delta or Notch activity, R7 presumptive cells become R1/R6. Moreover, ectopically expressing Notch in R1/R6 cells causes them to develop as R7.

Transcription Factor Dpax-2, transcriptional repressor TTk88, and adaptor protein Phyllopod control cell fate specification of R1-R7 cells (Shi and Noll, 2009). Both Dpax-2 and TTk88 function to promote cone cell development. Dpax-2 is expressed in the nuclei of cone cells, bristle cells, and in primary pigment cells (Fu and Noll, 1997). TTk88 also localizes to cone cells. Additionally, it can be found in the nuclei of undetermined basal cells (Lai et al., 1996). In ommatidia of *ttk*; *D-Pax-2* double mutants, all cone cells are lost (Shi and Noll, 2009). Additionally, ectopically co-expressing Dpax-2 and TTK88, results in the conversion of R precursor cell fate to cone cells (Shi and Noll, 2009). Independently, TTK88's role is to prevent inappropriate R cell differentiation of cone precursor cells but not to promote cone cell fate. In fact, ommatidia within the mutant patch contain extra R7 cells in *ttk* mutants (Lai et al., 1996) while there is increased cell death of R precursor cells in ommatidia where TTK88 is being ectopically expressed. Moreover, in this overexpression, R precursor cells are not converted to cone cells. D-pax2, on other hand, does promote cone cell specification while suppressing cone precursor cell death (Shi and Noll, 2009).

Phyl promotes R cell fate by both targeting TTK88 for degradation via the formation of a complex with other proteins (Tang et al., 1997) and blocking R cell fate by downregulating D-Pax (Shi and Noll, 2009). Phyllopod is expressed in undifferentiated

cells and R cells (Shi and Noll et al., 2009). Just as in ectopic expression of Dpax-2, loss-of-function Phyl mutants show transformation of R cell precursor cells into cone cells. Moreover, TTK88 (Li et al., 1997), and D-pax proteins (Shi and Noll, 2009) are ectopically expressed in these cells. Conversely, when Phyl is ectopically expressed, cone precursor cells are transformed into R cells while TTK88 (Chang et al., 1995; Dickson et al., 1995) and D-pax levels are reduced relative to wild type. This is a mechanism in which Phyl controls R cell fate by downregulating two proteins which promote cone cell fate in different ways.

1.6c.2 R cell target selection

The projection of R cells to their final destinations in the brain is also highly coordinated. These project through the optic stalk into the optic lobe, where they contact their targets. The optic lobe is composed of four optical ganglia: The lamina, medulla, lobula and lobula plate (Figure 25). R cells make connections with neurons in the lamina and medulla. R1–R6 photoreceptors terminate in the lamina, which lies directly beneath the retina (Figure 26). This process takes place in a single, morphologically defined step (Choe et al., 2006). The medulla is subdivided into 10 layers (M1-M10). R7 and R8 extend through the lamina to terminate in the M6 and M3 layers respectively, of the medulla (Lee et al., 2003; Araujo and Tear et al., 2003; Ting and Lee, 2007; Tomasi et al., 2008) (Figure 26). R7 and R8 reach their targets in two stages: First they sequentially extend to temporary layers. A later process of stabilization results in their concurrent termination to the desired layers (Ting et al., 2005).These connections are under the control of several distinct molecular signals.

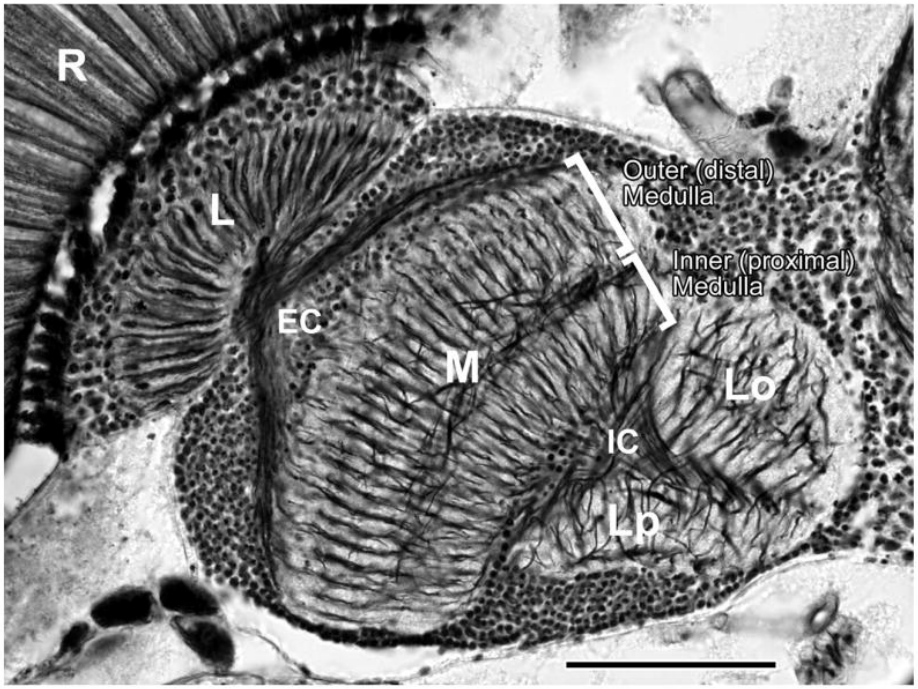

Figure 25. Horizontal Section of a *Drosophila* Visual System from a Preparation Stained by the Bodian Method. Up: direction of the animal's anterior. Horizontal rows of cartridges parallel to the equator in the lamina neuropile (L) connect to horizontal rows of columns in the medulla (M) by means of sheets of fibres that traverse the external chiasma (EC). The medulla is subdivided into two parts, outer (distal, strata M1–M6) and inner (proximal, strata M7–M10), by its middle stratum, which connects to Cuccatti's bundle and contains laterally-orientated axons of many medulla tangential neurons. Each input terminal from the lamina terminates in a specific stratum of the outer (distal) medulla. R, retina; IC, internal chiasma; Lo, lobula; Lp, lobula plate. Scale bar: 50 μm. (Takemura et al., 2008)

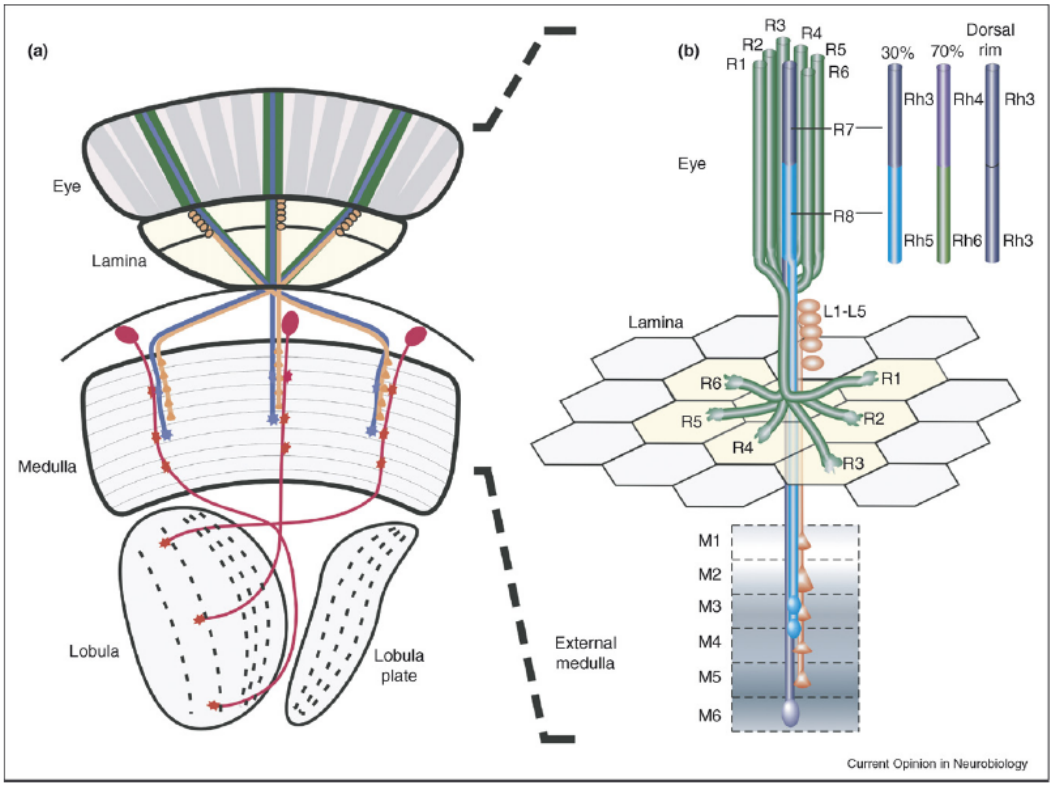

Figure 26. R cells Terminate in Various Regions of the Optic Lobe. (a) The medulla, lobula and lobula plate are organized into layers. Photoreceptor axons project into the lamina and medulla (green and purple lines) to form synapses with lamina (orange) and medulla (red) neurons, respectively, whereas lamina neurons make connections to the medulla, and medulla neurons connect to the lobula and lobula plate (only 1 of ~50 types of medulla neurons and none of the centrifugal neurons are shown). (b) Connection patterns of the photoreceptor neurons. The eye comprises ~750 ommatidia (green columns), each of which contains eight photoreceptor neurons termed R1–R8. The axons of R1–R8 form a common bundle to innervate the lamina and medulla in an invariant pattern. The R1–R6 axons defasciculate from the common bundle at the lamina and extend laterally to form synapses with the lamina neurons in the neighboring columns. The connection pattern of R1–R6 in the lamina is stereotyped and reflects the organization of their rhabdomeres (light-sensing structures) in the eye. The R7 and R8 axons extend through the lamina and terminate in two medulla layers, termed M3 and M6, respectively. Similarly, the lamina neurons (L1–L5) make layer-specific connections in the medulla (see Figure 3c) (Ting and Lee, 2007).

Receptor tyrosine phosphatase Dlar, classical cadherin N-cadherin (Ncad) and scaffolding protein Liprin-α have been shown to work together in a complex pathway to influence all R cell subtype connections. They can physically associate as Dlar binds to both Ncad and Liprin via its phosphatase domain (Prakash et al., 2009). Their expression

during development overlap as they are all distributed in both R cell axons and their targets in the lamina plexus and within the medulla neuropil (Lee et al., 2001; Clandinin et al., 2001; Choe et al., 2006) However, the localization of any of these proteins in a developing fly is not dependent on the activity of the other (Prakash et al., 2009). They all regulate R7 target selection as R7 axons terminate early in the M3 layer of *Ncad, liprin-α and Dlar* eye-specific mosaic mutants (Lee et al., 2001; Clandinin et al., 2001; Choe et al., 2006). Ncad plays a unique role in the regulation of topographic map formation: In *Ncad* mosaic mutants, R8 axon terminals exhibit defects in the formation of a normal topographic map (Lee et al., 2001; Clandinin et al., 2001). Furthermore, it has been shown that Ncad alone is required for the first phase of R7 and R8 layer-selection (Ting et al., 2005) while Ncad, Dlar, and Liprin-α cooperate to regulate the second phase (Clandinin et al., 2001; Ting et al., 2005; Choe et al., 2006;Prakash et al., 2009). Lastly with Ncad and Dlar, a phototaxis defect associated with R7 and R8 target selection has been demonstrated as *Ncad* and *Dlar* mosaic mutants prefer visible over UV light (Lee et al., 2001; Clandinin et al., 2001).

The regulation of R1-R6 cell target selection by these three proteins, further shows that they do not form a simple linear pathway (Prakash et al., 2009). In R1-R6 mutants, axons either completely fail to defasciculate from the ommatidial bundle and extend toward their targets in the lamina or make weak, morphologically abnormal extensions once within the lamina plexus (Lee et al., 2001; Choe et al., 2006). However, expression of a transgene of any one of these three proteins fails to rescue the mutant defects caused by inhibiting either of the other two proteins in R1-R6 target selection (Prakash et al., 2009). Additionally, only Ncad is required in lamina neurons for R1-R6 cell target selection, as

only Ncad shows R cell axons failing to extend to their corresponding targets in mutant lamina neurons (Choe et al., 2006). What's more, double mutants display more severe phenotypes than single mutants. For example, 40% of *Ncad, Dlar* double mutants and 60% of *Ncad, Liprin*-α double mutants exhibit no extension of R4 axons to targets as opposed to 20% in *Ncad* single mutants (Prakash et al., 2009). Lastly, Ncad and Dlar downregulate Liprin-α when it is not bound to Dlar (Prakash et al., 2009). Thus, Dlar, Ncad, and Liprin- α present a pathway in which the proteins have both overlapping and independent roles in R cell targeting despite forming a complex together (Prakash et al., 2009).

Another set of three proteins that work together to control R cell projection to *Drosophila* optic ganglions is Protocadherin Flamingo(Fmi), receptor tyrosine kinase Anaplastic lymphoma kinase (Alk), and LDL receptor repeat- containing secreted factor Jelly Belly (Jeb). Alk is activated by Jeb—which is essential for Alk's role in R cell targeting. Fmi is localized to all R cells and in target neurons in the lamina and medulla while Jeb is expressed in the former and Alk, in the latter (Senti et al., 2003; Bazigou et al., 2007). In *fmi*, *Alk*, and *jeb* mutant mosaic adult flies, R1-R6 axons extend to inappropriate targets in the lamina. Most recently, it has been shown that R1-R6 axon targeting is governed non cell-autonomously by a balance of Flamingo activity between an R cell and its neighbors. For instance, overexpression of *fmi* in a single R cell subtype is sufficient to cause mistargeting by adjacent axons (Chen and Clandini et al., 2008). Meanwhile, R8 axons of the three mutants, either terminate at superficial levels in the medulla, fasciculate with R8 axons in adjacent medulla columns, or terminate incorrectly in the

M6 layer of the medulla (Lee et al., 2003; Bazigou et al., 2007). Finally, R7 axons of the three mutants experience defects most likely as a consequence of the impact on R8 axon targeting (Senti et al., 2003; Lee et al., 2003).

Lastly, transmembrane protein Golden Goal (Gogo) has been shown to be required for R8 axons to properly reach their targets in the medulla. It is expressed in all R cell neurons and localizes to growth cones (Tomasi et al., 2008). In *gogo* mutants, R8 axons stall at the surface of the medulla (layer M1) and fail to innervate the medulla column (Tomasi et al., 2008). In fewer cases, R8 axons bypass the M3 layer and terminate in the M6 layer.

Chapter 2 Materials And Methods

2.1 For Actin Binding assays

2.1a.Molecular cloning

2.1a.1 Restriction enzyme digestion

All restriction digestion reactions contained clean DNA, 5 units of enzyme for every 25 µl reaction, and a final concentration of 1X buffer optimized for the specific restriction enzyme. The reactions were incubated at 37˚C for 1 hour.

2.1a.2 DNA Gel electrophoresis

0.7-1% agarose gels were made using agarose (Fisher) and 1X TAE (Tris base, Acetic acid, EDTA) buffer. After boiling the agarose with the TAE in a 250 ml Erlenmeyer flask, and cooling, 5-6 µl of Ethidium Bromide were added for visualization. The gel was then cast and allowed to cool for an hour. After removing the comb, samples were loaded and then the gel was run for approximately 1h30 minutes @ ~100V.

2.1a.3 Gel extraction/ band purification

After running an agarose gel, the band in question was cut out using a surgical blade. The band was placed in a 1.5ml Eppendorf tube and weighed. The Qiagen QIAX II DNA extraction kit for agarose gels was used to extract and purify DNA. The agarose gel was dissolved in QX1 buffer, whose volume used was equivalent to three times the weight of the DNA band isolated. Anywhere from 10 µl to 30 µl of QIAEX II silica beads were added to the suspension. The tube was then placed in a heating block at 50˚C for 15 minutes with gentle shaking every 2-3 minutes. The tube was then centrifuged at top speed for 30 seconds. The supernatant was removed and discarded. The pellet was

washed in QX1 buffer. The tube was centrifuged again, supernatant removed again, and the pellet was washed with PE buffer. After centrifuging, the supernatant was removed and the pellet was allowed to air dry until it turned slightly white in color. Then an appropriate volume of 10 mM Tris-HCl pH 8.0 was added to the pellet. The tube was vortexed and then placed on a heating block at 50˚C for 10 minutes. The tube was then centrifuged at top speed for 1 minute. Afterwards the supernatant was transferred to a new tube. The sample is ready to use at this point.

2.1a. 4 Generation of recombinant plasmid

All vectors used were cut with 30-60U of enzyme and digested overnight @37C to ensure complete digestion.

The pBluescript II SK(+), a 2961-bp phagemid derived from pUC19 was used as an intermediate vector to subclone Dunc115L into pT7Flag1(Figure 27) .

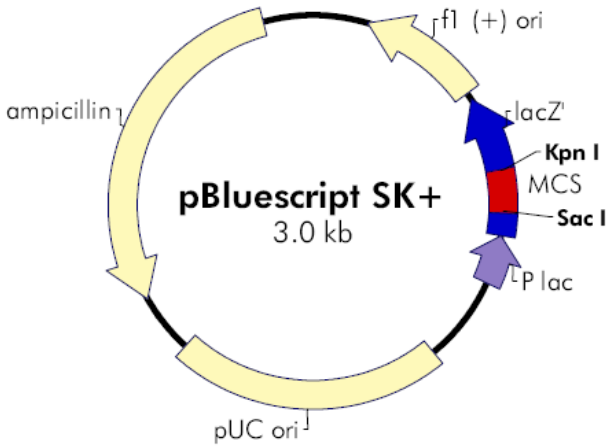

Figure 27. Organization of the pBluescript II SK(+) Vector.

The pUASTattB, a 8489bp vector was used to subclone Dunc115L and S for the purposes of generating *dunc115* mutant rescues. It is a pUAST vector that has been modified with loxP and attB recombination sites (Bischof et al., 2007)(Figure 28).

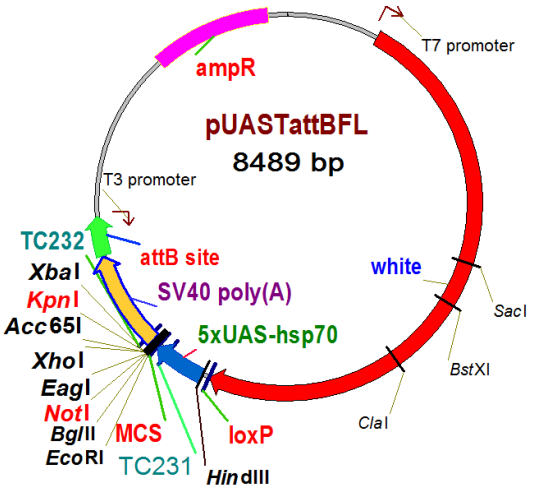

Figure 28. Organization of the pUASTattB Vector.

The pT7-FLAG-1, a 4889 bp *E. coli* expression vector was used to generate Dunc115L and S FLAG fusion proteins. DNA fragments inserted into this vector must be placed in frame to it. An N-terminal Met-FLAG fusion protein containing the FLAG epitope (DYKDDDDK) will result as consequence of proper subcloning to the polylinker site (Figure 29).

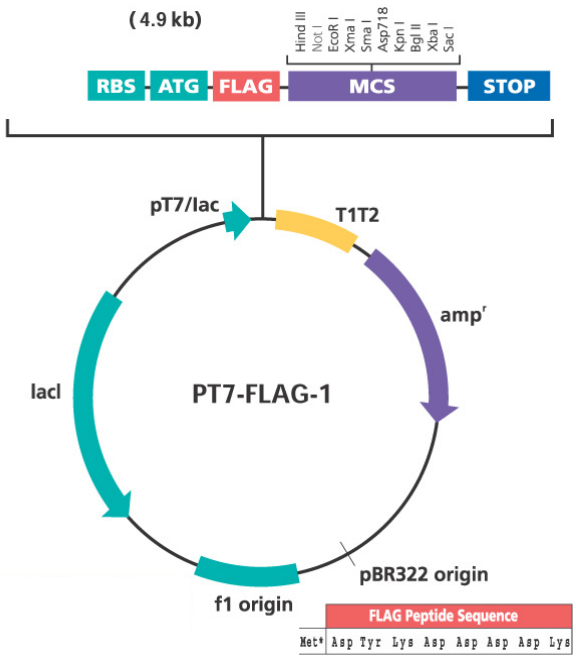

Figure 29. Organization of the pT7-Flag-1 Vector.

2.1a. 5 Dephosphorylation of vector using Shrimp Alkaline Phosphatase (SAP)

In order to dephosphorylate the vector prior to ligation with insert, 85 µl of digested vector was mixed with 5ul of 1u/µl Shrimp Alkaline Phosphatase (Promega) enzyme along with 10 µl 10X SAP buffer. The reaction was incubated at 37C for 15 minutes and stopped by heating at 75˚C for 15 minutes. The tube was then placed on ice for 5 minutes and then spun at top speed for 1 minute. At this point, the vector is ready to use.

2.1a. 6 Ligation

T4 DNA ligase (Fisher), ligase buffer, vector DNA and insert DNA were combined in a 1.5 ml Eppendorf tube for each reaction. Vectors were diluted in a 100 µl final volume and inserts were resuspended in a 30 µl volume. Different vector: insert ratios were used. Ingredients were mixed by pipetting up and down. A 16˚C water bath was set up and

ligation reactions were carried out over 4 hours. After the reaction, tubes were placed on ice for five minutes and then spun for 1 minute.

2.1a.7 Transformation

Calcium chloride competent DH5α cells made in the lab were used for all transformations. 100 µl of competent cells were thawed at room temperature and then added to a DNA sample of 1-10 µl in a 0.5ml Eppendorf tube. Mixing was done by flicking the tube. The tube was then placed on ice for 20 minutes. Afterwards, the tube was heat shocked by transfer to a 42˚C water bath for 90 seconds. Then the tube was placed back on ice for 10 minutes. After this, the contents of the tube were transferred to a 15ml conical tube and 500 µl SOC were added. The conical tube was then placed in a 37˚C ground shaker at 250 RPM for 50 minutes. Afterwards, the contents of the tube were placed into a 1.5 ml Eppendorf tube which was spun at 6000 RPM for 5 minutes in a tabletop centrifuge. Pellets were then resuspended in 200 µl LB broth and plated onto LB plates with the appropriate antibiotic. Plates were allowed to grow at 37˚C for 16 hours and then clones were screened for and selected.

2.1a.8 Selection of clones

<u>Ampicillin</u>

Selection of transformants was performed by plating on LB plates containing 70 µg/µl of Ampicillin. To make plates, a 100mg/ml solution of Ampicillin was made by dissolving it in water.

Blue- white

For blue/white selection, 20 µl isopropylthio-B-D galactosidase (IPTG)(200 mg/ml) and 100 µl 5-bromo-4-chloro-3-indolyl-B-D galactosidase(X-gal)(20 mg/ml) were mixed together on LB plates containing 70 µg/µl of Ampicillin. Transformants containing uncut pBluescript vector are blue. Transformants bearing a recombinant plasmid have a disrupted lac-Z gene and are therefore white instead of blue.

Chloramphenicol

Selection of transformants was performed by plating on LB plates containing 100µg/ml of Chloramphenicol. To make the plates, a Chloramphenicol solution was made by dissolving in ethanol to a 100 mg/ml concentration.

2.1a. 9 Growing overnight culture of transformant clones

Transformants were plated overnight at 37˚C. Single colonies were tip-picked onto a grid and grown overnight at 37˚C. Colonies from the grid were then cultured in 4 ml of LB liquid media containing 5 µg/ml of Ampicillin or Chloramphenicol and placed overnight in a ground shaker at 37˚C and 200 RPM.

2.1a.10 Plasmid DNA isolation: Miniprep

The QIAprep Miniprep kit was used for all minipreps. It is based on the alkaline lysis of bacterial cells followed by adsorption of DNA onto spin columns with silica beads at a high salt concentration. The procedure consists of the three standard steps 1) preparation

and clearing of bacterial lysate 2) adsorption of DNA onto the QIAprep spin columns 3) washing and elution of the plasmid DNA.

Plasmid DNA was isolated using a mini-prep kit (Qiagen). The cells were pelleted from culture by centrifugation in 1.5 ml tubes at top speed for two minutes and the supernatant was discarded. This takes three rounds of centrifugation as the cells were grown overnight in 4ml of LB broth. The cells were resuspended in 250 μl of P1 buffer, making sure to pipette up and down until the cells were completely in suspension. Cells were lysed by adding 250 μl of P2 lysis buffer. The lysis buffer was neutralized by adding 350 μl of N3 buffer. Samples were then centrifuged for 10 minutes at top speed and the supernatants were applied to spin columns and centrifuged for one minute at 6000 RPM. The flow-through was reapplied two more times to the column, centrifuging after each round for one minute. The flow-through was discarded after the final spin for one minute. Spin columns were then washed 2X each with PB and PE buffer along with top speed spins for 50 seconds. The flow-through was discarded after each spin. A final spin at top speed for 1 minute was done to remove residual wash buffer. The columns were then transferred to clean 1.5 ml tubes and the DNA was eluted from the columns with 10mM Tris-HCL pH 8.0. DNA elution was conducted by three rounds of adding 30 μl 10mM Tris-HCL pH 8.0 to the columns, and centrifuging at 6000 RPM for 1 minute. After the final elution, the samples were centrifuged at top speed for one minute. The DNA concentration and purity was determined by OD_{260} and OD_{280} spectrophotometric readings using Nanodrop 2000c (Thermo Fisher).

2.1a.11 Sequencing

Isolated plasmid DNA from each clone was submitted to GeneWIZ (North Brunswick, NJ) at a concentration of 50-60ng/µl. The necessary primers were included at a concentration of 2.5pmol/µl. Sequencing of the insert was considered complete when the sequence from opposing sides overlapped with high fidelity. It took 4 rounds of sequencing per clone to sequence the full insert. Sequences were analyzed using Applied Biosystems Sequence Scanner v1.0 and Finch TV.

2.1a.12 Generation of pT7Flag1 clones

Dunc115L

Dunc115L cDNA was originally inserted into pOT2 via EcoRI (5') and XhoI (3'). We excised it by EcoRV (5') and XhoI (3') enzyme digestion and subcloned it into a EcoRV/XhoI cut pBSII vector to give pBS-Dunc115L (Figure 30A). In order to subclone Dunc-115L into pT7Flag1, we generated a 2.4kb PCR product of pBS-Dunc115L that contained only the coding sequence of Dunc115L. This is because there is a stop codon upstream of the coding region (marked in red in Figure 30B) and this would prevent the Flag tag from being generated attached to the Dunc115L protein. We used the following primers: **Up115L** 5'-ATTGCGGCCGCCATGGGTAAACA and **Dwn115L** 5'-CGGGGTACCCTAGAAGAGCTTCACACG. We then cut our PCR product and pT7Flag1 with KpnI and NotI. After a ligation and subsequent transformation, clones were identified that contained Dunc115L in frame to pT7Flag1. These clones were sent out for sequencing and found to be correct. Clone 1J was used to generate Dunc115L protein in the acting binding assay.

A)

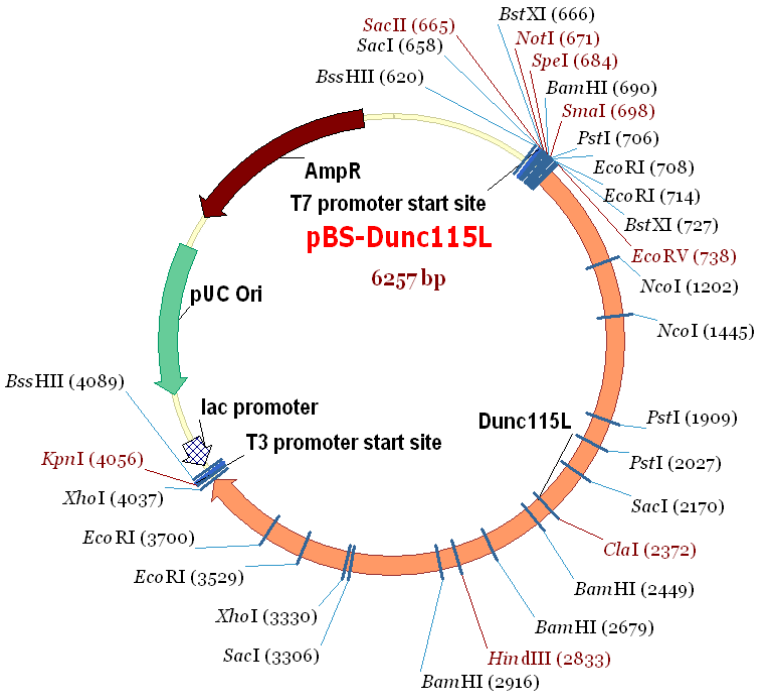

B) Upstream PCR primer

NotI

Up115L 5′-ATTGCGGC**CGCCATGGGTAAACA**

ggcacgagtgccgtcggtttcgttgctggtgcggtgcggtgttttttgctggtcgcag
ctccgatttgagaatcagacattcaggcatttcaaaaaggccaccattttccgctgtga
tctttgtcgtcaaatttaaagtgcgagaccacaccaaaagcaaatcgcacattcgtcat
tcgagctgcgaacgcattattaaccacactcctatccagactcacacatgtttacagtc
taacaatcgtgctacgcagattgcgaatgcatacggcgaaagatacaaatagaaaaaat
cttagcagaagaaaattttgttagtgaagtgaagaggaagtagtggtgacctgtgcgc
gagtatttgtgctttccccgtgtgtgtctctctgttctagtgtgcgtgattccctcccc
cgttttgcaggcgaaaaagcgaagagcacagcagtatatagtatct**cgcc**

atg ggt aaa caa aaa atc tac tgt gcg aaa tgc acg aag aag tgc

M G K Q K I Y C A K C T K K C

tcc ggc gag gtg ctc cgc gtg gcg gac aac cac

S G E V L R V A D N H

C) Downstream PCR primer

KpnI

Dwn115L 5′- CGGGGTACCCTAGAAGAGCTTCACACG

gag ttc tat cgg cta ccc cag tgg cga cgc aac gag ctg aag cgg

E F Y R L P Q W R R N E L K R

cgt gtg aag ctc ttc taggaggcaagtggaaggcgcagcatgcgaggatagc

R V K L F *

aacccaagtggaggaggaggctg

Figure 30. Generation of pT7FLAG-1-Dunc115L, A) Organization of pBS-Dunc115L B) Upstream PCR primer used to generate Dunc115L minus the noncoding exon region. Notice the stop codon marked in red. C) Downstream primer used to generate Dunc115L.

Dunc115S

Dunc115S cDNA was originally directionally inserted into pOTB7 via EcoRI (5') and XhoI (3') (Figure 31A). In order to subclone Dunc-115S into pT7Flag1, we generated a 2.3kb PCR product of pOTB7-Dunc115S that contained only the coding sequence of Dunc115S. Like with Dunc115S, there is a stop codon upstream of the coding region (marked in red in the Figure 31B) and this would prevent the Flag tag from being generated attached to the Dunc115S protein. We used the following primers: Up115S 5'-GCCGAATTCC GTTGTGATGTATATATTAA3' and Dwn115S 5'GGAAGATCTTTACAATTTTGCGTTAGC3'. We then cut our PCR product and pT7Flag1 with EcoRI and BglII. After a ligation and subsequent transformation, clones were identified that contained Dunc115S in frame to pT7Flag1. These clones were sent out for sequencing and found to be correct. Clone 2H was used to generate Dunc115S protein in the acting binding assay.

A)

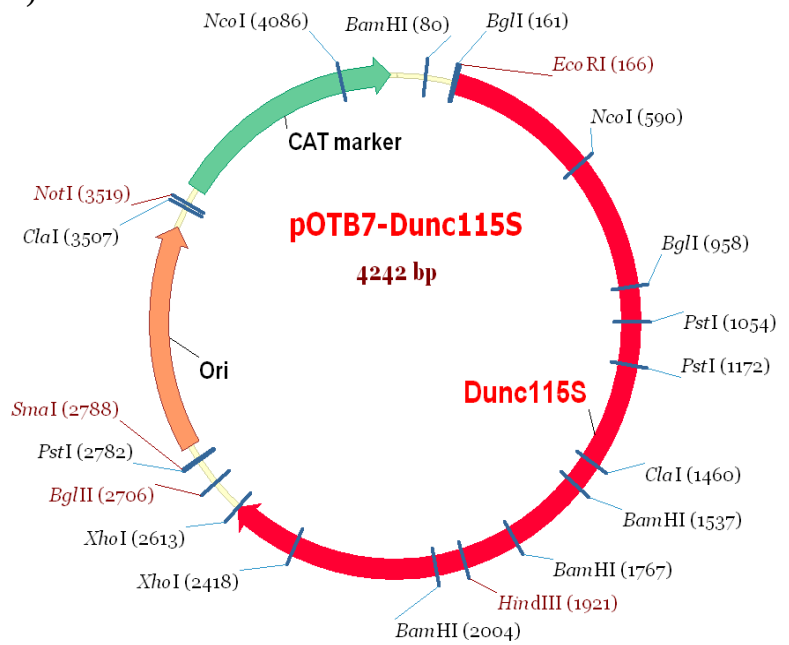

B) Upstream PCR primer

EcoRI

Up 115S 5′-GCCGAATTCC GTTGTGATGTATATATTAA3′

Ggcacgaggaacgcacacacacatacaacgaatctcgcaacatacgatatacgataagt
tgtg

atg tat ata tta ata tat atat cca ttc cga aac atc cac aaa

M Y I L I Y

cag aca aga cca ga

C) Downstream PCR primer

Bgl2

Dwn115S 5′GGAAGATCTTTACAATTTTGCGTTAGC3′

Tgc gct aac gca aaa ttg taa ctg aga aca act ata tga aag gaa

C A N A K L *

cat aaa atc cca ata

Figure 31. Generation of pT7FLAG-1-Dunc115S A) Organization of pOTB7-Dunc115S B) Upstream PCR primer used to generate Dunc115S minus the noncoding exon region. Notice the stop codon marked in red. C) Downstream primer used to generate Dunc115S.

2.1b Generation of Dunc115 fusion proteins: TnT T7 coupled reticulocyte lysate assay.

The TnT T7 coupled reticulocyte kit was used in order to generate FLAG-Dunc115 fusion proteins *in vitro* from Flag-Dunc115 DNA circular constructs. The lysate, and RNA polymerase were placed on ice while the other items were thawed at room temperature. Once all ingredients were thawed, the following were combined in a 1.5 ml Eppendorf:

Tnt lysate	25µl
TnT reaction buffer	2µl
TnT T7 RNA Polymerase	1µl
Amino Acid Mix, minus Leucine (1mM)	0.5µl
Amino Acid Mix, minus Methionine (1mM)	0.5µl
RNAsin ribonuclease Inhibitor	1µl
DNA sample (1ug/ul)	2µl
Water	18µl

The components were mixed gently by pipetting up and down. The tube was then incubated at 30˚C for 90 minutes. The reaction was stopped by placing the tube on ice.

2.1c Actin binding protein spin-down assay

The Actin Binding kit (Cytoskeleton Inc) was used to see if Dunc-115 proteins bind to actin. The Spin-down assay uses differential centrifugation to distinguish between non-actin binding versus actin binding proteins and also to qualify the activity of the actin-

binding proteins toward actin. Actin is a 43kD protein (Figure 32). It can exist in monomeric (Globular-actin) and multimeric (Filamentous-actin) forms. We used the kit under conditions that specifically tested for proteins that bind to the sides of Filamentous-actin. There are two types of such proteins: those that bind to one actin filament and those that are able to crosslink filaments by binding to two. We were interested in surveying the actin bundling activity of our protein. To do this, a centrifugation of 14,000 xg is carried out for one hour after the test protein is combined with F-actin in a tube. At this centrifugation speed, single filaments will remain in the supernatant even if they bind to the test protein. F-actin will pellet but only if it's in a large crosslinked bundle with the test protein. Still, some pelleting occurs as a result of self aggregation of actin. The key lies in observing if the protein pulls out more actin in the pellet versus the supernatant. This implies it is causing actin to polymerize to a greater extent than if it were alone.

Lyophilized actin was resuspended to 1 mg/ml by adding 250µl General Actin Buffer to 250ug of protein and pipetting vigorously up and down. Then it was left on ice for 30 minutes. Afterwards, 25 µl Actin Polymerization buffer were added to the actin tube with heavy pipetting up and down. The tube was incubated at room temperature for 1 hour. After these manipulations, the tube represents an actin stock of 23mM.

α-actinin is a 116kD protein (Figure 32). Actinin has been documented as being able to crosslink actin filaments and therefore serves as a positive control for actin binding. Lyophilized α-actinin was reconstituted to 1mg/ml by adding 50ul ddH_2O to 50µg of protein.

Bovine serum albumin is a 68kD protein (Figure 32). It does not bind to actin and serves as a negative control. Lyophilized BSA was reconstituted to 3.4mg/ml by adding 1 ml to 3.4mg in the tube.

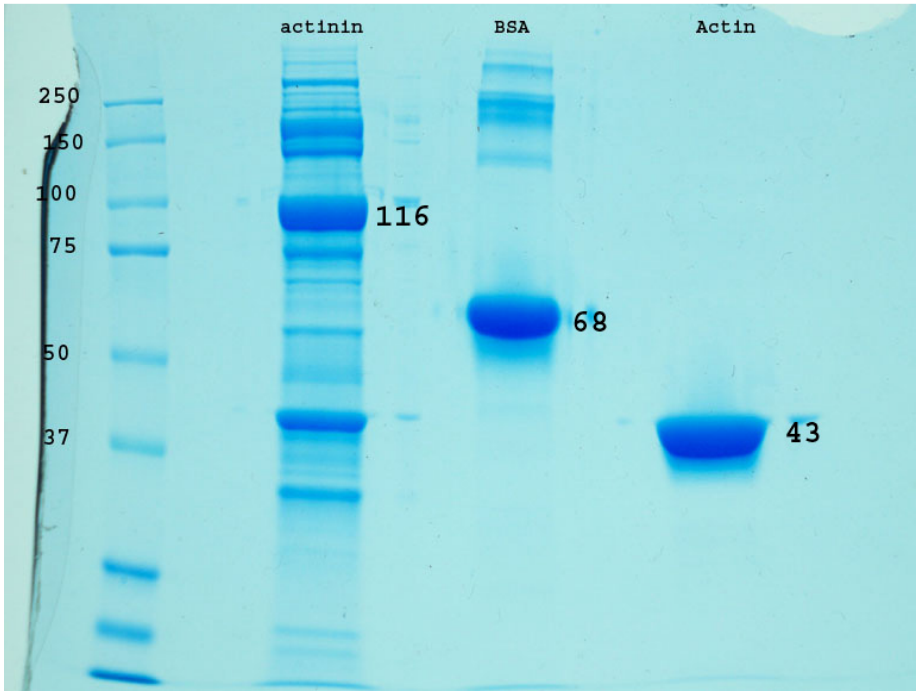

Figure 32. Actinin, BSA, and Actin. Coomassie stain of 10% Tris/Glycine gel showing purified samples of the three proteins: Actinin, 116kD; BSA, 68kD; Actin, 43kD.

To test the binding, several tubes were set up. Tube 1 was F-actin alone. Tube 2 was α-actinin alone. Tube 3 was α -actinin +F-actin. Tube 4 was BSA+F-actin. Tube 5 was Dunc115L alone. Tube 6 was Dunc115L +Actin. Tube 7 was Dunc115S alone. Tube 8 was Dunc115S + Actin. Tube 9 was rabbit reticulocyte lysate. Tube 10 was lysate + actin.

40 ul F-actin buffer were added to tubes 2, 5, 7, 9. 40 µl F-actin stock were added to tubes 1, 3, 4, 6, 8, 10. 10 ul Dunc115L were pipetted into tubes 5 and 6. 10 ul Dunc115S were added into tubes 7, and 8. 10 µl alpha-actinin (positive control) and 2 µl 1M Tris-HCl pH 6.5 were pipetted into tubes 2 and 3. 2 µl of BSA and 9 µl of H_2O were added to tube 4.

10 µl 1X PBS were pipetted into tube 1.10µl of lysate were added to tubes 9, and 10. The tubes were incubated at room temperature for 30 minutes.

The tubes were centrifuged at 14,000 xg for 1 hour. Supernatants were removed and placed in different tubes from the pellets.

The pellets were resuspended in 50 ul H_2O and pipetted up and down for 2 minutes. To all tubes, 10 µl of 6X sample buffer (with 5% β –Mercaptoethanol) were added for a total of 60 µl and then 25 µl were loaded into a PAGE gel for visualization.

2.1d. Visualization of proteins

2.1d.1 Western

When running proteins made by using the lysate kit:

5µl out of 50 µl of lysate mix, 20 µl H_2O, and 5 µl 6X SDS sample buffer containing 5% β - Mercaptoethanol were combined in a tube for a total volume of 30µl. When running pure proteins from a kit, 1 -10 µl of protein were used, the water was adjusted, and 5 µl 6X SDS sample buffer was still used. When running actin binding assays, 10 µl 6X SDS sample buffer were used for a 50 µl protein solution.

25 µl of each sample were loaded onto a precast 10% SDS PAGE precast gel (Promega). 10 µl of ladder were loaded and the gel was run for 1h 20m at 108V. The gel was transferred to a sheet of Whatman paper that had been pre-immersed in transfer buffer. A sponge was added below the Whatman. A nitrocellulose sheet, also soaked in transfer buffer, was placed on top of the gel. The right corner of the sheet was cut to account for orientation. A glass Pasteur pipette was used to roll away any bubbles. Then another

soaked Whatman was placed on top of the nitrocellulose sheet and then a sponge was placed. The cassette was closed and then placed in the transfer chamber. The transfer was run at 238 mA for 52 minutes. Afterwards, the gel was discarded and the nitrocellulose membrane was blocked in 5% TBST+ milk for 1 hour. Then the blocking solution was drained and the appropriate dilution of primary antibody was poured onto the nitrocellulose sheet in a small rectangular plastic box. It was shaken for 1 hour. Afterwards, the nitrocellulose sheet was quickly washed 3X in 5% milk +PBST and then 3 five minute washes. Then an appropriate dilution of secondary antibody was poured onto the sheet and shaken for 1 hour. Afterwards, the nitrocellulose sheet was quickly washed 3X in 5% milk +PBST and then one five minute wash, followed by two 10 minute washes. Then 30 ml of Supersignal West Pico chemiluminescent substrate were poured onto the sheet and allowed to shake for 5 minutes. Afterwards, the sheet was covered in saran wrap, taped to a cassette and then developed in the x-ray room.

Exposures varied from 1 second to 30 minutes depending on the concentration of proteins encountered.

2.1d.2 Coomassie stain

After running the gel, it was removed from the plastic. It was then placed in a microwavable container and enough Coomassie was added to fully immerse the gel in the stain. It was then placed on a shaker for 3 hours at room temperature. Within the hour, the strongest bands can be seen slightly as this point. After three hours, the stain was drained, destaining solution was added, and the gel was placed back on the shaker for 1 hour. The

destaining step was repeated until the bands were clearly visible and excess Coomasie no longer came off the gel. At this point, the gel was drained and a picture was taken.

2.2 For genetic interactions of Dunc-115 with Robo and Rho GTPases

2.2a Stocks

2.2a.1 Maintenance of Stocks: *Drosophila* Husbandry

Stocks in current use were kept at 25˚C in plastic vials or bottles with fly food at the bottom. Fly stocks in storage were kept at 18˚C. Fly stocks were flipped into a new vial every two weeks if reared at 25˚C, and every month if being reared at 18˚C.

2.2a.2 Fly Food Medium

First, 226.8 g of Jazzmix (Fisher scientific) were stirred into 1200 ml of H_2O in a Groen cooker. This mixture was boiled for approximately 7 minutes with regular stirring. Propionic acid, benzoic acid and methyl paraben contained in JazzMix act as antimicrobial agents. The food was then cooled for five minutes before dispensing. The mixture was poured into vials or bottles and allowed to harden. Yeast was sprinkled on the surface prior to putting flies in the vessels. This recipe yields 37 bottles or 131 vials.

2.2a.3 Fly strains: The following stocks have been used:

yw; P[dunc-115^{KG03651}], yw; GMC-rac1/TM6B, *yw; GMR-Mtl^{V15}*/ CyO

yw ; *GMR-Cdc42^{V12} /CyO, yw; If/CyO; TM2/TM6B, yw; slit^{1}robo^{5}/CyO*

yw; Pin/CyO, FRT2A Rac1/TM6B, w; Rac2; yw; GMR-Gal4

w; robo2^{4} P[w+] FRT40A/CyO, robo3^{1} FRT40A/CyO

2.2b. Staining

2.2b.1 Collection of Embryos

Canton S and Dunc-115 adults about five days old were put into a collecting chamber for 1 to two days for conditioning, and eggs were collected overnight for approximately 18 hours on grape juice plates coated with yeast paste. The plates were exchanged and embryos were removed from the overnight plate by using a small paint brush and washing with water in a collecting nylon basket, making sure to rinse well as to remove residual yeast.

The grape plates were made by boiling together 9.0 g of Fly agar(Sigma) , 23.2 g of glucose (Sigma), 11.6g sucrose, 170.4 ml grape juice, 220 ml water, and 7.2 g Baker's dry yeast. The mixture was cooled to 60˚C and then 4.5 ml Acid Mix A (16.7 ml 100% Propionic acid, 1.0 ml 85% Phosphoric acid, 22.3 ml H_2O) and 8.8 ml of 1.25N NaOH was added. The mixture was then poured into small Petri plates that fit the collecting chamber and allowed to harden. Water and yeast were mixed to form a paste that is spread on these plates.

2.2b.2 Fixation of Embryos

To remove the chorion, the embryos were soaked in 50% bleach for three minutes. The embryos were then rinsed thoroughly with water and placed into a glass test tube containing a mix of 1 ml of heptanes and 1ml of 45% paraformaldehyde with the fixative phase at the bottom. The vial was agitated for 1 hour at room temperature, followed by the removal of the aqueous phase leaving behind the heptanes and embryos. To remove

the vitelline membrane, 1 ml of methanol was added to the tube and shaken vigorously for 1 minute. Those embryos that had been devitellinized sank to the bottom and were washed three times with methanol following the removal of the liquid. Embryos were stored in methanol at -75˚C. Prior to staining, the embryos were re-hydrated by washing 2 times for five minutes and one time for 30 minutes with PBT. Embryos were blocked for 1 hour with BSTN prior to staining.

2.2b.3. Motoneurons and CNS dissection (light microscope phenotypic analysis only)
With forceps, embryos were gently placed dorsal side up onto a slide. Using a sharp tungsten needle, a longitudinal cut from the posterior end all the way up to between the optic lobes was made. With the edge of the needle, the flaps of the body wall were pushed down onto each side of the slide so that they adhere. Then the guts, trachea, and fat were cleaned out, adding 1XPBS to assist in the clean-up. This cleanup process will expose the ventral nerve cord for CNS analysis and the inner surface of the bodywall musculature for motoneuron analysis.

2.2b.4 Motoneurons and CNS Staining

To investigate the motoneurons, embryos were incubated overnight at 4˚C with 1:20 Fas II antibody 1D4 in BSTN. To remove residual antibody, the embryos, were washed, 4 times for 15 minutes each in PBT. Subsequently, embryos were blocked in BSTN for one hour and incubated overnight at 4˚C with 1:200 diluted Cy5-conjugated goat anti-mouse secondary antibody (Jackson ImmunoResearch Laboratories, Inc.).

Embryos were washed 4 times in PBT for 15 minutes each wash. Prior to mounting, embryos were put through a 25% and 50% glycerol series. The embryos were put in 70% glycerol plus an anti-quenching agent for mounting.

2.2c Microscopy

2.2c.1 Confocal microscopy

A Nikon PCM-2000 confocal microscope equipped with dual HENe-Argon lasers was used to analyze the samples. The scope has a FITC filter set, power stage control and the Simple-32 computer software.

2.3. For Bioinformatic analysis

2.3a. Obtanining fully sequence genomes 12 *Drosophila* species

Firstly, eleven fully sequenced genomes were downloaded from Flybase and formatted in FASTA format.

2.3b Identifying Dunc-115 orthologs: BLAST

We then ran BLAST (Altschul et al., 1990) on the cDNA sequence of Dunc-115L from *Drosophila melanogaster* against each *Drosophila* genome in order to identify potential orthologs. We looked at genomes closest to *D. melanogaster* first. We looked for gene sequences within BLAST info that share orthologs. Afterwards, we translated the coding sequence from each ortholog.

Similarly, we ran BLAST on Dunc-115L against two other Dipterans: *Culex pipiens* (house mosquito) and *Anopheles gambiae* (African malaria mosquito) and aligned each

protein sequence to Dunc-115L. We also performed searches for additional isoforms of Dunc-115. As with Dunc115L, we ran BLAST (Altschul et al., 1990) of the cDNA sequence of Dunc-115M, and S from *Drosophila melanogaster* against each *Drosophila* genome in order to identify potential orthologs.

2.3c. Aligning DNA and protein sequences: Clustal W

We then aligned each ortholog with the protein sequence of Dunc-115L using ClustalW. After aligning each ortholog separately with Dunc-115L, we aligned all 14 protein sequences together with ClustalW in order to verify conservation across species (Figure 7).

2.3d. Generating phylogenetic tree: Seqboot, Consense, Ape

Using the PHYLIP package (Felsenstein, 1981), we then generated 100 bootstraps (**Seqboot**) in order to construct a maximum likelihood tree. It allows you to generate multiple data sets that are resampled versions of input data set. With **Dnaml**, the purpose of running multiple data sets is to generate a big output file as well as tree file with trees from 100 data sets. Then we ran **Consense** and **Ape** from the **R-project** package **(**Paradis et al., 2004**)** to visualize a majority rule consensus tree.

2.3e. Quantify conservation of Dunc-115L across Drosophila species: PAML

In order to quantify the level of sequence conservation of Dunc-115L across *Drosophila* species, we applied a maximum likelihood algorithm known as PAML (Yang, 1997), which allowed us to calculate the ratio of nonsynonymous-to-synonymous nucleotide substitutions Ka/Ks for each codon. In the case of nonsynonymous substitutions (Ka), a

substitution of one base for another in a gene coding for a protein produces a change in the translated amino acid sequence whereas synonymous substitutions (Ks) do not (Nekrutenko et al., 2002). The comparison between the number of nonsynonymous substitutions (Ka), and the number of synonymous substitutions (Ks) tells us whether deleterious mutations are selected against (negative selection) or whether mutations that may be advantageous in response to an environmental change are favored (positive selection). When positive selection dominates, the Ka/Ks ratio is greater than 1 whereas when negative selection dominates, the Ka/Ks ratio is less than 1(Nekrutenko et al., 2002). When these two forces are in equilibrium, the Ka/Ks ratio is close to 1.

2.3f Mapping intron-exon borders

We performed a BLAST on the genomic sequence of Dunc-115 (CG31352) against the genomic sequence of Dunc-115 from other species. We sorted the results by regions of homology in order to spot the coding regions. We first did this with species closest to Dunc-115 in *D.melanogaster*: *D. simulans, D. sechellia, D. yakuba, D. erecta.* We then isolated each Dunc-115 genomic sequence and performed ClustalW sequence alignment on the whole genomic sequence of all Dunc-115s. Since all isoforms of *Drosophila melanogaster* Dunc115 differ by only the first exon, we searched for the M and S isoforms of orthologs by looking for their first exon coding sequences.

Afterwards, we did a ClustalW alignment with just the M, and S candidate first exon coding sequences of the Dunc-115s (using about 120 bps for each Dunc-115). We then looked for certain landmarks to discern candidate isoforms in other *Drosophila* species:

1-Indels/stop codons:

Within this alignment, we looked for indels or stop codons within these candidate coding regions. If these were found, then it is unlikely that these regions are true coding regions, and since S, M, and L isoforms differ by their first exons, it would be unlikely that those isoforms are conserved in the other *Drosophila* species being compared.

2- Existence of intron-exon border sequences AGGT (exon-intron), and AGGT (intron-exon) flanking the exons.

3- translatable coding sequences:

We then translated the candidate S, and M 1st exon coding sequences. If they didn't translate, then again, they could not be true coding sequences. If these three factors checked out, then we could discern that the isoform exists in that Drosophila species.

For *D. melanogaster* Dunc115L, we used the following info for the first exon: (position refers to position within Dunc115 gene).
Beginning of exon: 1bp
Begins to code at: 496bp
Ends: 499bp

For *D. melanogaster* Dunc115S, we used the following info for the first exon:
Beginning of exon: 5762 bp
Begins to code at: 5816bp
Ends: 5933bp

For *D. melanogaster* Dunc115M, we used the following info for the first exon:
Beginning of exon: 5745 bp
Begins to code at: 6013bp
Ends: 6393bp

The beginning and end for each of the remaining exons in *Drosophila melanogaster* Dunc-115 were recorded , and they were used to derive the coordinates of the beginning and end for these exons in the orthologs as well. Once all the information was collected, the map could be formed. It is important to note that the sequences had to be in the right orientation to *D. melanogaster* Dunc-115. So sequences were complemented, reversed or reverse complemented in order to maintain the consistent orientation. The map was then created using the coordinates for the beginning and end of each exon.

Chapter 3 Acting Binding Of Dunc-115

3.1 Generation of Flag-Dunc115 cDNA clones

Our cDNA sequence analysis reveals that Dunc-115L is an isoform containing an actin-binding villin headpiece domain (VHD). Furthermore, our molecular modeling demonstrates that the VHD domain in Dunc-115L is capable of binding to actin. To test direct binding between the VHD domain and actin (Barrientos et al., 2007), full-length Dunc-115L cDNA insert was subcloned in frame into vector pT7-Flag1 (Sigma-Aldrich) for generating fusion protein Flag-Dunc-115 L (Figure 30). This was achieved by removing it from the POT2 vector, where it was originally inserted into EcoRI and XhoI sites, by cutting it with XhoI and EcoRV. It was then subcloned into pBluescript via digestion with the same enzymes and subsequent ligation. From here, PCR was performed on pBluescript-Dunc115L in order to only copy the coding region of Dunc115L. A 2.4Kb product was generated. This was done because the 5' noncoding region contained stop codons, which would prevent the Dunc115L fusion protein from being made. Afterwards, this PCR product was digested with NotI and KpnI. PT7-Flag-1 was cut with the same enzymes and pT7-Flag-1-Dunc115L was generated.

In order to show that actin binding in Dunc-115 does not occur in absence of the VHD domain, Dunc115S cDNA was also subcloned into pT7-Flag-1 (Figure 31). This was achieved by performing PCR on POTB7-Dunc115S. It was then digested with BglII and EcoRI and ligated to pT7-Flag-1 that had been cut with the same enzymes.

3.2 Generation/ isolation of Flag-dunc 115 fusion proteins

Flag-Dunc-115 L and S were then expressed *in vitro* with the cell free TNT® T7 coupled reticulocyte lysate system (Promega) to produce the fusion proteins. The proteins were visualized via western analysis.

3.3 Actin Binding Assay: Dunc115L binds to actin and Dunc115S does not

Once generated, Dunc-115L and S proteins were identified via western analysis with Anti-FLAG antibody. These proteins were found to be 89kD and 84kD respectively (Figure 33). F-actin binding analysis was then conducted using an actin binding protein spin-down assay kit (Cytoskeleton, Inc), which has been used widely [see for example Barrientos et al., (2007)]. After mixing Flag-Dunc-115 fusion proteins S and L with non-muscle F-actin (from the kit), a low force (14,000xg) centrifugation was carried out. At this centrifugation, bundling of F-actin occurs if more of the sample is found in the pellet with F-actin versus the supernatant. If Flag-Dunc-115 binds to F-actin, it will co-sediment with actin filaments and form a pellet, and Western blot analysis using an Anti-Flag antibody (F1804, Sigma-Aldrich) should detect bands in the pellet, not the supernatant. By comparing results from Flag-Dunc-115L and S, we would be able to determine their actin-binding ability and if only Flag-Dunc-115L binds actin, it will be clear that it is due to the VHD domain.

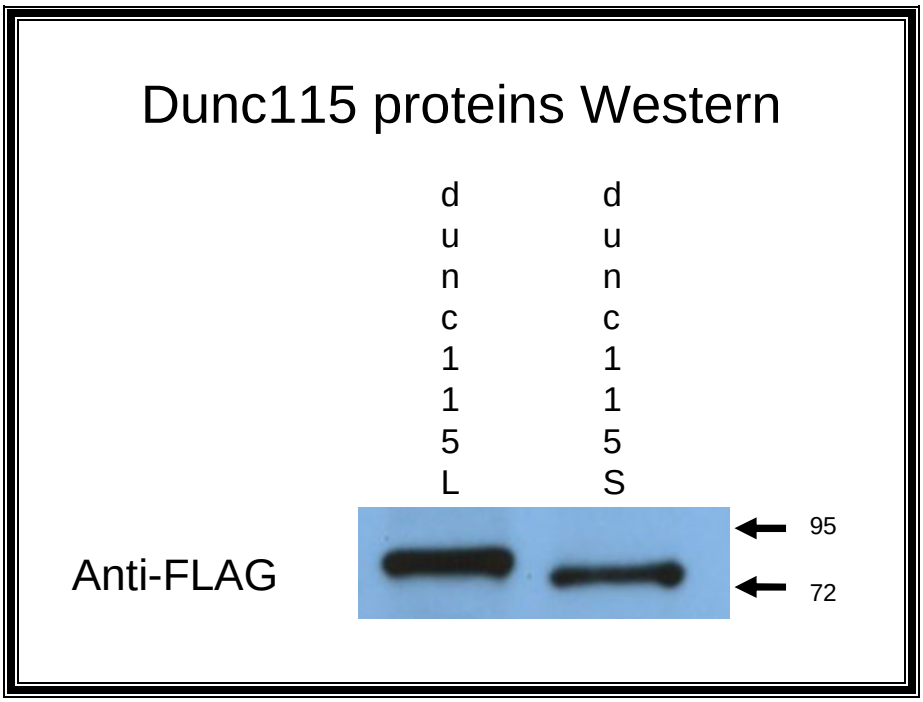

Figure 33. Dunc115L and Dunc115S. Anti-Flag stained Western of 10% Tris/Glycine gel. Dunc115L and S are 89kD and 84kD, respectively.

In addition to Dunc-115 isoforms, several controls were carried out: The binding of F-actin with alpha-actinin, BSA, and lysate alone was also tested (Figure 34). Alpha-actinin has been well documented as an actin binding protein. When alpha-actinin was combined with F-actin, 40% of it was found in the pellet versus the supernatant. With alpha-actinin alone less than 1% of it was found in the pellet. 80% of the F-actin was found in the pellet. BSA has been shown to not bind to actin. In the case of BSA+ F-actin, all the BSA was found in the supernatant. 50 % of the F-actin was found in the pellet. We also tested the actin binding ability of the lysate to cross out any actin binding ability that is intrinsic to the lysate system used (Figure 36). When the lysate was mixed with the F-actin, 95% of the actin stayed in the supernatant, while all of the background lysate bands stayed in the supernatant as well. This indicates that the lysate does not have any intrinsic actin binding ability.

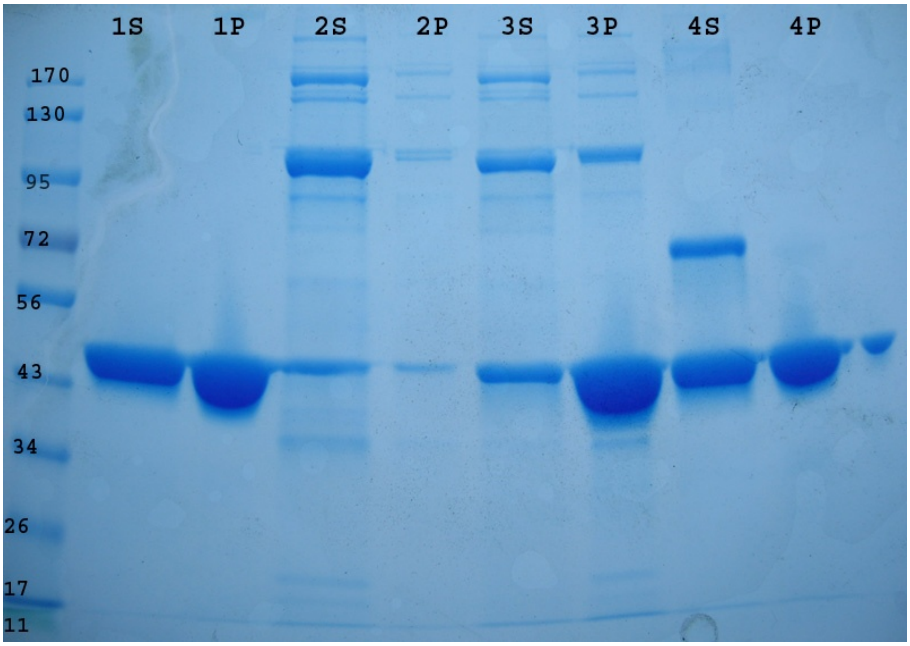

Figure 34. Actin Binding Assay of Actinin and BSA. Coomasie stained 10% Tris/Glycine gel. S=Supernatant P=pellet **Lane 1**=Actin alone **Lane2**=Actinin alone **Lane 3**=Actinin + Actin **Lane4**=BSA+Actin

We then tested Dunc-115S and L (Figure35, 36). In Dunc-115L alone, all of it was found in the supernatant. When F-actin was added, all of the Dunc-115L was found in the pellet (Figure 35) with 90% of the F-actin found in the pellet (Figure 36). With Dunc-115S alone and with F-actin added, all of the Dunc-115S was found in the supernatant (Figure 35). When combined with Dunc-115S, less than 1% of the F-actin was found in the pellet (Figure 36). Together, these results indicate that Dunc-115L binds to actin while Dunc-115S does not. This is likely to be because of the existence of the VHD domain in Dunc-115L.

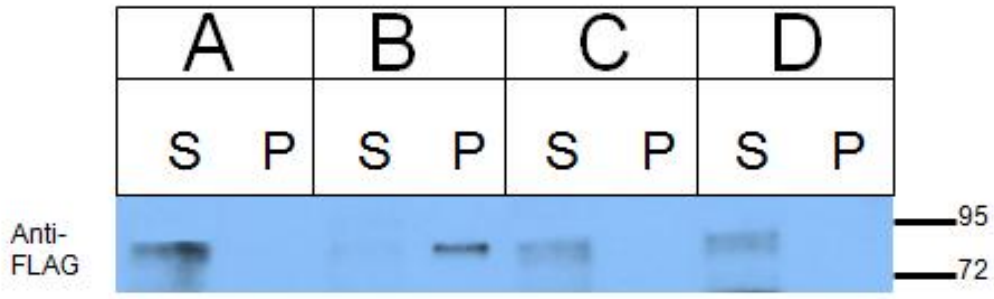

Figure 35. Actin Binding Assay of Dunc115L and S. Anti-FLAG stained Western of 10% Tris/Glycine gel. S=Supernatant P=pellet. A=dunc115L only B=dunc115L+actin C=dunc115S only D=dunc115S+actin.

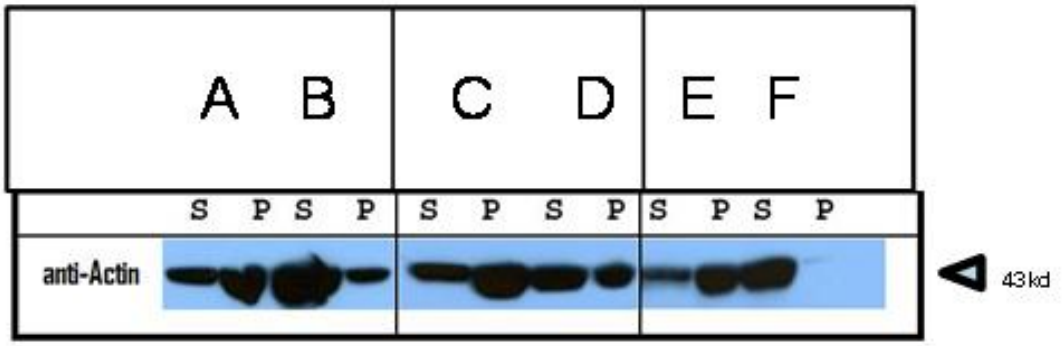

Figure 36. Actin Binding Assay of Lysate, Actinin, BSA, Dunc115L and S. Anti-Actin stained Western of 10% Tris/Glycine gel. S=Supernatant P=pellet. A=actin only B=lysate only C=actinin+actin D=BSA+actin E=dunc115L+actin F=dunc115S+actin

Chapter 4 Determining Robo as an upstream regulator of Dunc-115

The Slit/Robo pathway is a critical guidance mechanism during CNS development for both commissural and longitudinal axons in *Drosophila*, while our prior analysis has shown that Dunc-115 plays a role in axon pathfinding in the CNS (Garcia et al., 2007). In search for the upstream guidance signal that is relayed by Dunc-115, we set out to examine the genetic interaction between the Slit/Robo pathway and Dunc-115.

4.1 Dunc-115 regulates axon projection for subsets of neurons at the CNS

To characterize Dunc-115 functions, we have identified a SUPor-P inserted line from the P-element Screen/Gene Disruption Project, KG03651 as a *dunc-115* mutant and designated it as *dunc-115*^{KG03651}. We have sequenced the flanking sequences of the P-element and determined that the insertion is at 260bps from the first exon. We have the following evidence to conclude that KG03651 is a *dunc-115* mutant. First, *dunc-115*^{KG03651} has axon projection defects in the CNS midline and motoneurons (see below). Second, excising the P-element completely restores the wild-type phenotype (see below), indicating the defects are the result of the P-element insertion. Third, *dunc-115*^{KG03651}/*Df(3R)by10* double heterozygous embryos have almost identical phenotypes as *dunc-115*^{KG03651} homozygous [*Df(3R)by10* is a deficiency strain covering the *dunc-115* locus]. Finally, RT-PCR using RNA prepared from *dunc-115*^{KG03651} does not amplify the expected 830bp band shared by all three isoforms, though the same band is readily detectable in the wild-type.

We have conducted analyses on Dunc-115's role in axon projection at the midline and motoneuron pathfinding. Using the anti-Fasciclin II antibody 1D4, we have examined CNS axon projection in stage 17 embryos. In the wild type, the longitudinal axon bundles run in two parallel groups with each containing three tight fascicles, inner, medial and outermost (Figure 37A and B) (Winberg et al., 1998). The three axon fascicles in each group are clearly separated with the outermost bundle slightly thinner than the other two. By contrast, the anti-Fasciclin II staining in the *dunc-115*^{KG03651} CNS, shows that the outermost fascicle has been frequently disrupted by large gaps (black and white arrows in Figure 37C) while the medial and inner fascicles are often fused together forming a much thicker bundle (Figure 37C white arrows) (see Figure 37D for explanation). Approximately 23% of the hemisegments scored from stage 17 *dunc-115*^{KG03651} embryos [28/(n=)120] have CNS defects, compared to 2% in the wild type (n=115) and 5% in P-element excised embryos (n=90) (the precise P-element excision was confirmed by PCR and sequencing). Thus, Dunc-115 is involved in axon projection at the midline.

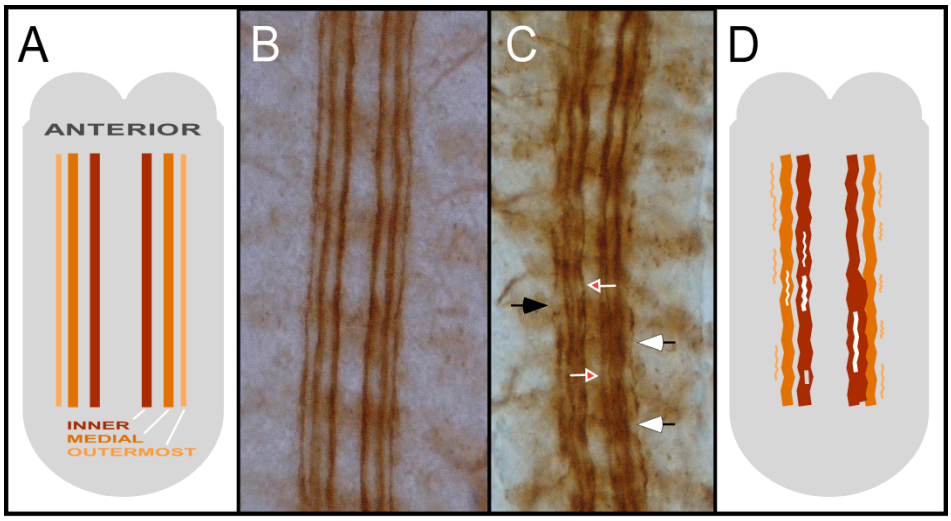

Figure 37. CNS Projection Defects in *dunc-115*^{KG03651}.
(A) Schematics for stage 17 wild-type embryos showing the CNS staining pattern with the use of anti-Fasciclin II antibody 1D4. Two sets of axon bundles run in parallel and each has three tight fascicles termed inner, medial and outermost.
(B) Viewing of the dorsal-ventral perspective of a filleted preparation of a stage 17 wild-type embryo stained with 1D4. The outermost fascicle is slightly thinner.
(C) Same as in (B) but with *dunc-115*^{KG03651} embryos. The outermost fascicle is disrupted frequently by breaks (black and white arrows). The medial and inner fascicles at some regions are fused into a thick bundle (white arrows), or have abnormal splitting (red arrows).

To test the requirement for Dunc-115 by motoneuron axons, we have examined motoneuron axon projections to their peripheral muscle targets. In the wild-type, the b branch of the intersegmental nerve (ISN) ISNb separates from the ISN after exiting the CNS and proceeds into the ventral domain forming three major branches, one between muscle fibers 6 and 7, one each at the ventral edges of muscle 13 and 12 (Figure 38A and arrowheads in Figure 38B) (Winberg et al., 1998). The TN (transverse nerve) projects along the segmental border of adjacent segments.

In *dunc-115*^{KG03651} embryos, ISNb axons often do not defasciculate from each other at choice points and bypass muscle fibers 6 and 7 (Figure 38C black *arrows) and the ventral edge of muscle 13 (Figure 38C black arrows). Some ISNb axons proceed to and

innervate the ventral edge of muscle 13 (Figure 38C white arrowhead at the center) and then fail to innervate muscle 12 and project beyond normal targets (again having the "bypass" phenotype) (Figure 38C red arrow), while other ISNb axons fail to innervate muscle fibers 6/7 and 13 but proceed to innervate muscle 12 (Figure 38C white *arrowheads) (see Figure 38D for illustration). About 9% of the *dunc-115*^{KG03651} hemisegments scored (16/180) have ISNb projection defects like the one marked by the red arrows in Figure 38C, compared to 0% in the wild type embryos (n=70) and 1% in the P-element excised line (n=109). Defects as failure to innervate muscle fibers 6 and 7 or the ventral edge of muscle 13 are 30% among the hemisegments examined (n=180). Therefore, Dunc-115 plays a role in ISNb pathfinding.

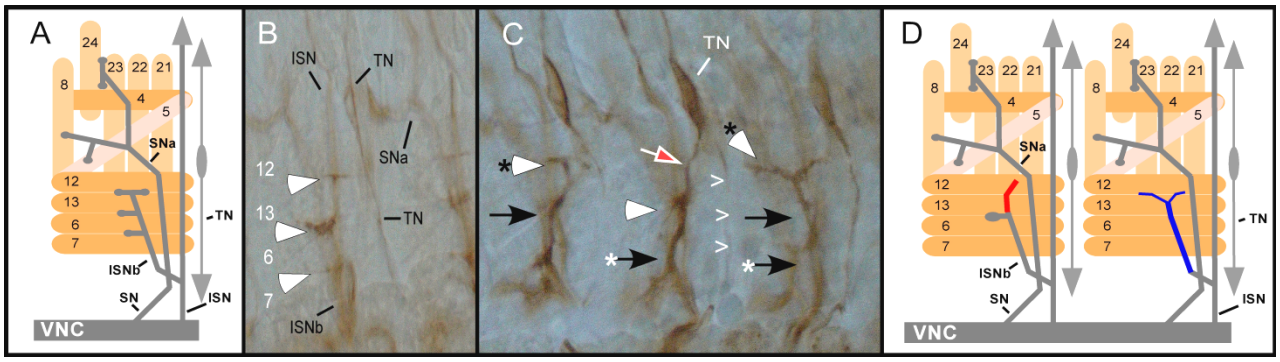

Figure 38. Projection Defects in the Motoneuron Axons of *dunc-115*^{KG03651}.
(A) Schematics of a hemisegment in the wild-type stage 17 embryo illustrating projection of motoneuron axons. ISN, intersegmental nerve; ISNb, the b branch of ISN; SN, segmental nerve; SNa, the a branch of SN; TN, transverse nerve; VNC, ventral nerve cord. Anterior is to the right and dorsal up in all panels. Schematics were based on and inspired by Ayoob et al. (2006).
(B) A filleted preparation of a stage 17 wild-type embryo stained with 1D4. TN travels along the segmental border while the SNa has its characteristic bifurcation (out of focus). The typical three branches form ISNb are marked by white arrowheads, one at the cleft between muscle fibers 6 and 7, one each at the ventral edge of muscle 13 and 12.
(C) Same preparation as in (B) but with *dunc-115*^{KG03651} embryos. ISNb axons fail to innervate muscle fibers 6 and 7 (black *arrows at center and right) and the ventral edge of muscle 13 (black arrows at left and right). The ISNb axon at the center reaches the ventral edge of muscle 13 and innervates it (white arrowhead), but then fails to innervate muscle 12 and projects beyond the ventral edge of muscle 12 (red arrow). ISNb axons at the left and right project to the ventral edge of muscle 12 and form innervation (white *arrowheads). The trajectory of TN axon at the center is marked with (>).
(D) Schematics showing two adjacent hemisegments as seen in (C) (center and right hemisegments). For simplicity, all motoneuron axons are depicted above muscle fibers in (A) and (D).

4.2 Dunc-115 is a downstream effector of the Slit/Robo pathway

Given the involvement of Dunc-115 in axonal pathfinding, it is important to determine the origin of the guidance signals that are relayed by Dunc-115. There are several actin binding proteins that have been characterized and thus it is possible that different guidance mechanisms may utilize different downstream effectors to relay signals to the cytoskeleton. Similarly, overlapping downstream effectors are also likely where different guidance cues may use the same downstream effector. Thus assessing downstream effectors of a guidance pathway is inevitably complicated. As a first attempt, we decided

to determine the genetic interaction between Dunc-115 and a guidance pathway using a well established scheme involving a sensitized genetic background. The basic principle is that by decreasing the expression levels of a gene in a given pathway, the animals so manipulated will be sensitive to dosage changes (or expression levels) of other genes in the same pathway.

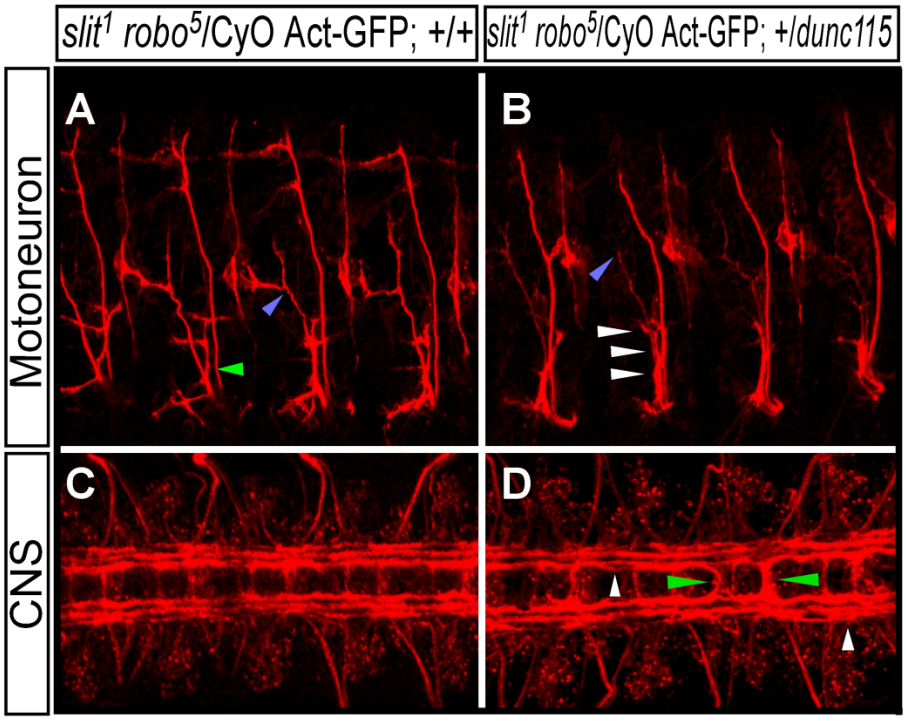

Figure 39. Axon Projection Defects.
(A) A stage 17 *slit*^{1} *robo*^{5}*/CyO Act-GFP* embryo stained with FasII antibody 1D4 (see Figure 4A and B for comparison). SNa has its characteristic bifurcation (blue arrowhead). Apart from occasional reduced branches (e.g. green arrowhead), the projection is basically wild-type.
(B) Removal of one copy of *dunc-115* (*slit*^{1} *robo*^{5}*/CyO Act-GFP; +/dunc-115*) causes significant axon projection defects where the typical three branches of ISNb are disappeared in most segments (white arrowheads). Some SNa neurons also lose the typical bifurcation (blue arrowhead).
(C) The CNS of a similar embryo as in (A) stained with 1D4. It is essentially wild-type.
(D) The CNS of a similar embryo as in (B) stained with 1D4. It has the defects seen in homozygous *dunc-115* mutants such as fused axon bundles and abnormal splitting (white arrowheads, compare with Figure 3C). In addition, it has the defects typical for the Robo pathway, i.e. abnormal longitudinal axon crossing at the midline to the contralateral side (green arrowheads). All panels are stacked confocal images after 1D4 and secondary antibody staining.

Given the involvement of the Slit/Robo pathway in axon projection in the midline and Dunc-115's role as described above, we reasoned Dunc-115 might operate downstream of the Robo receptor. To test this, we generated embryos with genotype *slit*^{1} *robo*^{5}*/CyO Act-GFP; +/dunc-115* and examined the axonal pathfinding at the midline and of motoneurons. Both *slit*^{1} and *robo*^{5} are null and homozygous lethal mutants. The *slit*^{1} *robo*^{5}*/CyO Act-GFP* double heterozygous offers the most sensitive background to test components of the Slit/Robo pathway (for example Yang and Bashaw, 2006), with the CyO Act-GFP balancer making it possible to select the desired embryos for phenotyping.

While *slit*^{1} *robo*^{5}*/CyO Act-GFP* embryos are basically wild-type (Figure 39A and C), the removal of one copy of *dunc-115* in *slit*^{1} *robo*^{5}*/CyO Act-GFP; +/dunc-115* embryos generates projection defects for the ISNb branch: the three landmark innervations are missing in most hemisegments of nearly 25% of the embryos scored [17/(n=)70] (Figure 39B white arrowheads, compare to Figure 38B). Some SNa axons do not have the typical bifurcation (blue arrowhead in Figure 39B). At the CNS, removal of one *dunc-115* copy causes the typical Slit/Robo defects where longitudinal axons cross the midline abnormally (Figure 39D). Collectively, with the *slit* and *robo* sensitized background (*slit*^{1} *robo*^{5}*/CyO Act-GFP*), reduction of one *dunc-115* copy generates significant projection defects in motoneurons and at the midline, indicating that Dunc-115 is a downstream effector of the Slit/Robo pathway.

Chapter 5 Establishing Dunc-115L As A Downstream Effector of Rho GTPAses

The Slit/Robo pathway starts at the plasma membrane where Slit binds to the Robo receptor to initiate the signaling process leading to the reorganization of the cytoskeleton. Given that Dunc-115 is an actin binding protein, there will be other guidance signal relaying posts before reaching Dunc-115. Accumulating evidence indicates that the Rho family GTPases function as a guidance signal integration hub where signals from different guidance pathways could be integrated and relayed downstream. Moreover, a direct linkage between the Robo receptor and members of the Rho GTPases has been established (Fan et al., 2003). Furthermore, actin-binding proteins involved in axon guidance have been shown to be targets of the Rho GTPases. For all these reasons, we decided to examine the possibility that Dunc-115 may function downstream of members of the Rho GTPase subfamily.

We chose to investigate the matter in the adult eye that has been wildly used for studying signal transduction and genetic interactions. Our working hypothesis was that by over-expressing members of the Rho GTPases, the eye will show the roughened eye morphology as shown by many (e.g. Hariharan et al., 1995; Nolan et al.,1998) and that if Dunc-115 was downstream, reducing its dosage would ameliorate the rough eye phenotype.

5.1 Overexpression of Rac1, Mtl and Cdc42 results in roughened *Drosophila* eyes

We thus chose the *Drosophila* visual system to examine the relationship between Dunc-115 and the Rho GTPases. The fly compound eyes have been used widely in analyzing GTPase signaling pathways (for example Nolan et al., 1998; Hu et al., 2005), where overexpression of the Rho GTPases often results in a roughened eye phenotype. We first examined the eye phenotype of GMR-rac1, GMR-Mtl^{V15} and GMR-Cdc42^{V12} animals, where GMR is a retinal-specific promoter and Mtl^{V15} and Cdc42^{V12} are constitutively active. Unlike in the wild-type eye where ommatidia are organized in orderly rows (Figure 40A), compound eyes overexpressing Rac1, Mtl^{V15} and Cdc42^{V12} have disrupted ommatidium patterns with disorganized and missing bristles and irregular ommatidial sizes (Figure 40B–D, compare to A). The compound eyes in the hemizygous Dunc-115 animals (P[*dunc-115*^{KG03651}]/+) have wild-type eyes (Figure 40E, compare to A).

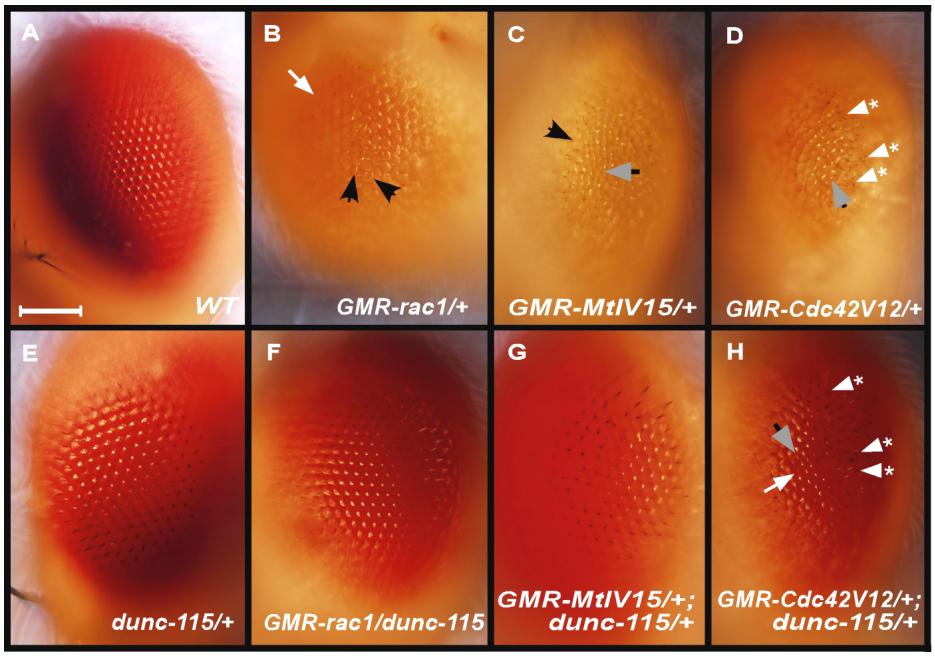

Figure 40. Suppression of Rho GTPases by Dunc-115.
(A) A wild-type compound eye has well organized ommatidial facets and bristles.
(B) to (D) Overexpression of Rac1, Mtl^{V15} and Cdc42^{V12} disrupt the ommatidial arrangement and cause disoriented (black arrows in B and C) and missing (white arrow in B) bristles. Some ommatidia have irregular sizes (gray arrow in C and D), while some bristles are duplicated (white ⁎arrowheads in D).
(E) The eye of the Dunc-115 hemizygous mutant (P[*dunc-115*^{KG03651}]/+) is wild-type.
(F) and (G) Removal of one copy of *dunc-115* drastically suppresses Rac1 and Mtl overexpression defects resulting in a wild-type appearance.
(H) Reduction of one copy of the *dunc-115* gene does not significantly change the roughened eye phenotype in the Cdc42^{V12} overexpressing eye with ommatidia having irregular sizes (gray arrow) and disorganized (white arrow), while bristles are frequently duplicated (⁎arrowheads). All panels are light microscopic images of adult *Drosophila* eyes and are representative of at least five flies analyzed for each genotype. Scale bar, ~100 μm for all.

5.2 Dunc-115 is a downstream effector of the Rho GTPase family

If Dunc-115 is a downstream effector of a Rho GTPase (for example Rac1), removal of one copy of the *dunc-115* gene will ameliorate the roughened eye phenotype caused by Rac1 overexpression. To test this, one copy of *dunc-115* is removed from Rac1, Mtl and Cdc42 overexpressing animals and the eye phenotype was examined. The results show that the roughened eye phenotype is dramatically suppressed with the removal of a single copy of *dunc-115* in Rac1 and Mtl^{V15} overexpressing animals but not in eyes with Cdc42

overexpression (Figure 40F–H). Indeed, the ommatidial facets in Rac1 and Mtl^{V15} overexpressing eyes with one copy of *dunc-115* have near wild-type appearance with much improved bristle patterns (compare Figure 5F and G to B and C, respectively). By contrast, removal of one *dunc-115* copy in Cdc42 overexpressing animals does not significantly change either the ommatidial facets or bristle arrays (compare Figure 7H to D). We have also repeated these analyses using the deficiency line Df(3R)by10 that removes the dunc-115 locus and the results are the same as with the P[dunc-115KG03651]/+ strain (data not shown). Together, these results suggest that Dunc-115 operates downstream of Rac1 and Mtl but not Cdc42.

Chapter 6 Analyzing The Genomic Evolution Of Dunc-115 Gene.

As discussed earlier, Dunc-115 has been analyzed in *Drosophila melanogaster*, where it functions as a critical regulator for establishing neural connections in both the eye and central nervous system (Garcia et al., 2007). In addition, Dunc-115L shares extensive sequence identity with its orthologs in *C. elegans* (UNC-115) and in mammals (AbLIM). For instance, *Drosophila* LIM domain 4 is 63% and 69% identical to human LIM domain 4 and *C. elegans* LIM domain 3, respectively, while the *Drosophila* VHD domain is 58% and 64% identical to the counterpart from humans and *C. elegans* (Garcia et al., 2007).

6.1 Dunc-115L orthologs in other Drosophila species and two other Dipterans

In this study, we used the availability of 12 sequenced *Drosophila* genomes (*Drosophila* 12 Genomes consortium, 2007) to investigate the level of sequence conservation of Dunc-115 across the *Drosophila* genus. So far, Dunc-115 has only been identified in *Drosophila melanogaster*. Our motivation was to find *Dunc-115* in other *Drosophila* species as well was in other Dipterans. The conservation of this gene across evolution would indicate that it is of functional importance to Dipterans.

Firstly, eleven fully sequenced genomes were obtained from Flybase. We then ran BLAST (Altschul et al., 1990) on the cDNA sequence of Dunc-115L from *Drosophila melanogaster* against each *Drosophila* genome in order to identify potential orthologs. Afterwards, we translated the coding sequence from each ortholog. We then aligned each ortholog with the protein sequence of Dunc-115L using ClustalW. *Drosophila persimilis*

had the lowest level of sequence identity with 90% while both *Drosophila sechellia* and *Drosophila yakuba* were 99% identical to Dunc-115L (Table 1).

Table 1 | Protein Length and % Sequence Identity of Dunc-115L in *Drosophila melanogaster* and of its Orthologs in Other Species

Name	Protein length(aa)	% Protein sequence identity(to Dunc-115L)
D. melanogaster	806	100
D. mojavensis	846	93
D. grimshawi	811	92
D. virilis	883	93
D. willistoni	807	92
D. pseudoobscura	804	94
D. persimilis	753	90
D. simulans	839	99
D. sechellia	839	99
D. yakuba	845	99
D.erecta	848	98
D.ananassae	810	96
C.pipiens	812	69
A.gambiae	830	71

Similarly, we ran BLAST on Dunc-115L against two other Dipterans: *Culex pipiens* (house mosquito) and *Anopheles gambiae* (African malaria mosquito) and aligned each protein sequence to Dunc-115L. These show 69 and 71% protein sequence identity, respectively. After aligning each ortholog separately with Dunc-115L, we aligned all 14 protein sequences together with ClustalW in order to verify conservation across species (Figure 41).

Protein Sequence Comparison of Dunc-115L from Different Species

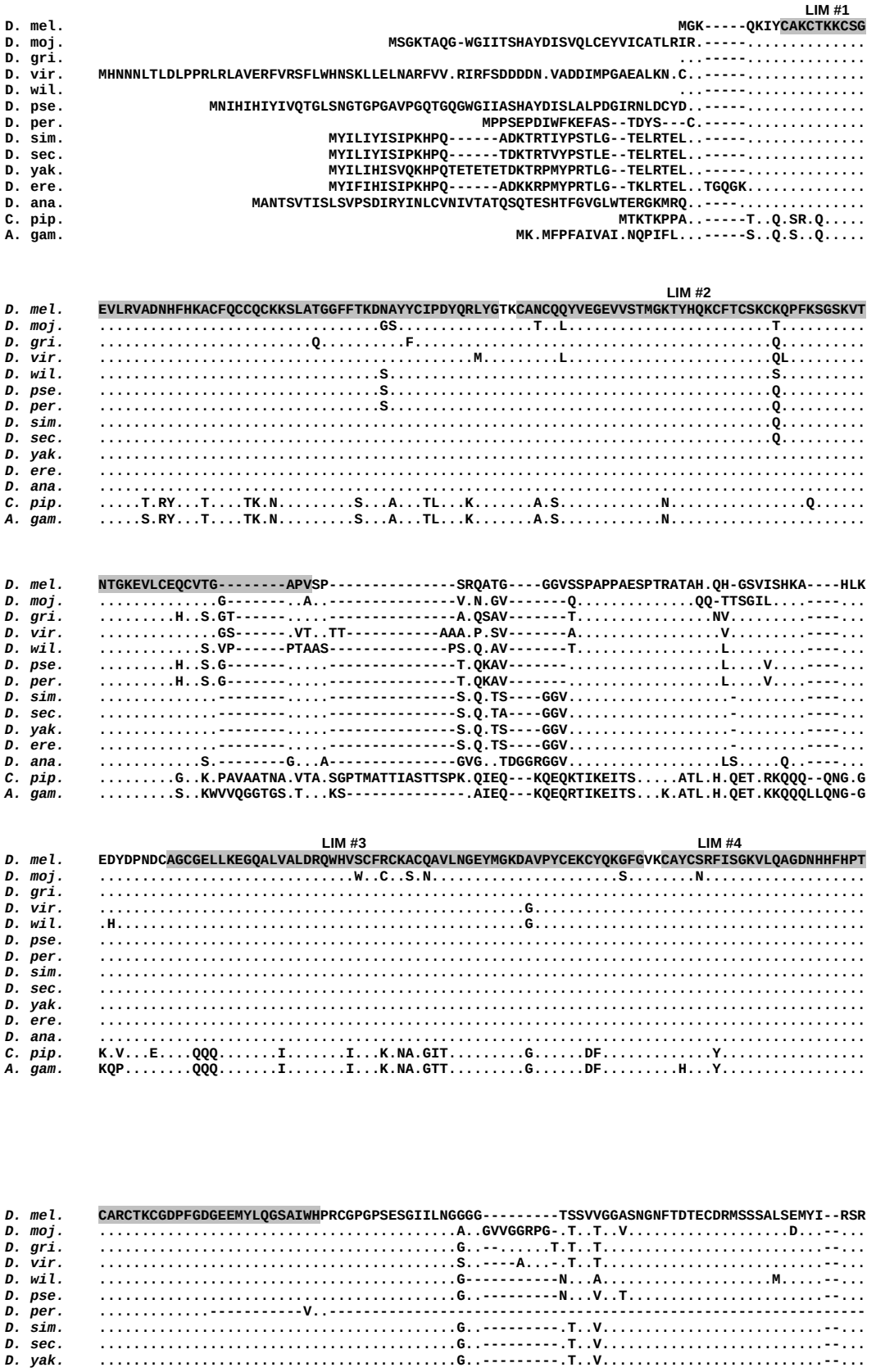

```
D. ere.    .....................................G.R---------.T..V.....................--...
D. ana.    .....................................G..---------ST..A.....................--...
C. pip.    ..............................SADS----------------AALLN.VE....N.E..F..T.T..M..IQ------
A. gam.    ..............................SE------------------AGILN.VDT...N.E..F..T.T.GM..IQFTY..Q


D. mel.    TPSFNGSLYSSS--RKHYRTVSPGLILREYG-RPNAEDISRIYTYSYLTDAPHYLRKPIDPYDKTPLSPHFHRPSSYATTAS--NAGSVA   540
D. moj.    ............--.............-..IG.....................................T.....-.--.......
D. gri.    ....L.......................................................................A.....-.--.......
D. vir.    ...........................................................................A.....-.--.......
D. wil.    ...........P.....................................................A.............--.......
D. pse.    ...I.......................................................................A.....-.--.......
D. per.    -------.QNTD...............................................................A.....-.--.......
D. sim.    ...........................................................................................--.......
D. sec.    ...........................................................................................--.......
D. yak.    ...........................................................................................--.......
D. ere.    ..................A........................................................................--.......
D. ana.    ...................................................E...R.............P.P.--.......
C. pip.    ------------.--Y...T.........NRQGY.D..A..........E........E....A.V.......HQ.G----------.-
A. gam.    ...V...V..PYTH..Y...T.........KNQGY-...A.........EE.G...R..E...RA.V.......VQHYSSMGVGGTA.SI


                                                                UAD Domain
D. mel.    GSRPPS--RPHSRTRSAMKVLVDAIRSETPRPKSPGMNNEEPIELSHYPAAKKPPPGEQPKIERDDFPAPPYPYTDPERRRRYSDTYKGV   630
D. moj.    .......--..................................................................................
D. gri.    .......-..................................................................................
D. vir.    .......--..................................................................................
D. wil.    .......--.....................................................................ES.H..
D. pse.    .......--.....................................D....L.....................................
D. per.    .......--.....................................D....L.....................................
D. sim.    .......-...................................................................................
D. sec.    .......--..................................................................................
D. yak.    .......--..................................................................................
D. ere.    .......--..................................................................................
D. ana.    .......--..................................................................................
C. pip.    .P.SS.GS.S...S.........S.....................M....G........K.........................S..NI
A. gam.    .K.SA.GS.S...S.........S.................................K.........................S....


D. mel.    PASDDEDENVENGK----PNGKVKNGEEQQRLQREAEQLEKLN-SGIGSAIAKDLKEHAKYRKWKQNNLDPRNASRTPSASKEPLYKLRY   720
D. moj.    .V...D..EN....R---T......D...T............K-.....................................
D. gri.    .......-DI.........---T......G......H..........-.....V.....................................
D. vir.    ........D.........---T......G...S..H..........-...C.V.....................................V.....
D. wil.    .......--DEN..DQ---A......GD..I..K..........-.....................................
D. pse.    .....E..NVQ...Q---T..NA......R......AE.....-.....V..........H.....................
D. per.    .....E..NVQ...Q---T..NA......R......AE.....-.....V..........H.....................
D. sim.    .A...E..NV.....----P......G...Q.............-.....................................V.....
D. sec.    .A...E..NV.....----.......G...Q.............-.....................................V.....
D. yak.    .A...E..NV....Q----......G...Q.............-.....................................
D. ere.    .A...E..NV....Q---.......G...Q.............-.....................................I.....
D. ana.    .....E..NV.....----T...I..G...Q.............-.....................................
C. pip.    -E...EVDHQAKHQQQVGAGRED.ENQTER..RK.E.E.S...S..M.-KVL...Q.QK..ET..RE.................T.R...
A. gam.    .E...EVDHAN-----------N.ENVTEK.HTK.E.E.R...S..M.TV.L...Q.KKR.EH...E.................M.RM..


D. mel.    ESPIGASPSRNLDHQKPFYEDEMFDRSTSYRGSLGKSLGNAPSYNAIHSYRSPPKPGYGFKTTTLP--YIRNGFSSDFSYGG-LGDKTHS   810
D. moj.    .................C.....................................................P-.....Y........-.......
D. gri.    ..........H.....................................................-.....Y........-.......
D. vir.    ...........................................................S.M.P-.....Y...................
D. wil.    ..........H.....................................................--.....Y........G.......
D. pse.    ..........H..S..................................................--.....Y........-.......
D. per.    ..........H..S.....................................................-.....Y........-.......
D. sim.    ...........................................................................-.....-.......
D. sec.    ...........................................................................-.....-.......
D. yak.    ...........................................................................-.....Y........-.......
D. ere.    ...........................................................................-.....Y........-.......
D. ana.    ...........................................................................-.....Y........-.......
C. pip.    ...V...........RASED-.Y.........V.RAI.....................S....SSL...Y.....F..-.......
A. gam.    ...V.................-DE.........V.RAI...T.................S.....SL...Y.....FS.-.......
```

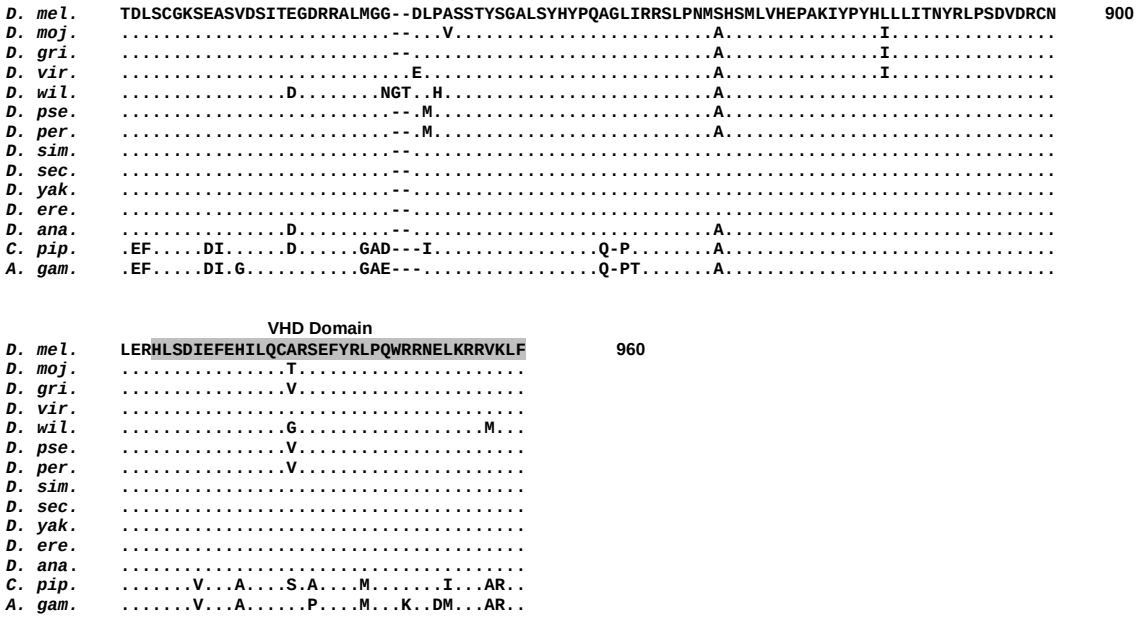

Figure 41. Protein Sequence Comparison of Dunc-115L from Different Species.
Dunc-115L protein sequences from 12 Drosophila species along with 2 mosquito species are aligned using the CLUSTAL W(1.81) program. *Drosophila melanogaster* Dunc-115L sequence was used as the template to establish consensus sequences where dots represent identical amino acids and dashes are introduced to maximize the alignment. Shaded segments are structural motifs of the LIM, UAD and VHD domains. *D. mel., D. melanogaster; D. moj., D. mojavensis; D. Gri., D. grimshawi; D. vir., D. virilis; D. wil., D. willistoni; D. pse., D. pseudoobscura; D. per., D. persimilis; D. sim., D. simulans; D. sec., D. sechellia; D. yak., D. yakuba; D. ere., D. erecta; D. ana., D. ananassae; C. pip., Culex pipiens; A. gam., Anopheles gambiae.*

6.2 Generation of phylogenetic tree of Dunc115L across Drosophila species

Using the PHYLIP package (Felsenstein, 1981),we then generated 100 bootstraps (**Seqboot**) in order to construct a maximum likelihood tree (**Dnaml**) and ran **Consense** and **Ape** from the **R-project** package **(**Paradis et al., 2004**)** to get a majority rule consensus tree (Figure 42). In the resulting tree, *Anopheles gambiae* and *Culex pipiens* serve as outgroups. This tree is consistent with the *Drosophila* species tree recently published (*Drosophila* 12 Genomes Consortium, 2007), with exception of the branch of *D. grimshawi* and *D. mojavensis* which—with a bootstrap value of 61—is weakly supported.

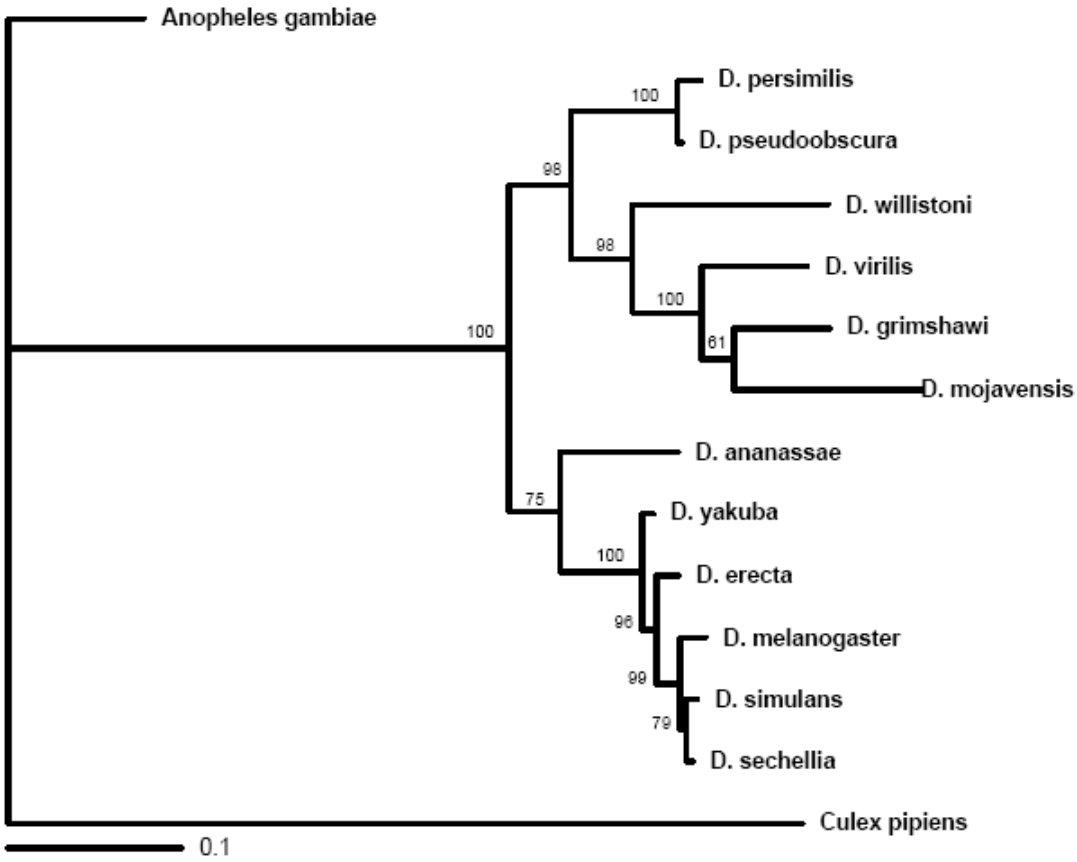

Figure 42. Phylogenetic Tree of Dunc-115L across the 12 Sequenced Species of *Drosophila* and Two Genera of Mosquito. The numbers above each node represent bootstrap values. The scale represents .1 substitutions per site. *Anopheles gambiae* and *Culex pipiens* represent outgroups of the *Drosophila* species.

6.3 Quantifying sequence conservation of Dunc-115L and specific domains across Drosophila species.

In order to quantify the level of sequence conservation of Dunc-115L across *Drosophila* species, we applied a maximum likelihood algorithm known as PAML (Yang, 1997), which allowed us to calculate the ratio of nonsynonymous-to-synonymous nucleotide substitutions Ka/Ks for each codon. In the case of nonsynonymous substitutions (Ka), a substitution of one base for another in a gene coding for a protein produces a change in the translated amino acid sequence whereas synonymous substitutions (Ks) do not (Nekrutenko et al., 2002). The comparison between the number of nonsynonymous substitutions (Ka), and the number of synonymous substitutions (Ks) tells us whether deleterious mutations are selected against (negative selection) or whether mutations that may be advantageous in response to an environmental change are favored (positive selection). When positive selection dominates, the Ka/Ks ratio is greater than 1 whereas when negative selection dominates, the Ka/Ks ratio is less than 1(Nekrutenko et al., 2002). When these two forces are in equilibrium to each other, the Ka/Ks ratio is close to 1.

Table 2 | Ka/Ks Ratios of Dunc-115L Domains

Region of sequence	Ka	Ks	Ka/ks (+-1sd)
Whole seq	.18456	3.67144	.05027 (0.04672, 0.05398)
LIM1	.05049	3.48373	.01449 (0.008269, 0.02224)
LIM2	.18704	6.26063	.02988 (0.02255, 0.03844)
LIM3	.08241	7.29230	.01130 (0.007451,0.015724)
LIM4	.02439	3.35599	.00727 (0.002810, 0.01285)
UAD	.12482	15.87872	.00786 (0.002619, 0.01387)
VHD	0.06056	4.95642	.01222 (0.006253,0.01943)

The average Ka/Ks of Dunc-115 was found to be .05027 (Table 2). Such a low Ka/Ks ratio suggests that this gene has undergone negative selection and that it is highly conserved. Investigation of specific domains demonstrates even stronger conservation. The VHD domain shows 5X the average conservation of *Dunc-115L*. The other domains were similarly conserved with Ka/Ks ratios ranging from .00727 to .02988. Thus, these domains are highly conserved across all *Drosophila* species.

6.4 Looking for existence other Dunc-115 isoforms across Drosophila species

We also wanted to know whether the other two isoforms of Dunc-115 were conserved in other Drosophila species. To answer this question, we performed a BLAST on the genomic sequence of *Drosophila melanogaster* Dunc-115 (CG31352) against the genomic sequence of Dunc-115 from other species. We then performed ClustalW sequence alignment on the whole genomic sequence of all *Drosophila* Dunc-115 genomic sequences recovered. Since all *Drosophila melanogaster* Dunc-115 isoforms differ by only the first exon, we looked specifically for the M, and S first exon coding sequences in the other *Drosophila* species. Afterwards, we did a ClustalW alignment with just the M, and S candidate first exon coding sequences of the Dunc-115S (using about 120 bps for each Dunc-115).

We looked for certain landmarks to discern candidate isoforms in other *Drosophila* species: Absence of indels/stop codons, existence of intron-exon border sequences AGGT(exon-intron) , and AGGT(intron-exon), and translatable coding sequences. If

these three factors checked out, then we could discern that that isoform exists in a particular *Drosophila* species.

When investigating the candidate 1st exon coding region of Drosophila species closest to *D.melanogaster*, we obtained the following results:

For the S form

	Indels	Translatable
D.simulans	No	Yes
D.sechellia	No	Yes
D.erecta	No	Yes
D.yakuba	No	Yes

For the M form

	Indels	translatable
D.simulans	Yes	No(2 stop codons)
D.sechellia	Yes	No (1 stop codon)
D.erecta	Yes	No (2 stop codons)
D.yakuba	Yes	No (1 stop codon)

Thus, we can conclude that for the species closest to *D. melanogaster*, Dunc-115S was conserved across *Drosophila* species while Dunc-115M was not. We did not investigate further ortholog isoforms of *Drosophila melanogaster* Dunc-115M as it is highly unlikely that it is conserved in species more distantly related to it since it is not conserved in those species closest to it. We recorded Dunc-115S candidate first exon info for the remaining *Drosophila* species.

We then used the beginning and end of all exons of Dunc-115 as obtained through the process above, in order to map the intron-exon borders of the Dunc-115 gene genomic

structure for the twelve *Drosophila* species (Figure 43). In this manner, we were able to confirm both L and S isoforms in eight out of twelve *Drosophila* species. Dunc-115 in *Drosophila mojajensis* and *Drosophila willistoni* most closely resemble the S isoform. Dunc115 in *Drosophila grimshawi* most closely resembles the L isoform. *Drosophila virilis* has a unique form of Dunc-115, unlike the S or the L isoform. Thus, Dunc-115S, is for the most part, conserved across species.

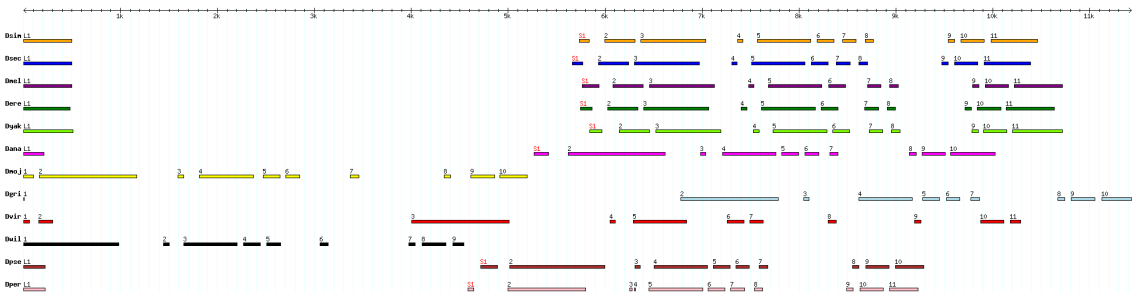

Figure 43. Map of Intron-Exon Borders of Dunc115 Gene in 12 Drosophila Isoforms. The L and S isoforms in *Drosophila melanogaster* as well as most closely related species differ only by the first exon used. In species that bear both isoforms, the L isoform 1st exon is labeled L1 and the S isoform 1st exon is labeled S1. In species that bear only one isoform, 1st exons are simply labeled 1.

We have shown that Dunc-115L is highly conserved among 12 *Drosophila* species and two mosquito genera. Moreover, in the case of the former, sequence identity becomes even more compelling at the individual domain level. Such level of conservation for the VHD domain among *Drosophila* species, which has been shown both in *C. elegans* and in humans to bind to actin (Roof et al., 1997; Struckhoff and Lundquist, 2003), combined with 3D modeling predictions (Garcia et al., 2007), strongly supports the likelihood that this domain binds to actin in *Drosophila melanogaster*. Additionally, we have confirmed the existence of an S isoform in 10 out of 12 species. The M isoform is not conserved across different *Drosophila* species.

Chapter 7 General Discussion

7.1 The VHD domain in Dunc-115L is required for actin binding

Our mutant analyses indicate that Dunc-115 is required for axon pathfinding in subsets of neurons. Furthermore, protein sequence data indicate that the long isoform Dunc-115L contains a VHD domain that has the potential to interact with actin. If such binding can be established experimentally, it will offer one mode of function for Dunc-115 where signals from guidance cues can be relayed to Dunc-115 that in turn regulates cytoskeleton.

The VHD domain of Dunc-115 has key residues such as Trp64 in a hydrophobic patch termed “cap” and Phe76 that are required for binding to F-actin (Vardar et al., 1999; Vardar et al., 2002; Vermeulen et al., 2004; Garcia et al., 2007). Indeed this is a feature also found in Dunc-115 homologs such as Unc-115 (Struckhoff and Lundquist, 2003). Thus in the computer modeling done previously, it was found that Dunc-115 is capable of binding to actin (Garcia et al., 2007).

The absence of the VHD domain in isoform Dunc-115S provides a convenient construct to determine the requirement for VHD domain in actin binding. Our cosedimentation assay clearly shows that only Dunc-115L—not S—is capable of binding to actin, suggesting that the VHD domain is required (and thus necessary) for actin binding. Combined with our bioinformatics data and evidence from *in vitro* VHD domain/actin binding analyses from other species in the literature, we propose that the VHD domain in Dunc-115L functions as a binding target for actin *in vivo*.

How then does the actin binding ability of Dunc-115 impact growth cone projection? One tempting possibility is that Dunc-115 may regulate filopodial formation. Our actin binding assay shows that Dunc-115 bundles actin, a process seen in the formation of filopodia.

7.2 Dunc-115 is a downstream effector of the Robo receptor and Rho GTPases.

While Slit/Robo is a well known guidance pathway, it remains elusive how guidance signals from Slit/Robo are relayed to the cytoskeleton. Our analysis here offers one possible route for subsets of CNS neurons in *Drosophila* where guidance signals of the Slit/Robo pathway are sent to Dunc-115, which in turn regulates the cytoskeleton through actin binding. Indeed, a similar functional mode has been found in *C. elegans* where guidance signals from the Netrin receptor are relayed to Unc-115, which then, presumably, regulates actin.

Thus the emerging picture is that actin binding proteins such as Dunc-115 function as the final recipient of guidance signals and thus play a critical role in regulating the cytoskeleton in response to growth cone navigation. One remaining challenge is to decipher the cytoplasmic network involved in connecting the surface guidance receptors such as Robo and Netrin to actin binding proteins such as Dunc-115. While significant amount of information has been accumulated where important landmarks have been identified, large gaps in our understanding still exist. Our demonstration that the Rho family GTPases function as an intermediate signal integration hub between the Robo

receptor and Dunc-115 provides one other example as how guidance signals may be delivered to the cytoskeleton.

Finally, how Dunc-115 affects growth cone dynamics and morphology *in vivo* during axon outgrowth remains unknown. One possible route is to use Total Internal Reflection Microscopy (TIRM) or fluorescent speckle microscopy to observe directly cytoskeletal dynamics in living growth cones as they respond to guidance cues (Geraldo and Gordon-Weeks, 2009; Lowery and Van Vactor, 2009).

7.3 Conservation of Dunc-115 isoforms across species

7.3a. Dunc115 L and S isoforms are largely conserved across *Drosophila* species and Dipterans

It is not surprising that Dunc-115L was conserved throughout all *Drosophila* species as it is the isoform that shows most sequence similarity with *C. elegans* and vertebrate orthologs (Garcia, 2007). Our tree demonstrates that the evolution of Dunc-115L in *Drosophila* species is in line with the evolution of the *Drosophila* species themselves. Additionally, this conservation across *Drosophila* species is a good preliminary indicator of the Robo/Rho GTPase/Dunc-115 signaling cascade possibly being evolutionarily conserved across species. Additional experimentation must take place. Also, our finding of the great similarity with two mosquitos is the first demonstration of Dunc-115 orthologs in other insects. The conservation of this gene across evolution would indicate that it is of functional importance to Dipterans.

Overall, the C-terminus of Dunc-115L shows much greater conservation than the N-terminus. The LIM domains do show great conservation despite being closer to the N-terminus. Variability at the N-terminus lies outside these domains. Additionally, analysis of the coding sequence alignment of *Drosophila* species shows that the VHD domain undergoes much variability at the DNA level. This further supports the fact that the VHD domain is functionally conserved as all orthologs are nearly identical at the protein level. It is interesting that all *Drosophila* species of the *melanogaster* group (*D. melanogaster, D. simulans, D. sechellia, D. yakuba, D. erecta*, and *D. ananassae*) contain an Alanine in the 917th position of the protein sequence alignment, which falls in the VHD domain. This may point to an evolutionary change that distinguishes this group of Drosophila from those of other groups like the *obscura* group whose members (*D. pseudoobscura* and *D. persilillis*) contain a Valine at this position.

It is noteworthy that Dunc-115S was conserved throughout subgenus Sophophora but missing in subgenus *Drosophila*. This distinction in Dunc-115S isoform points possibly to a key evolutionary event differentiating subgenus Sophophora from subgenus *Drosophila.*

7.3b. Dunc115M is not conserved across species

When trying to generate an intron-exon border map for all three Dunc-115 isoforms, we could not clearly define a *Drosophila melanogaster* Dunc-115M first exon. It was interesting to find that Dunc115M does not have a coding region in the Dunc115S first exon. It begins at 5745bp, begins coding at 6013 bp, and ends at 6393bp while the S first

exon form begins at 5762bp, begins to code at 5816bp, and ends at 5933bp. Dunc115M begins coding in S's intron region between its first 2 exons. Additionally, when trying to isolate orthologs of *Drosophila melanogaster* Dunc-115M from the coordinates of its first exon, we could not find any orthologs—even in *Drosophila* species closest to *D. melanogaster*: *D. simulans*, *D. sechellia, D. erecta, or D. yakuba*! We found indels in each candidate first exon and the sequences were untranslatable. Further research is needed to fully elucidate the nature of the M isoform.

7.4 Conclusions

(a) The VHD domain of Dunc-115L is required for binding to actin.

(b) Dunc115L and the VHD domain are both highly conserved across *Drosophila* species.

(c) Dunc-115 is a downstream effector of the Slit/Robo pathway.

(d) Dunc-115 relays signals from members of the Rho GTPase family.

Based on our findings, we propose the following model for Dunc-115 (Figure 44). Guidance cues such as the Slit/Robo pathway initiate the axon projection process at the plasma membrane and guidance signals are relayed to a processing hub like the Rho GTPases, which in turn relays signals to Dunc-115. Dunc-115 will regulate cytoskeleton through binding to actin.

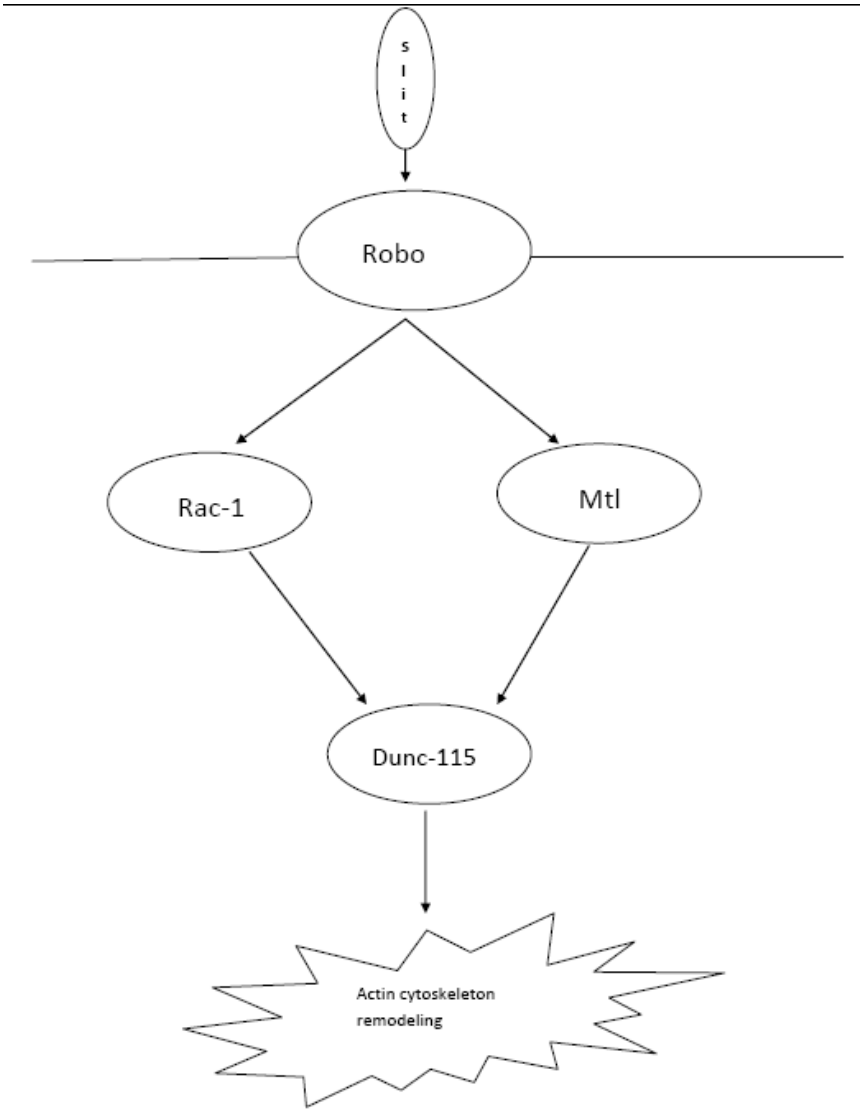

Figure 44. Signaling Cascade Involving Dunc115. Slit binds to its receptor Robo, which signals via Rho GTPases Rac-1 and Mtl. These then stimulate Dunc115 to bind to actin and subsequently affect cytoskeletal dynamics and axon guidance.

It should be noted that pathways like Slit/Robo may send signals to multidownstream effectors and conversely, downstream effectors including the Rho GTPases and Dunc-115 can receive guidance signals from different surface receptors.

7.5 Future research

One remaining issue is how these Dunc-115 isoforms may function differently. As a first step to address this question, we will express individual isoforms in a *dunc-115* mutant background to examine the rescue effect of each isoform. Independent transgenic stocks will be established and stocks with the transgene on the 2nd chromosome selected and balanced since endogenous Dunc-115 is on the 3rd chromosome. Then the following genotype, UAS-Dunc-115/CyO, Act-GFP; P[*dunc-115*^{KG03651}]/P[*dunc-115*^{KG03651}], will be synthesized from available stocks, UAS-Dunc-115/CyO, Act-GFP and Sco/CyO, Act-GFP; P[*dunc-115*^{KG03651}]/TM3, Ser (available in the PI's laboratory):

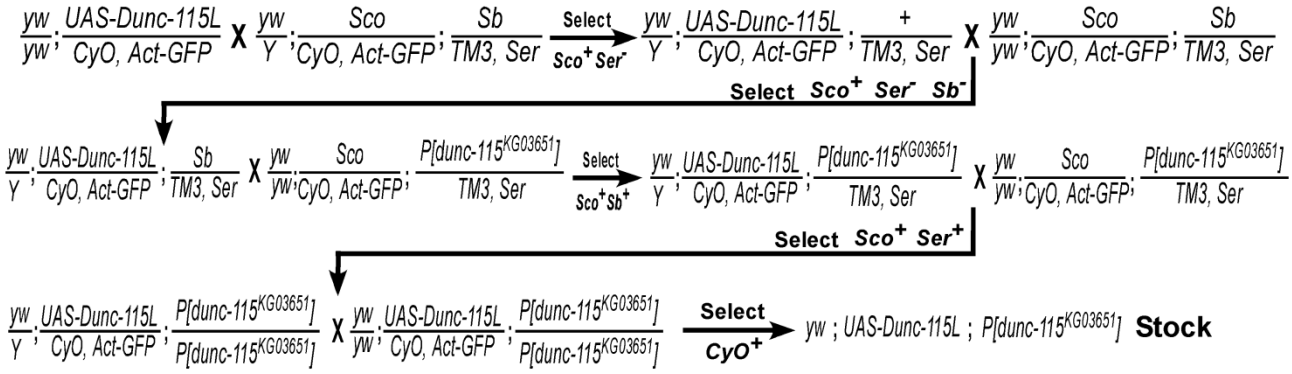

Similarly,*elav*-GAL4/CyO, Act-GFP; P[*dunc-115*^{KG03651}]/P[*dunc-115*^{KG03651}] strain will be created and used to generate the following cross:

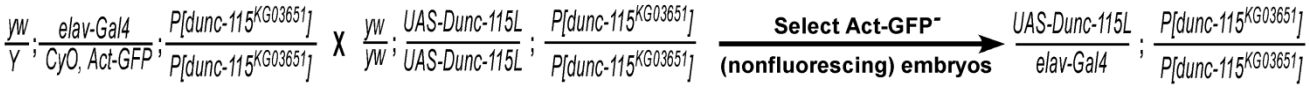

UAS-Dunc-115S strains in *dunc-115* mutant background will be similarly created as well. Eggs at stage 17 from these crosses will be collected and stained with anti-FasII antibody (1D4) to determine the rescuing effect of Dunc-115 individual isoforms. We will test multiple lines for each construct to make certain any distinctive rescuing effects with different isoforms are not due

to expression levels, and we will conduct carefully controlled blind statistical data analyses. We will also express Dunc-115 isoforms in a wild-type background to test defects generated by overexpression. From this set of experiments, we will be able to determine which isoforms are capable of restoring the wild-type phenotype. Given the existence of the VHD domain, we expect Dunc-115L will rescue the defects in axon projection while Dunc115S will not.

References

Altschul S, Gish W, Miller W, Myers EW, Lipman DJ (1990) Basic local alignment search tool. J Mol Biol. 215, 403-410.

Aizawa H, Sutoh K, Yahara I (1996) Overexpression of cofilin stimulates bundling of actin filaments, membrane ruffling, and cell movement in Dictyokstelium. J Cell Biol 132, 335-344.

Amann KJ, and Pollard TD (2001) Direct real-time observation of actin filament branching mediated by Arp2/3 complex using total internal reflection fluorescence microscopy. Proc Natl Acad Sci USA 98, 15009-15013.

Araujo, SJ, and Tear G (2003) Axon guidance mechanisms and molecules: lessons from invertebrates. Nat. Rev. Neurosci. 4, 910-922.

Ayoob JC, Yu HH, Terman JR, and Kolodkin AL (2004) The Drosophila receptor guanylyl cyclase Gyc76C is required for semaphorin-1a-plexin A-mediated axonal repulsion. J Neurosci. 24, 6639-6649.

Ayoob JC, Terman JR, and Kolodkin AL (2006) Drosophila Plexin B is a Sema-2a receptor required for axon guidance. Development 133, 2125-2135.

Bagnard D, Lohrum M, Uziel D, Püschel AW, and Bolz J (1998) Semaphorins act as attractive and repulsive guidance signals during the development of cortical projections. Development 125, 5043–5053.

Bamburg JR, Harris HE, and Weeds AG (1980) Partial purification and characterization of an actin depolymerizing factor from brain. FEBS Lett.121, 178-182.

Banerjee U, Renfranz PJ, Pollock JA and Benzer S(1987) Molecular characterization and expression of sevenless, a gene involved in neuronal pattern formation in the Drosophila eye. Cell 49, pp. 281–291.

Bao S, Fischbach K-F, Corbin V, and Cagan RL (2010) Preferential adhesion maintains separation of ommatidia in the *Drosophila* eye. Developmental Biology 344, 948-956.

Barallobre MJ, Pascual M, Del Rio JA, and Soriano E (2005) The Netrin family of guidance factors: emphasis on Netrin-1 signalling. Brain Research Reviews 49, 22– 47

Barrientos T, Frank D, Kuwahara K, Bezprozvannaya S, Pipes GC, Bassel-Duby R, Richardson JA, Katus HA, Olson EN, and Frey N (2007) Two novel members of the ABLIM protein family, ABLIM-2 and -3, associate with STARS and directly bind F-actin. J Biol Chem 282, 8393-8403.

Bazigou E, Apitz H, Johansson J, Loren CE, Hirst EMA, Chen P-L, Palmer RH, and Salecker I (2007) anterograde Jelly belly and Alk Receptor tyrosone kinase signaling mediates retinal axon targeting in *Drosophila*. Cell 128, 961-976.

Begemann G, Michon AM, vd voorn L, Wepf R, Mlodzik M (1995) The Drosophila Orphan nuclear receptor seven-up requiresthe Ras pathway for its function in photoreceptor determination. Development 121, 225-235.

Bhat KM (2005) Slit-Roundabout signaling neutralizes netrin-Frazzled-mediated attractant cue to specify the lateral positioning of longitudinal axon pathways. Genetics 170, 149-159.

Bhat KM, Gaziona I, Krishnan S (2007) Regulation of axon guidance by slit and netrin signaling in the Drosophila ventral nerve cord. Genetics 176, 2235-2246.

Billard C, Delaire S, Raffoux E, Bensussan A, and Boumsell L (2000) Switch in the protein tyrosine phosphatase associated with human CD100 semaphorin at terminal B-cell differentiation stage. Blood 95, 965-972.

Bio.Research. ucsc.edu (http://bio.research.ucsc.edu/people/hinck/netrinoverview.html)

Bischof J, Maeda RK, Hediger M, Karch F, Basler K (2007) An optimized transgenesis system for Drosophila using germ-line-specific phiC31 integrases. PNAS 104, 3312-3317.

Bork P, and Beckmann G (1993) The CUB domain. A widespread module in developmentally regulated proteins. J Mol Biol.231, 539-545.

Brambilla E, Constantin B, Drabkin H, and Roche J (2000) Semaphorin SEMA3F localization in malignant human lung and cell lines: A suggested role in cell adhesion and cell migration. Am J Pathol. 156, 939-950

Brankkatschk M, and Dickson BJ (2006) Netrins guide Drosophila commissural axons at short range. Nature Neuroscience 9, 188-194.

Brittis PA, Lu Q, and Flanagan JG (2002) Axonal protein synthesis provides a mechanism for localized regulation at an intermediate target. Cell 110, 223-235.

Brose K, Bland KS, Wang KH, Arnott D, Henzel W, Goodman CS, Tessier-Lavigne M, and Kidd T (1999) Slit proteins bind Robo receptors and have an evolutionarily conserved role in repulsive axon guidance. Cell 96, 795-806.

Brown MD, Cornejo BJ, Kuhn TB, and Bamburg JR (2000) Cdc42 stimulates neurite outgrowth and formation of growth cone filopodia and lamellipodia. J Neurobiol 43, 352-364.

Carlier MF, Laurent V, Santolini J, Melki R, Didry D, Xia GX, Hong Y, Chua NH, Pantaloni D (1997) Actin depolymerizing factor (ADF/cofilin) enhances the rate of filament turnover: implication in actin-based motility. J Cell Biol 136, 1307-1322.

Carter N, Nakamoto T, Hirai H, and Hunter T (2002) EphrinA1-induced cytoskeletal re-organization requires FAK and p130(cas). Nat Cell Biol 4, 565-573.

Chang HC, Solomon NM, Wassarman DA, Karim FD, Therrien M, Rubin GM, Wolff T (1995) Phyllopod functions in the fate determination of a subset of photoreceptors in *Drosophila.* Cell 80, 463-472.

Chen H, Chedotal A, He Z, Goodman CS, and Tessier-Lavigne M (1997) Neuropilin-2, a novel member of the neuropilin family, is a high affinity receptor for the semaphorins Sema E and Sema IV but not Sema III. Neuron 19, 547–559.

Chen H, Bagri A, Zupicich JA, Zou Y, Stoeckli E, Pleasure SJ, Lowenstein DH, Skarnes WC, Ch´edotal A, Tessier-Lavigne M (2000) Neuropilin-2 regulates the development of selective cranial and sensory nerves and hippocampal mossy fiber projections. Neuron 25, 43–56.

Chen J, Godt D, Gunsalus K, Kiss I, Goldberg M, Laski FA (2001) Cofilin/ADF is required for cell motility during Drosophila ovary development and oogenesis. Nat Cell Biol 3, 204-209.

Chen P-L, and Candinin TR (2008) The Cadherin flamingo mediates level- dependent interactions that guide photoreceptor target choice in *Drosophila.* Neuron 58, 26-33.

Chien CB, Rosenthal DE, Harris WA, and Holt CE (1993) Navigational errors made by growth cones without filopodia in the embryonic Xenopus brain. Neuron 11, 237-251.

Chilton JK (2006) Molecular mechanisms of axon guidance. Developmental Biology 292, 13-24.

Choe K-M, Prakash s, Bright A, Clandinin TR (2006) Liprin-α is required for photoreceptor target-selection in *Drosophila.* PNAS 103, 11601-11606.

Chrzanowska-Wodnicka M, Burridge K (1996) Rho-stimulated contractility drives the formation of stress fibers and focal adhesions. J Cell Biol 133, 1403-1415.

Clandinin TR, Lee C-H, herman T, Lee RC, Yang AY, Ovasapyan S, and Zipursky SL (2001) *Drosophila* LAr regulates R1-R6 and R7 target specificity in the visual system. Neuron 32, 237-248.

Coleman HA, Labrador JP, Chance RK, Bashaw GJ (2010) the Adam family metalloprotease Kuzbanian regulates the cleavage of the roundabout receptor to control axon repulsion at the midline. Development 137, 2417-2426.

Comeau MR, Johnson R, DuBose RF, Petersen M, Gearing P, VandenBos T, Park L, Farrah T, Buller RM, Cohen JI, Strockbine LD, Rauch C, and Spriggs MK (1998) A poxvirus-encoded semaphorin induces cytokine production from monocytes and binds to a novel cellular semaphorin receptor, VESPR. Immunity 8, 473-482.

Cooper GM. (2000) Structure and Organization of Actin Filaments.The Cell : A molecular approach. 2nd Edition.

Cutforth T, and Harrison CJ (2002) Ephs and ephrins close ranks. Trends Neurosci 25, 332-334.

Davy A, and Soriano P (2005) Ephrin signaling in vivo: look both ways. Developmental Dynamics 232, 1-10.

Dent EW, and Gertler FB (2003) Cytoskeletal dynamics and transport in growth cone motility and axon guidance. Neuron 40, 209-227.

Dickson BJ, Dominguez M, van der Straten A, Hafen E (1995) Control of Drosophila photoreceptor cell fates by phyllopod, a novel nuclear protein acting downstream of the Raf kinase. Cell 80, 453-467.

Dickson BJ (2002) Molecular mechanisms of axon guidance. Science 298, 1959-1964.

Dickson BJ, and Gilestro GF (2006) Regulation of commissural axon pathfinding by slit and its Robo receptors. Annu Rev Cell Dev Biol 22, 651-675

Drosophila 12 Genomes Consortium (2007) Evolution of genes and genomes on the Drosophila phylogeny. Nature 450, 203-218.

Elhabazi A, Delaire S, Bensussan A, Boumsell L, and Bismuth G (2001) Biological activity of soluble CD100. I. The extracellular region of CD100 is released from the surface of T lymphocytes by regulated proteolysis. J Immunol 166, 4341-4347.

Enomoto T (1996) Microtubule disruption induces the formation of actin stress fibers and focal adhesions in cultured cells: possible involvement of the rho signal cascade. Cell Struct Funct 21, 317-326.

Erkman L, Yates PA, McLaughlin T, McEvilly RJ, Whisenhunt T, O'Connell SM, Krones AI, Kirby MA, Rapaport DH, Bermingham JR, O'Leary DD, and Rosenfeld MG (2000) A POU domain transcription factor-dependent program regulates axon pathfinding in the vertebrate visual system. Neuron 28,779-792.

Eurekah.com and Landes Bioscience. 2003.

Evans TA, Beshaw GJ (2010) Functional diversity of robo receptor immunoglobulin domains promotes distinct axon guidance decisions. Current Biology 20, 567-572.

Fan J, and Raper JA (1995) Localized collapsing cues can steer growth cones without inducing their full collapse. Neuron 14, 263-274.

Feiner L, Webber AL, Brown CB, Lu MM, Jia L, Feinstein P, Mombaerts P, Epstein JA, and Raper JA (2001) Targeted disruption of semaphorin 3C leads to persistent truncus arteriosus and aortic arch interruption. Development 128, 3061-3070.

Feldheim DA, Kim YI, Bergemann AD, Frisén J, Barbacid M, and Flanagan JG (2000) Genetic analysis of ephrin-A2 and ephrin-A5 shows their requirement in multiple aspects of retinocollicular mapping. Neuron 25, 501-503.

Felsenstein J (1981) Evolutionary trees from DNA sequences: a maximum likelihood approach. J Mol Evol.17, 368-376.

Freeman M (1996) Reiterative use of the EGf receptor triggers differentiation of all cell types in the *Drosophila* eye. Cell 87, 651-660.

Friederich E, Vancompernolle K, Huet C, Goethals M, Finidori J, Vandekerckhove J, Louvard D (1992) An actin-binding site containing a conserved motif of charged amino acid residues is essential for the morphogenic effect of villin. Cell 70, 81–92.

Friederich E, Vancompernolle K, Louvard D, and Vandekerckhove J (1999)Villin function in the organization of the actin cytoskeleton. Correlation of in vivo effects to its biochemical activities in vitro. J Biol Chem 274, 26751-26760.

Frisen J, Yates PA, McLaughlin T, Friedman GC, O'Leary DD, and Barbacid M (1998) Ephrin-A5 (AL-1/RAGS) is essential for proper retinal axon guidance and topographic mapping in the mammalian visual system. Neuron 20, 235-243.

Fu W, and Noll M (1997) The Pax2 homolog sparkling is required for development of cone and pigment cells in the Drosophila eye. Genes Dev. 11, 2066-2078.

Fujisawa H (2004) Discovery of semaphorin receptors, neuropilin and plexin, and their functions in neural development. J Neurobiol. 59, 24-33

Fujisawa K, Wrana JL, Culotti JG (2007) The Slit Receptor EVA-1 coactivates a SAX-3/Robo-mediated guidance signal in C. elegans. Science 317, 1934-1938

Garbe DS and Bashaw GJ (2004) Axon Guidance at the Midline: From Mutants to Mechanisms. Critical Reviews in Biochemistry and Molecular Biology 39, 319–341.

Garbe DS, and Bashaw GJ (2007) Independent functions of Slit-Robo repulsion and Netrin-Frazzled attraction regulate axon crossing at the midline in Drosophila. Journal of Neuroscience 27, 3584-3592.

Garcia MC, Abbasi M, Singh S, and He Q (2007) Role of Drosophila gene dunc-115 in nervous system. Invertebrate Neuroscience 7, 119-128.

Geraldo S and Gordon-Weeks PR (2009) Cytoskeletal dynamics in growth-cone steering. Journal of Cell Science 122, 3595-3604.

Giger RJ, Cloutier JF, Sahay A, Prinjha RK, Levengood DV, Moore SE, Pickering S, Simmons D, Rastan S, Walsh FS (2000) Neuropilin-2 is required in vivo for selective axon guidance responses to secreted semaphorins. Neuron 25, 29–41.

Gitai Z, Yu TW, Lundquist EA, Tessier-Lavigne M, Bargmann CI (2003) The netrin receptor UNC-40/DCC stimulates axon attraction and outgrowth through enabled and, in parallel, Rac and UNC-115/AbLIM. Neuron 37,53-65.

Gitler AD, Lu MM, Epstein JA (2004) PlexinD1 and semaphorin signaling are required in endothelial cells for cardiovascular development. Dev Cell 7,107-116.

Gong Q, Rangarajan R, Seeger M, and Gaul U (1999) The netrin receptor frazzled is required in the target for establishment of retinal projections in the Drosophila visual system. Development 126, 1451-1456.

Govek EE, Newey SE, and Van Ael L (2005) The Role of the Rho GTPases in neuronal development. Genes & Development 19, 1-49

Grill B, Bienvenut WV, Brown HM, Ackley BD, quadroni M, Jin Y (2007) C. elegans RPM-1 regulates axon termination and synaptogenesis through the Rab GEF GLO-4 and the Rab GTPase GLO-1. Neuron 55, 587-601.

Guan, KL and Rao Y.(2003) Signalling mechanisms mediating neuronal responses to guidance cues. Nat. Rev. Neurosci.
4, 941–956.

Hakeda-Suzuki S, Ng J, Tzu J, Dietzl G, Sun Y, Harms M Nardine T, Luo L, and Dickson BJ (2002) Rac function and regulation during Drosophila development. Nature 416, 438-442.

Hall A (1998) Rho GTPases and the actin cytoskeleton. Science 279, 509-514.

Hall A and Lalli G (2010) Rho and Ras GTPases in Axon Growth, Guidance, and Branching. Cold Spring Harbor Perspective s in Biology 2, a001818.

Hall KT, Boumsell L, Schultze JL, Boussiotis VA, Dorfman DM, Cardoso AA, Bensussan A, Nadler LM, Freeman GJ (1996) Human CD100, a novel leukocyte semaphorin that promotes B-cell aggregation and differentiation. Proc Natl Acad Sci U S A 93, 11780-11785

Hamelin M, Zhou Y, Su MW, Scott IM, and Culotti JG (1993) Expression of the UNC-5 guidance receptor in the touch neurons of C. elegans steers their axons dorsally. Nature 364, 327-330.

Hansen MJ, Dallal GE, and Flanagan JG (2004) Retinal axon response to ephrin-as shows a graded, concentration-dependent transition from growth promotion to inhibition. Neuron 42, 717-730.

Hariharan IK, Hu K-Q, Asha H, Quintanilla A, Ezzell RM, and Settleman (1995) Characterization of rho GTPase family homologues in *Drosophila melanogaster* : overexpressing *Rho1* in retinal cells causes a late developmental defect. The EMBO Journal 14, 292-302.

Harris WA, Stark WS, and walker JA (1976) Genetic dissection of the photoreceptor system in the compound eye of *Drosophila melanogaster*. Journal of Physiology 236, 415-439.

Harris, R., Sabatelli, L. M. and Seeger, M. A. (1996). Guidance cues at the Drosophila midline: identification and characterization of two Drosophila netrin/unc6 homologs. Neuron 17, 217-228.

He Z, Tessier- Lavigne M (1997) Neuropilin is a receptor for the axonal chemorepellent Semaphorin III. Cell 90, 739-751.

Heberlein U, Wolff T, and Rubin GM (1993) The TGFβ homolog *dpp* and the segment polarity gene *hedgehog* are required for propagation of a morphogenetic wave in the *Drosophila* retina Cell 75, 913-926.

Hiramoto M, Hiromi Y, Giniger E, and Hotta Y (2000) The Drosophila Netrin receptor Frazzled guides axons by controlling Netrin distribution. Nature 406, 886-889.

Hiramoto M, and Hiromi Y (2006) ROBO directs axon crossing of segmental boundaries by suppressing responsiveness to relocalized Netrin. Nature Neuroscience 9, 58-66.

Holland SJ, Gale NW, Mbamalu G, Yancopoulolos GD, Henkemeyer M, and Pawson T (1996) Bidirectional signalling through the EPH-family receptor Nuk and its transmembrane ligands. Nature 383, 722-725.

Hu H, Li M, Labrador JP, McEwen J, Lai EC, Goodman CS, and Bashaw GJ (2005) Cross GTPase-activating protein (CrossGAP)/Vilse links the Roundabout receptor to Rac to regulate midline repulsion. Proc Natl Acad Sci U S A 102, 4613-4618.

Huber AB, Kolodkin AL, Ginty DD, Cloutier JF (2003) Signaling at the growth cone: ligand-receptor complexes and the control of axon growth and guidance.Annu Rev Neurosci. 26, 509-563.

Hummel T, Schimmelpfeng K, Klambt C (1999) Commissure formation in the embryonic CNS of *Drosophila*. Developmental Biology 209, 381-398.

Ishida I, Kumanogoh A, Suzuki K, Akahani S, Noda K, and Kikutani H Involvement of CD100, a lymphocyte semaphorin, in the activation of the human immune system via CD72: implications for the regulation of immune and inflammatory responses. Int Immunol. 15, 1027-1034.

Isbister CM, Tsai A, Wong ST, Kolodkin AL, and O' Connor TP (1999) Discrete roles for secreted and transmembrane semaphorins in neuronal growth cone guidance in vivo. Development 126, 2007-2019

Ito T, Kagoshima M, Sasaki Y, Li C, Udaka N, Kitsukawa T, Fujisawa H, Taniguchi M, Yagi T, Kitamura H, and Goshima Y. Repulsive axon guidance molecule Sema3A inhibits branching morphogenesis of fetal mouse lung. Mech Dev 97, 35-45.

Jaffe AB, Hall A (2002) Rho GTPases in transformation and metastasis. Advances in Cancer Research 84, 57-80.

Jarman AP, Grell EH, Ackerman L, Jan LY, Jan YN (1994) *atonal* is the proneural gene for *Drosophila* photoreceptors. Nature 369, 398-400.

Jin Z, and Strittmatter SM (1997) Rac1 mediates collapsing-1-induced growth cone collapse. Journal of Neuroscience 17, 6256-6263.

Johansen J, Halpern ME, Keshishian H (1989) Axonal Guidance and the Development of Muscle Fiber-Specific Innervation in *Drosophila* embryos. Journal of Neuroscience 9, 4318-4332.

Jurney WM, Gallo G, Letourneau PC, McLoon SC (2002) Rac1- mediated endocytosis during ephrin-A2 and semaphoring 3A-induced growth cone collapse. Journal of Neuroscience 22, 6019-6028.

Kagoshima M, and Ito T (2001) Diverse gene expression and function of semaphorins in developing lung: positive and negative regulatory roles of semaphorins in lung branching morphogenesis. Genes Cells 6, 559-571.

Kaprielian Z, Runko E, and Imondi R (2001) Axon Guidance at the midline Choice Point. Developmental Dynamics 221, 154-181.

Kaufmann N, Wills ZP, Van Vactor D (1998) *Drosophila* Rac1 controls motor axon guidance. Development 125, 453-461.

Keleman K, and Dickson BJ (2001) Short- and long-range repulsion by the Drosophila Unc5 netrin receptor. Neuron 32, 605-617.

Kelleher JF, Atkinson SJ, and Pollard TD (1995) Sequences, structural models, and cellular localization of the actin-related proteins Arp2 and Arp3 from Acanthamoeba. Journal of Cell Biology 131, 385-397.

Keleman K, Rajagopalan S, Cleppien D, Teis D, Paiha K, Huber LA, Technau GM, and Dickson BJ (2002) Comm sorts robo to control axon guidance at the Drosophila midline. Cell 110, 415-427.

Keleman K, Ribeiro C, Dickson BJ (2005) Comm function in commissural axon guidance: cell autonomous sorting in vivo. Nature Neuroscience 8, 156-163.

Kidd T, Brose K, Mitchell KJ, Fetter RD, Tessier-Lavigne M, Goodman CS, and Tear G (1998) Roundabout controls axon crossing of the CNS midline and defines a novel subfamily of evolutionarily conserved guidance receptors. Cell 92, 205-215.

Kidd T, Bland KS, and Goodman CS (1999) Slit is the midline repellent for the robo receptor in Drosophila. Cell 96, 785-794.

Kim AS, Kakalis LT, Abdul-Manan N, Liu GA, and Rosen MK (2000) Autoinhibition and activation mechanisms of the Wiskott-Aldrich syndrome protein. Nature 404, 151-158.

Kim MD, Kolodziej P, and Chiba A (2002) Growth cone pathfinding and filopodial dynamics are mediated separately by Cdc42 activation. Journal of Neuroscience 22, 1794-806.

Kitsukawa T, Shimono A, Kawakami A, Kondoh H, and Fujisawa H (1995) Overexpression of a membrane protein, neuropilin, in chimeric mice causes anomalies in the cardiovascular system, nervous system and limbs. Development 121, 4309-4318.

Kitsukawa T, Shimizu M, Sanbo M, Hirata T, Taniguchi M, Bekku Y, Yagi T, Fujisawa H (1997) Neuropilin-semaphorin III/D-mediated chemorepulsive signals play a crucial role in peripheral nerve projection in mice. Neuron 19, 995-1005.

Klambt C, Jacobs JR, Goodman CS (1991) The midline of the Drosophila central nervous system: a model for the genetic analysis of cell fate, cell migration, and growth cone guidance. Cell 64, 801-815.

Kolodkin AL, Matthes DJ, O'Connor TP, Patel NH, Admon A, Bentley D, and Goodman CS (1992) Fasciclin IV: sequence, expression, and function during growth cone guidance in the grasshopper embryo. Neuron 9, 831-845.

Kolodkin AL, Matthes DJ, Goodman CS (1993) The semaphorin genes encode a family of transmembrane and secreted growth cone guidance molecules. Cell 75, 1389-1399.

Kolodkin AL, Levengood DV, Rowe EG, Tai YT, Giger RJ, and Ginty DD (1997) Neuropilin is a semaphorin III receptor. Cell 90, 753-762.

Kolodziej P A., Timpe LC, Mitchel KJ., Fried SR, Goodman CS, Jan LY, and Jan YN (1996) frazzled encodes a Drosophila member of the DCC immunoglobulin subfamily and is required for CNS and motor axon guidance. Cell 87, 197-204.

Kozma R, Ahmed S, Best A, Lim L (1995) The Ras-related protein Cdc42Hs and bradykinin promote formation of peripheral actin microspikes and filopodia in Swiss 3T3 fibroblasts. Mol Cell Biol 15,1942-1952.

Korey CA, and Van Vactor D (2000) From the growth cone surface to the cytoskeleton: one journey, many paths. J Neurobiol 44, 184-193.

Knust E (2007) Photoreceptor morphogenesis and retinal regeneration: lessons from *Drosophila.* Current Opinion in Neurobiology 17, 541-547.

Kramer H, Cagan RL, & Zipursky SL (1991) Interaction of bride of sevenless membrane-bound ligand and the sevenless tyrosine-kinase receptor. Nature 352, 207-212.

Kramer S, West SR, Hiromi Y (1995) cell fate control in the Drosophila retina by the orphan receptor seven-up: its role in the decisions mediated by the ras signaling pathway. Development 121, 1361-1372.

Kruger RP, Aurandt J, and Guan KL (2005) Semaphorins command cells to move. Nature Reviews Molecular Cell Biology 6, 789-800.

Kuhn TB, Brown MD, Wilcox CL, Raper JA, Bamburg JR (1999) Myelin and collapsing-1 induce motor neuron growth cone collapse through different pathways: inhibition of collapse by opposing mutants of rac1. Journal of Neuroscience 19, 1965-1975.

Kullander K, and Klein R (2002) Mechanisms and functions of Eph and ephrin signalling. Nat Rev Mol Cell Biol. 3, 475-486.

Lai Z-C, Harrison SD, Karim F, Li Y, and Rubin GM (1996) Loss of tramtrack gene activity results in ectopic R7 cell formation, even in a *sina* mutant background. PNAS 93, 5025-5030.

Lee C-H, herman T, Clandinin TR, Lee R, and Zipursky SL (2001) N-Cadherin regulates target specificity in the *Drosophila* visual system. Neuron 30, 437-450.

Lee RC, Clandinin TR, Lee CH, Chen PL, Meinertzhagen IA, Zipursky SL (2003) The protocadherin Flamingo is required for axon target selection in the *Drosophila* visual system. Nature Neuroscience 6, 557- 563.

Li H, Kulkarni G, Wadsworth WG (2008) RPM-1, a caenorhabditis elegans protein that functions in presynaptic differentiation, negatively regulates axon outgrowth by controlling SAX-3/ robo and UNC-5/UNC5 activity. Journal of Neuroscience 28, 3595-3603.

Li S, Li Y, Carthew RW, Lai ZC (1997) Phtoreceptor cell differentiation requires regulated proteolysis of the transcriptional repressor Tramtrack. Cell 90, 469-478.

Liu BP, Chrzanowska-Wodnicka M, and Burridge K (1998) Microtubule depolymerization induces stress fibers, focal adhesions, and DNA synthesis via the GTP-binding protein Rho. Cell Adhes Commun 5, 249-255.

Liu Z, Patel K, Schmidt H, Andrews W, Pini A, Sundaresan V (2004) Extracellular Ig domains 1 and 2 of Robo are important for ligand (Slit) binding. Mol Cell Neurosci 26, 232-240.

Long H, Sabatier C, Ma L, Plump A, Yuan W, Ornitz DM, Tamada A, Murakami F, Goodman CS, Tessier-Lavigne M (2004) Conserved roles for Slit and Robo proteins in midline commissural axon guidance. Neuron 42, 213-223.

Lowery LA, and Van Vactor D (2009) The trip of the tip:understanding the growth cone machinery. Nature Reviews Molecular Cell Biology 10, 332-343.

Lu C, Huang X, Ma HF, Gooley J J, AparacioJ, Roof D J, Chen C, Chen DF and Li T (2003) Normal retinal development and retinofugal projections in mice lacking the retina-specific variant of actin-binding LIM domain protein. Neuroscience 120, 121–131.

Luo L (2000) Rho GTPases in neuronal morphogenesis. Nature Reviews Neuroscience 1, 173-180.

Luo L (2002) Actin cytoskeleton regulation in neuronal morphogenesis and structural plasticity.Annual Review of Cell and Developmental Biology.18, 601-635.

Luo Y, Raible D, and Raper JA (1993) Collapsin: a protein in brain that induces the collapse and paralysis of neuronal growth cones. Cell 75, 217-227

Luo Y, Shepherd I, Li J, Renzi MJ, Chang S, and Raper JA (1995) A family of molecules related to collapsin in the embryonic chick nervous system. Neuron 14,1131-1140

Lundquist EA, Herman RK, Shaw JE, and Bargmann CI (1998) UNC-115, a conserved Protein with predicted LIM and actin-binding domains, mediates axon guidance in C. elegans. Neuron 21, 385–392.

Lundquist EA, Reddien PW, Hartwieg E, Horvitz HR, and Bargmann CI (2001) Three C. elegans Rac proteins and several alternative Rac regulators control axon guidance, cell migration and apoptotic cell phagocytosis. Development 128, 4475-4488.

Lundquist EA (2003) Rac proteins and the control of axon development. Curr.ent Opinion In. Neurobiology 13, 384–390.

Lundquist EA (2006) Small Gtpases. Wormbook, ed. The *C.elegans* Research Community. Wormbook. http:// wormbook.org

Maciver SK, Zot HG, Pollard TD (1991) Characterization of actin filament severing by actophorin from Acanthamoeba castellanii. J Cell Biol 115, 1611-1620.

Maciver SK and Hussey PJ (2003) The ADF/cofilin family: actin-remodeling proteins. Genome Biol 3, reviews3007.1–reviews3007.12.

Mann F, Ray S, Harris W,and Holt C (2002) Topographic mapping in dorsoventral axis of the Xenopus retinotectal system depends on signaling through ephrin-B ligands. Neuron 35, 461-473.

Mann F, Harris WA, and Holt CE (2004) New views on retinal axon development: a navigation guide. Int J Dev Biol. 48, 957-964.

Mark MD, Lohrum M, and Püschel AW (2000) Patterning neuronal connections by chemorepulsion: the semaphorins. Cell and Tissue Research 290, 299-306.

McGough A, Pope B, Chiu W, Weeds A Cofilin changes the twist of F-actin: implications for actin filament dynamics and cellular function (1997) J Cell Biol 138, 771-781.

Messersmith EK, Leonardo ED, Shatz EJ,Tessier-Lavigne M, Goodman CS, and Kolodkin AL (1995) Semaphorin III can function as a selective chemorepellent to pattern sensory projections in the spinal cord. Neuron 14, 949–959.

Miao HQ, Soker S, Feiner L, Alonso JL, Raper JA, and Klagsbrun M (1999) Neuropilin-1 mediates collapsin-1/semaphorin III inhibition of endothelial cell motility: functional competition of collapsin-1 and vascular endothelial growth factor-165. J Cell Biol. 146, 233-242

Miki H, and Takenawa T (2003) Regulation of actin dynamics by WASP family proteins. Journal of Biochemistry134, 309-313.

Mitchison T, and Kirschner M (1988) Cytoskeletal dynamics and nerve growth. Neuron 1, 761-772.

Morlot C, Thielens NM, Ravelli RB, Hemrika W, Romijn RA, Gros P, Cusack S, and McCarthy AA (2007) Structural insights into the Slit-Robo complex. Proc Natl Acad Sci USA 104; 14923-14928.

Mueller BK (1999) Growth cone guidance: First Steps Towards a Deeper Understanding. Annu. Rev. Neurosci. 22, 351-358

Mullins RD, Heuser JA, Pollard TD (1998) The interaction of Arp2/3 complex with actin: nucleation, high affinity pointed end capping, and formation of branching networks of filaments. Proc Natl Acad Sci U S A 95, 6181-6186.

Nagaraj K, and Hortsch M (2006) Phosphorylation of L1-type cell-adhesion molecules--ankyrins away! Trends Biochem Sci. 31, 544-546.

Nakagawa S, Brennan C, Johnson KG, Shewan D, Harris WA, and Holt CE (2000) Ephrin-B regulates the Ipsilateral routing of retinal axons at the optic chiasm.. Neuron 25, 599-610.

Nakamoto T, Kain KH, Ginsberg MH (2004) Neurobiology: New connections between integrins and axon guidance. Curr Biol 14, R121-123

Nakamura H (2001) Regionalisation and acquisition of polarity in the optic tectum. Prog Neurobiol 65, 473-488.

Negishi M, and Katoh H (2002) Rho family GTPases as key regulators for neuronal network formation. Journal of Biochemistry 132, 157-166.

Nekrutenko A, Makova KD, and Li WH (2002) The KA/Ks ratio test for assessing the protein-coding potential of genomic regions: an empirical and simulation study. Genome Res. 12, 198-202.

NewsomeTP, Schmidt S, Dietzl G, Keleman K, Asling B, Debant A, and Dickson BJ (2000) Trio combines with Dock to regulate Pak activity during photoreceptor axon pathfinding in *Drosophila.* Cell 101, 283-294.

Nobes CD, and Hall A (1995) Rho, Rac, and Cdc42 GTPases regulate the assembly of multimolecular focal complexes associated with actin stress fibers, lamellipodia, and filopodia. Cell 81, 53-62.

Nolan KM, Barrett K, and Lu Y. (1998) Myoblast city, the Drosophila homolog of Dock 180/CED-5, is required in a Rac signaling pathway utilized for multiple developmental processes. Genes Dev 12, 3337-3342.

Norris AD, Dyer JO, Lundquist EA (2009) The Arp2/3 complex, UNC-115/abLIM, and UNC-34/Enabled regulate axon guidance and growth cone filopodia formation in Caenorhabditis elegans. Neural Development 4.

Ng J, Nardine T, Harms M, Tzu J, Goldstein A, Sun Y, Dietzl G, Dickson BJ, and Liqun Luo (2002) Rac GTPases control axon growth, guidance and branching. Nature 416, 442-447.

O'Donnell M, Chance RK, and Bashaw GJ (2009) Axon Growth and Guidance: Receptor Regulation and Signaling Transduction. Annu.Rev. Neuroscience 32, 383-412.

Paradis E, Claude J, Strimmer K. (2004) APE: Analyses of Phylogenetics and Evolution in R language. Bioinformatics 20, 289-290.

Pascual M, Pozas E, Soriano E (2005) Role of class 3 semaphorins in the development and maturation of the septohippocampal pathway. Hippocampus 15, 184-202.

Pasquale EB (2005) Eph receptor signaling casts a wide net on cell behavior. Nat Rev Mol Cell Biol 6, 462-475.

Pfeiffenberger C, Cutforth T, Woods G, Yamada J, Rentería RC, Copenhagen DR, Flanagan JG, and Feldheim DA (2006) Ephrin-As and neural activity are required for eye-specific patterning during retinogeniculate mapping. Nature Neuroscience 8, 1022-1027.

Pollard TD, and Borisy GG (2003) Cellular motility driven by assembly and disassembly of actin filaments. Cell 112, 453-465.

Plump AS, Erskine L, Sabatier C, Brose K, Epstein CJ, Goodman CS, Mason CA, Tessier-Lavigne M (2002) Slit1 and Slit2 cooperate to prevent premature midline crossing of retinal axons in the mouse visual system. Neuron 33, 219-232.

Prakash S, McLendon HM, Dubreuil CI, Ghose A, Hwa J, Dennehy KA, Tomalty KMH, clark KL, Van Vactor D, Clandinin TR (2009) Complex interactions amongst N-cadherin, DLAR, and Liprin- α regulate Drosophila photoreceptor axon targeting. Developmental Biology 336, 10-16.

Rajagopalan S, Vivancos V, Nicolas E, and Dickson BJ (2000) Selecting a longitudinal pathway: Robo receptors specify the lateral position of axons in the Drosophila CNS. Cell 103, 1033-1045.

Raper JA (2000) Semaphorins and their receptors in vertebrates and invertebrates. Curr. Opin. Neurobiol. 10, 88 -94.

Ready DF, Hanson TE, Benzer S (1976) Development of the *Drosophila* retina, a neurocrystalline lattice. Developmental Biology 53, 217-240.

Ridley AJ, and Hall A (1992) The small GTP-binding protein rho regulates the assembly of focal adhesions and actin stress fibers in response to growth factors. Cell 70, 389-399.

Ridley AJ, Paterson HF, Johnston CL, Diekmann D, Hall A (1992) The small GTP-binding protein rac regulates growth factor- induced membrane ruffling. Cell 70, 401-410.

Rogge RD, Karlovich CA, Banerjee U (1991)Genetic dissection of a neurodevelopmental pathway: Son of sevenless functions downstream of the sevenless and EGF receptor tyrosine kinases. Cell 64, 39-48.

Roignant J-Y, and Treisman JE (2009) Pattern formation in the *Drosophila* eye disc. Int. J. Dev.Biol. 53, 795-804.

Roof DJ, Hayes A, Adamian M, Chishti AH, and Li T (1997) Molecular characterization of abLIM, a novel actin-binding and double zinc finger protein. The Journal of Cell Biology 138, 575-588.

Round J and Stein E (2007) Netrin signaling leading to directed growth cone steering. Current Opinion in Neurobiology 17, 15-21.

Sahay A, Molliver ME, Ginty DD, and Kolodkin AL (2003) Semaphorin 3F is critical for development of limbic
system circuitry and is required in neurons for selective CNS axons guidance events. J Neurosci 23, 6671– 6680.

Seeger M, Tear G, Ferres-Marco D, and Goodman CS (1993) Mutations affecting growth cone guidance in Drosophila: genes necessary for guidance toward or away from the midline. Neuron 10, 409-426.

Semaphorin Nomenclature Committee (1999) Unified nomenclature for the semaphorins/ collapsins. Cell 97, 551-552

Senti K-A, Usul T, Boucke K, Greber U, Uemura T, Dickson BJ (2003) flamingo regulates R8 axon-axon and axon-target interactions in the *Drosophila* visual system. Current Biology 13, 828-832.

Serafini T, Kennedy TE, Galko MJ, Mirzayan C, Jessell TM, and Tessier-Lavigne M (1994) The netrins define a family of axon outgrowth-promoting proteins homologous to C. elegans UNC-6. Cell 78, 409-424.

Satoh T, Nakafuku M, and Kaziro Y (1992) Function of Ras as a molecular switch in signal transduction. Journal of Biological Chemistry 267, 24149-24152.

Shakir MA, Gill JS, Lundquist EA (2006) Interactions of UNC-34 Enabled with Rac GTPases and the NIK kinase MIG-15 in Caenorhabditis elegans axon pathfinding and neuronal migration. Genetics 172, 893-913.

Shepherd I, Luo Y, Raper JA, and Chang S (1996) The distribution of collapsing-1 mRNA in the developing chick nervous system.. Dev Biol. 173, 185-199

Shi W, Kumanogoh A, Watanabe C, Uchida J, Wang X, Yasui T, Yukawa K, Ikawa M, Okabe M, Parnes JR, Yoshida K, and Kikutani H (2000) The class IV semaphorin CD100 plays nonredundant roles in the immune system: defective B and T cell activation in CD100-deficient mice. Immunity 13, 633-642.

Shi Y and Noll M. Determination of cell fates in the R7 equivalence group of the Drosophila eye by the concerted regulation of D-Pax2 and TTk88 Developmental Biology 331, 68-77.

Simpson JH, Bland KS, Fetter RD, and Goodman (2000a) Short-range and long-range guidance by Slit and its Robo receptors: a combinatorial code of Robo receptors controls lateral position. Cell 103, 1019-1032.

Simpson JH, Kidd T, Bland KS, Goodman CS(2000b) Short-range and long-range guidance by slit and its Robo receptors. Robo and Robo2 play distinct roles in midline guidance. Neuron 28, 753-766.

Skeath JB, and Thor S (2003) Genetic Control of Drosophila nerve cord development. Current Opinion in Neurobiology 13, 8-15.

Song H, and Poo M (2001) The cell biology of neuronal navigation. Nat Cell Biol 3, E81-8.

Spitzweck B, brankatschk M, Dickson BJ (2010) Distinct protein domains and expression patterns confer divergent axon guidance functions for Drosophila Robo receptors. Cell 140, 409-420.

Stein E, Zou Y, Poo M, and Tessier-Lavigne M (2001) Binding of DCC by netrin-1 to mediate axon guidance independent of adenosine A2B receptor activation. Science 291, 1976–1982.

Steup A, Ninnemann O, Savaskan NE, Nistch N, Püschel AW, and Skutella, T (1998) Semaphorin D acts as a repulsive factor for entorhinal and hippocampal neurons. Eur. J. Neurosci. 11, 729–734.

Stoeckli E and Zou Y (2009) How are Neurons wired to form functional and plastic circuits? Embo Reports 10, 326-330.

Struckhoff EC and Lundquist EA (2003) The actin-binding protein UNC-115 is an effector of Rac signaling during axon pathfinding in C. elegans. Development 130, 693–704.

Tamagnone L, Artigiani S, Chen H, He Z, Ming G-L, Song H-J, Ch´edotal A, Winberg ML, Goodman CS, Poo M-M (1999) Plexins are a large family of receptors for transmembrane, secreted, and GPI-anchored semaphorins in vertebrates. Cell 99, 71– 80.

Tang AH, Neufeld TP, Kwan E, Rubin GM (1997) PHYL acts to down-regulate TTK88, a transcriptional repressor of neuronal cell fates by a SINA-dependent mechanism. Cell 90, 459-467.

Takagi S, Tsuji T, Amagai T, Takamatstu T, and Fujisawa H (1987) Specific cell surface labels in the visual centers of Xenopus luevis tadpole identified using monoclonal antibodies. Dev. Biol. 122, 90-100.

Takahashi T, Fournier A, Nakamura F, Wang LH, Murakami Y, Kalb RG, Fujisawa H, Strittmatter SM (1999)
Plexin-Neuropilin-1 complexes form functional semaphorin- 3A receptors. Cell 99, 59–69.

Takahashi T, and Strittmatter SM (2001) Plexina1 autoinhibition by the plexin sema domain. Neuron 29, 429-439.

Takemura S-y, Lu Z, and Meinerzhagen IA (2008) Synaptic circuits of the *Drosophila* optic lobe: the input terminals to the medulla.Jcomp Neurol 509, 493-513.

Terman JR, Mao T, Pasterkamp RJ, Yu HH, Kolodkin AL (2002) MICALs, a family of conserved flavoprotein oxidoreductases, function in plexin-mediated axonal repulsion. Cell 109, 887-900.

Tessier-Lavigne M, and Goodman CS (1996) The molecular biology of axon guidance. Science 274, 1123-1133.

Thomas T, Kurihara H, Yamagishi H, Kurihara Y, Yazaki Y, Olson E N, Srivastava D (1998) A signaling cascade involving endothelin-1, dHAND, and Msx1 regulates development of neural crest-derived bran- chial arch mesenchyme. *Development.* 125, 3005–3014.

Ting C-Y, Yokenura S, Chung P, Hsu S-N, Robertson HM, Chiba A, Lee C-H (2005) *Drosophila* N-cadherin functions in the first stage of the two-stage layer-selection process of R7 photoreceptor afferents. Development 132, 953-963.

Ting CY and Lee CH (2007) Visual circuit development in Drosophila. Current Opinion in Neurobiology 2007, 17:1–8

Tomasi T, Satoko H-S, Ohler S, Schleiffer A, and Suzuki T (2008) The transmembrane protein Golden Goal regulates R8 photoreceptor axon-axon and axon-target interactions. Neuron 57, 691-704.

Tomlinson A, Ready DF (1986) Sevenless: a cell-specific homeotic mutation of the *Drosophila* eye. Science 231, 400-402.

Valera-Echavarria A, Tucker A, Püschel AW, Guthrie S (1997) Motor axon populations respond differently to the chemorepellents netrin-1 and semaphorin D. Neuron 18, 193-207.

van Roessel, P. and Brand, A.H. (2000) Gal-4 mediated ectopic gene expression in *Drosophila*. In: Sullivan, W., Ashburner, M., Hawley, R.S. (eds) *Drosophila* Protocols. Cold Spring Harbor Laboratory Press, New York, pp439-448.

Vardar D, Buckley DA, Frank BS, McKnight CJ (1999) NMR structure of an F-actin-binding "headpiece" motif from villin. JmolBiol. 294, 1299-310.

Vardar D, Chishti AH, Frank BS, Luna EJ, Noegel AA, Oh SW, Schleicher M, McKnight CJ (2002) Villin-type Headpiece Domains show a wide range of F-actin-binding affinities. Cell Mtotility and Cytoskeleton 52, 9-21.

Vastrik I, Eickholt BJ, Walsh FS, Ridley A, Doherty P (1999) Sema3A-induced growth cone collapse is mediated by Rac1 amino acids 17-32. Current Biology 9, 991-998.

Vermeulen W, Vanhaesebrouck P, Van Troys M, Verschueren M, Fant F, Goethals M, Ampe C, Martins JC, Borremans FAM
(2004) Solution structures of the C-terminal headpiece subdomains of human villin and advillin, evaluation of headpiece Factin-binding requirements. Protein Sci 13, 1276–1287.

Wang T, and Montell C (2007) Phototransduction and retinal degeneration in *Drosophila.* Pflugers Arch-Eur J Phys 454, 821-847.

Wasserman JD, Urban S, Freeman M (2000) A family of rhomboid-like genes: Drosophila *rhomboid-1* and roughoid/ rhomboid-3 cooperate to activate EGF receptor signaling. Genes & Development 14, 1651-1663.

Watanabe C, Kumanogoh A, Shi W, Suzuki K, Yamada S, Okabe M, Yoshida K, and Kikutani H (2001)Enhanced immune responses in transgenic mice expressing a truncated form of the lymphocyte semaphorin CD100. J Immunol 167, 4321-4328.

Watari-Goshima N, Ogura K, Wolf FW, Goshima Y, Garriga G. (2007) C. elegans VAB-8 and UNC-73 regulate the SAX-3 receptor to direct cell and growth-cone migrations. Nat Neurosci 10, 169-176.

Weinl C, Drescher U, Lang S, Bonhoeffer F, and Löschinger J (2003) On the turning of Xenopus retinal axons induced by ephrin-A5. Development 130, 1635-1643.

Wightman B, Baran R, Garriga G (1997) Genes that guide growth cones along the C. elegans ventral nerve cord. Development 124, 2571-2580.

Williams SE, Mann F, Erskine L, Sakurai T, Wei S, Rossi DJ, Gale NW, Holt CE, Mason CA, and Henkemeyer M (2003) Ephrin-B2 and EphB1 mediate retinal axon divergence at the optic chiasm. Neuron 39, 919-935.

Winberg ML, Noordermeer J N, Tamagnone L, Comoglio P M, Spriggs MK, Tessier-Lavigne M and Goodman C S (1998). Plexin A is a neuronal semaphorin receptor that controls axon guidance. Cell 95, 903-916.

Wolf FW, Hung MS, Wightman B, Way J, Garriga G (1998) Vab-8 is a key regulator of posteriorly directed migrations in C. elegans and encodes a novel protein with kinesin motor similarity. Neuron 20, 655-666.

Yang L and Bashaw GJ (2006) Son of sevenless directly links the Robo receptor to rac activation to control axon repulsion at the midline. Neuron 52, 595-607.

Yang L, Garbe DS , Bashaw GJ (2009) a frazzled/DCC-dependent transcriptional switch regulates midline axon guidance Science 324, 944-947.

Yang Y, and Lundquist EA (2005) The actin-binding protein UNC-115/abLIM controls formation of lamellipodia and filopodia and neuronal morphogenesis in Caenorhabditis elegans. Mol Cell Biol 25, 5158-5170.

Yang Z (1997) PAML: a program package for phylogenetic analysis by maximum likelihood Computer Applications in BioSciences 13, 555-556.

Yogev S, Schejter ED, and Shito B-Z (2008) Drosophila EGFR signaling is modulated by differential compertalization of Rhomboid intramembrane proteases. The EMBO Journal 27, 1219-1230.

Yu HH, Araj HH, Ralls SA, Kolodkin AL (1998) The transmembrane Semaphorin Sema I is required in Drosophila for embryonic motor and CNS axon guidance. Neuron 20, 207-220.

Yu WT, and Bargmann CI (2001) Dynamic regulation of axon guidance. Nature Neuroscience 4, 1169-1176.

Yuan XB, Jin M, Xu X, Song YQ, Wu CP, Poo MM, Duan S (2003) Signalling and crosstalk of Rho GTPases in mediating axon guidance. Nature Cell Biology 5, 38-45.

Yuasa-Kawada J,Kinoshita-Kawada M, Rao Y, Wu JY (2009) Deubiquinating enzyme USP33/ VDU1 is required for Slit signaling in inhibiting breast cancer cell migration. PNAS 106, 14530-14535.